ESTIMATION OF ABOVEGROUND BIOMASS/ CARBON STOCK AND CARBON SEQUESTRATION USING UAV IMAGERY AT KEBUN RAYA UNMUL SAMARINDA EDUCATION FOREST, EAST KALIMANTAN, INDONESIA

MD. ABUL HASHEM
February 2019

SUPERVISORS:
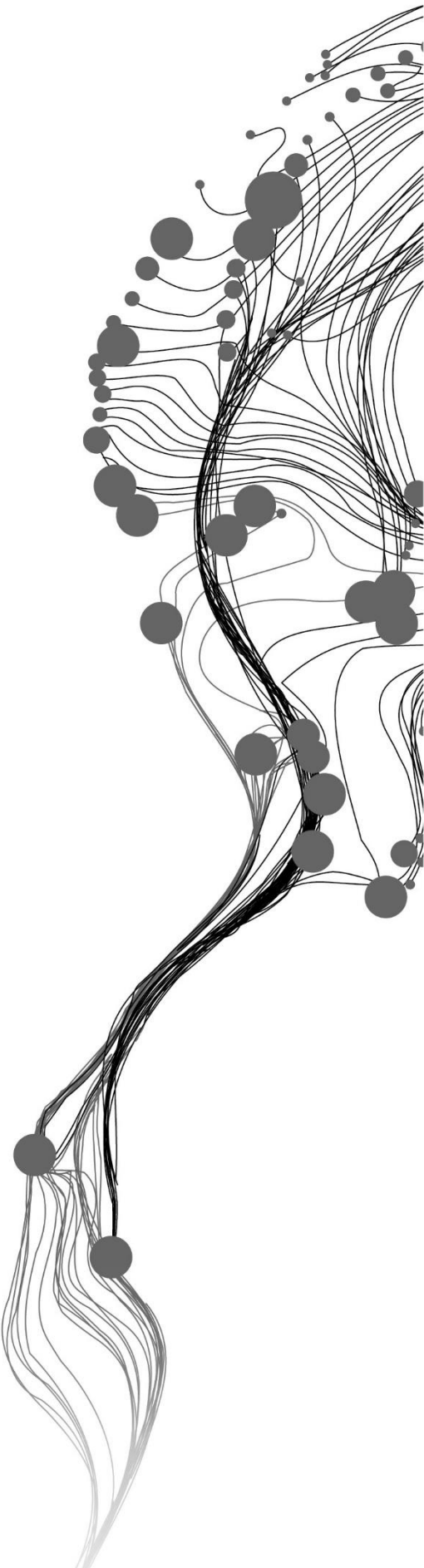Ir L.M. van Leeuwen-de- Leeuw
Dr. Y.A. Hussin

ADVISOR:
Dr. Y. Budi Sulistioadi
University of Mulawarman, Samarinda, Indonesia

ESTIMATION OF ABOVEGROUND BIOMASS/ CARBON STOCK AND CARBON SEQUESTRATION USING UAV IMAGERY AT KEBUN RAYA UNMUL SAMARINDA EDUCATION FOREST, EAST KALIMANTAN, INDONESIA

MD. ABUL HASHEM
Enschede, The Netherlands, February 2019

Thesis submitted to the Faculty of Geo-Information Science and Earth
Observation of the University of Twente in partial fulfilment of the
requirements for the degree of Master of Science in Geo-Information
Science and Earth Observation.
Specialization: Natural Resource Management

SUPERVISORS:
Ir L.M. van Leeuwen-de- Leeuw
Dr. Y. A. Hussin

ADVISOR:
Dr. Y. Budi Sulistioadi
University of Mulawarman, Samarinda, Indonesia

THESIS ASSESSMENT BOARD:
Prof. Dr. A.D. Nelson (Chair)
Dr. Tuomo Kauranne (External Examiner, Lappeenranta University of
Technology, Finland)

ABSTRACT

The accurate assessment of AGB/ carbon stock and carbon sequestration in the forest is the burning issue to the global community for taking mitigation and adaptation measures. REDD+ activities need to be evaluated scientifically which requires MRV mechanism of carbon emissions to follow the UNFCCC principles that would be transparent, consistent, comparable, complete and accurate. Quantification and monitoring of tropical rainforest carbon sequestration are essential to understanding the role of the tropical rainforest on the global carbon cycle. The important forest inventory parameters such as tree height and diameter at breast height (DBH) are needed to assess biomass and carbon stock. These tree parameters can be acquired by direct measurement and indirect estimation. The measuring of tree height and DBH from the direct field-survey is time-consuming, labor-intensive, and costly. However, it is quite challenging to acquire accurate tree height from the field due to the multi-layer canopy structure of the tropical forest.

Remote sensing is a suitable and cost-effective technique to assess biomass and carbon stock due to periodic monitoring of forest ecosystem. Three sources of remotely sensed data such as airborne laser scanning (ALS), radio detection and ranging (RADAR), and optical images (e.g., satellite or aerial images) can be used to extract the tree parameters. Unmanned aerial vehicles (UAVs) can acquire high resolution remotely sensed data to estimate biomass and carbon stock. The application of UAV is effective and efficient in assessing biomass with a relatively low cost for a small area at regular intervals. The purpose of this study is to assess forest aboveground biomass/carbon stock and carbon sequestration using high-resolution UAV images. The DSM, DTM, and orthomosaic were generated based on structure from motion (SfM) and 3D point clouds filtering techniques. The canopy height model (CHM) was generated from the DSM and DTM. The height extracted from the CHM and the predicted DBH calculated from the CPA based on the quadratic model were used as input in the generic allometric equation to estimate AGB and carbon stock.

The F-test and t-test revealed that the tree height extracted from CHM and the field-measured tree height had no significant difference. The relationship between field DBH and manually delineated CPA was made and showed the highest coefficient of determination and lowest RMSE for the quadratic model. The model validation also performed and showed a strong correlation between observed DBH and predicted DBH. The results of the F-test and t-test revealed that there was no statistically significant difference between field-based AGB and UAV-based AGB. The total amount of sequestered carbon for one year was assessed 6.32 Mg ha^{-1}. The difference of UAV-based AGB with and without inflated/deflated height was found 21.66 Mg ha^{-1} which is equivalent to 8.73% of original estimated UAV-based AGB without inflation and deflation of height. The single factor/ one-way ANOVA test revealed that there was a statistically significant difference between estimated UAV-based AGB with 8.94% inflation and deflation of height and UAV-based AGB without inflation/deflation of height. The average variation of biomass due to 1% inflation and deflation of CPA was 2.47 Mg ha^{-1} and showed statistically insignificant influence on biomass estimation. For 5% inflation and deflation of CPA, the average variation of biomass was estimated 12.37 Mg ha^{-1}. Despite its large variation, it had no statistically significant difference from original biomass, but the amount of AGB was observed very much close to the estimated amount of sequestered biomass for one year. On the other hand, the average variation of biomass 24.70 Mg ha^{-1} was estimated due to 10% inflated and deflated CPA that showed a statistically significant difference and it affected 9.96% variation of AGB from the original biomass. The estimated amount of carbon due to CPA error was double compared to the amount of sequestered carbon for one year. To summarise, this study showed a novelty by assessing carbon sequestration using UAV images for two consecutive years.

Keywords: Above ground biomass, carbon sequestration, Unmanned Aerial Vehicle, error propagation, canopy height model, Digital surface model, Digital terrain model

ACKNOWLEDGMENTS

TABLE OF CONTENTS

LIST OF FIGURES

LIST OF TABLES

LIST OF EQUATIONS

LIST OF APPENDICES

LIST OF ACRONYMS

AGB	Aboveground biomass
AGC	Aboveground carbon
ALS	Airborne Laser Scanner
ANOVA	Analysis of variance
CF	Carbon Fraction
CHM	Canopy Height Model
Cm	Centimetre
CO_2	Carbon dioxide
CP	Check Point
CPA	Crown projection area
DBH	Diameter at Breast Height
DGPS	Differential Global Positioning System
DSM	Digital Surface Model
DTM	Digital Terrain Model
GCP	Ground Control Points
GHG	Green House Gas
GIS	Geographic Information System
GNSS	Global Navigation Satellite System
GPS	Global Positioning System
GSD	Ground Sampling Distance
IMU	Inertial Measurement Unit
IPCC	Intergovernmental Panel on Climate Change
KRUS	Kebun Raya UNMUL Samarinda
LiDAR	Light Detection and Ranging
Mg	Megagram
MT	Missing Tree
MRV	Monitoring, Reporting and Verifications
OBIA	Object-Based Image Analysis
RADAR	Radio Detection and Ranging
REDD+	Reducing Emissions from Deforestation and Forest Degradation
RMSE	Root Mean Square Error
SfM	Structure from Motion
TLS	Terrestrial Laser Scanner
UAV	Unmanned Aerial Vehicle
UNFCCC	United Nations Framework Convention on Climate Change
UNMUL	University of Mulawarman
2D	Two Dimensional
3D	Three Dimensional

1. INTRODUCTION

1.1. Background Information

Environmental degradation from deforestation and forest degradation as well as land use change is one of the major concerns for the global community because 17% of total greenhouse gas (GHG) are being released from this source (IPCC, 2003). The importance of forests as both a sink and a source of greenhouse gas emissions is globally recognized (Brown, 2002). Around 30% of the earth's land surface is covered by the forest while 45% of the total carbon is stored on land (Saatchi et al., 2011). Tropical rainforests have been considered as one of the dominant types of forest that can play a crucial role in the context of biodiversity conservation and climate change mitigation and adaptation. They can sequester and store more carbon than any other forests (Gibbs et al., 2007). As stated by Saatchi et al. (2011) tropical forests can sequester around 247 billion tons of carbon, of which 78.14% is sequestered in aboveground biomass while the 21.86% of carbon is stored in belowground biomass. Tropical forests are recognized as the potential sink of sequestering carbon from the atmosphere through protecting forested lands, slowing deforestation, reforestation and agroforestry (Brown et al., 1996). However, deforestation and forest degradation occurred in tropical forests due to natural and anthropogenic interventions (Ota et al., 2015). According to the Intergovernmental Panel on Climate Change (IPCC), 1.6 billion tons of carbon are being released every year, exclusively from deforestation and forest degradation (IPCC, 2003). The tropical forest located in Southeast Asia contains 26% of the world's tropical carbon, and unfortunately, this region is experiencing more deforestation and forest degradation since 1990 (Saatchi et al., 2011). The climate change issue has brought attention to the global community to protect the forest from deforestation and forest degradation, specifically tropical forest. In 2005, UNFCCC commenced a process called "Reducing Emissions from Deforestation and Forest Degradation, plus the role of conservation, sustainable management of forests and enhancement of forest carbon stock (REDD+)" which is one of the key climate change mitigation mechanism. Sustainable, consistent and robust monitoring, reporting and verification (MRVs) mechanism should be operationalized to implement the REDD+ program successfully in every country. The estimation of AGB and carbon stock is a prerequisite to achieving the objectives of REDD+ program and eventually, to get the benefit from the newly emerging issue namely carbon trading.

Carbon stock is typically measured from the above ground biomass by assuming that half of the biomass is carbon (Basuki et al., 2009). Cutting trees and weighing their different parts is the destructive method for accurate estimation of biomass and carbon (Ebuy et al., 2011). This method is costly, labor-intensive and time-consuming. This destructive method is supportive and helpful to develop allometric equations to assess biomass and carbon stock (Clark et al., 2001). The forest parameters such as DBH, tree height, and wood density are required as input in these allometric equations to estimate the forest aboveground biomass/ carbon stock (Basuki et al., 2009, Ketterings et al., 2001).

Remote sensing techniques are a better choice than field measurement for capturing the spatiotemporal information of forest biophysical properties to assess biomass and carbon stock (Ota et al., 2017). Owing to applications in the forestry sector, there are mainly three sources of remotely sensed data such as (i) airborne laser scanning (ALS), (ii) radio detection and ranging (RADAR) (e.g., synthetic aperture radar), and (iii) optical images (e.g., satellite or aerial images).

The data acquisition using UAV-based platform has high operational flexibility in terms of cost, time, platforms, place and repeatability compared to the satellite-based platform and traditional manned photogrammetric operations (Stöcker et al., 2017). UAV has the capability of providing high spatial and temporal resolution data which is useful in assessing AGB and carbon stock (Fritz et al., 2013). UAV platform can capture high-resolution images that can be used effectively and efficiently to generate the digital terrain model (DTM), digital surface model (DSM), and ortho-mosaic image (Stöcker et al., 2017).

The captured images from the UAV platform are used to generate DSM, DTM, and orthomosaic based on structure from motion (SfM) technique. Structure from motion (SfM) represents the process to obtain a three-dimensional structure of a scene of an object from a series of digital images (Micheletti et al., 2015). SfM photogrammetry is cost and time-effective to estimate forest AGB and carbon stock. SfM uses a sequence of overlapping images to produce a sparse 3D model of the scene. SfM photogrammetry approach is capable of generating a digital surface model, reflecting the top of the canopy in the case of a forest and a digital terrain model (Mlambo et al., 2017). Canopy height model (CHM) can be generated from DSM and DTM. From CHM, the tree height can be extracted that would be the input for allometric equations to assess biomass and carbon (Magar, 2014).

Among all biophysical parameters of the tree, diameter at breast height (DBH) is one of the essential variables to assess the biomass and carbon because it explains more than 95% variation in biomass (Gibbs et al., 2007). Studies have proved that there is a significant relationship between CPA and DBH (Anderson et al., 2000). The correlation was demonstrated between CPA and all parts of trees such as foliage mass, branch mass, stem mass for biomass (Kuuluvainen, 1991). The above ground biomass and carbon stock can be assessed based on the relationship between CPA and DBH using regression model and allometric equations (Basuki et al., 2009; Chave et al., 2005).

1.2. Problem Statement and Justification

Most of the studies on assessment of AGB/carbon stock and carbon sequestration in tropical rainforest has been conducted using optical images (Du et al., 2012; Dube & Mutanga, 2015; Gibbs et al., 2007; Lu et al., 2004; (Powell et al., 2010). The data collected from optical remote sensing can have problems due to clouds, shadows, high saturation, low spectral variability, 2-D in nature and it is quite challenging to assess AGB and carbon stock using these data (Kachamba et al., 2016). Although some medium-resolution remote sensing data such as Landsat, Sentinel, etc. are freely available, it is difficult to use them to assess the forest aboveground biomass and carbon stock due to pixel size, resolution versus tree crown size. Some very high-resolution data such as QuickBird, IKONOS, etc. can estimate biomass accurately, but they are costly and need highly technical knowledge to process. (Koh & Wich, 2012). The application of radar backscatter to estimate AGB/carbon stock is challenging and leads to underestimation of AGB in the tropical forest because of its high density and complex structure(Minh et al., 2014; Villard et al., 2016). L-band radar data can be used to estimate AGB accurately up to 150 Mg ha^{-1} and it tends to saturate with AGB is greater than 150 Mg ha^{-1} (Villard et al., 2016). The decrease of intensity of radar backscatter also known as saturation effect is the main reason for under-estimation of AGB (Minh et al., 2014). Recently, Lidar has proved to be the best remote sensing technique to estimate biomass/ carbon stock accurately and precisely. However, it is very expensive to assess biomass and carbon stock over a large area (Strahler et al., 2008). Unmanned aerial vehicles (UAVs) can acquire high resolution remotely sensed data to estimate biomass and carbon stock. The application of UAV is effective and efficient in assessing biomass with a relatively low cost for a small area (Senthilnath et al., 2017). Furthermore, limited expertise is good enough to operate and acquire data from the UAV platform.

Conventional remote sensing techniques can provide horizontal forest structure accurately rather than vertical forest structure. On the contrary, UAV is capable of providing horizontal and vertical forest structure (Böttcher et al., 2009). In tropical rainforests, the estimation of above ground biomass and carbon stock is quite challenging because of its complex stand structure and plentiful verities of species composition (Nelson et al., 2000). A very limited number of researches were carried out using UAV images and Lidar in a tropical forest. Clark et al. (2001) stated that the research on carbon flux and atmosphere is still insufficient in a tropical forest. Based on that reason, it is essential to conduct research on quantifying and monitoring carbon sequestration in a tropical forest. Few studies were carried out to estimate carbon sequestration annually using high resolution remotely sensed data. The research on the accuracy of the assessment of the AGB and carbon stock and specifically carbon sequestration using high-resolution UAV images of two consecutive years would be helpful in the decision-making process to implement the REDD+ initiatives, sustainable forest management and eventually natural resources management using its mechanism on MRV.

Despite having some benefits UAV also has limitations. The captured images by the UAV can only cover the upper canopy of the tree. In the tropical forest, the lower canopy of trees is not visible because it is fully or partially covered by the upper canopy trees. The point clouds are generated based on the captured images that covered upper canopy, and it has an impact on assessing the total AGB and carbon stock. The different sources of error or uncertainty have direct effects on AGB/ carbon stock and especially sequestration estimation. The choice of remote sensing techniques influences the level of uncertainty in the estimate of biomass (Gonzalez et al., 2010). The major sources of error in assessing AGB/carbon stock and carbon sequestration are UAV data processing, tree parameter collection, allometric equations, ground-based sampling, regression modeling. In a tropical forest, the measurement of height is challenging because of the complex nature of the structure. It is quite challenging to extract accurate height form UAV-derived point clouds. The height variation affects the total AGB/carbon stock estimation, and finally, it influences assessing carbon sequestration. The variation of the amount of AGB and carbon stock of two years due to height error might be affected more on carbon sequestration estimation. The manually delineated CPA or automatic segmented CPA might have a certain level of inaccuracy, and it also has effects on biomass and carbon sequestration estimation because the predicted DBH is found based on CPA. In order to have complete and accurate biomass and carbon stock estimation, the identification and estimates of error are an essential part of the process (Brown, 2002). Therefore, it is significant to identify and quantify these errors and analyze the effect on biomass estimation and more specifically, how will that affect the carbon sequestration.

1.3. Research Objective

1.3.1. General Objective

This study is aiming at the assessing of AGB/ carbon stock, carbon sequestration and evaluating the effects of height and CPA delineation error on biomass estimation from very high-resolution UAV images based on SfM photogrammetry approach at Kebun Raya UNMUL (University of Mulawarman) Samarinda (KRUS) Education Forests, East Kalimantan, Indonesia.

1.3.2. Specific Objectives

1. To estimate the AGB/carbon stock of tropical rainforest for 2017 and 2018.
2. To assess the amount of sequestered carbon in the tropical forest for one year using UAV images.
3. To assess the accuracy of aboveground biomass of tropical rainforest estimated from UAV images.
4. To assess the effect of the error of tree parameters extracted from UAV images on AGB estimation.

1.4. Research Questions

1. What is the estimated amount of the AGB/carbon stock for 2017 and 2018?
2. What is the estimated amount of sequestered carbon?
3. What is the accuracy of the aboveground biomass estimated from UAV images?
4. What is the error of UAV-derived tree height and how does that affect the AGB estimation?
5. How much the CPA delineation error affect the AGB estimation?

1.5. Research Hypothesis

1. Ho: There is no significant difference between estimated biomass from UAV imagery and field-based biomass.
   Ha: There is a significant difference between estimated biomass from UAV imagery and field-based biomass.
2. Ho: The error of UAV-derived height has no significant influence on the AGB/ carbon estimation.
   Ha: The error of UAV-derived height has a significant influence on the AGB/ carbon estimation.
3. Ho: The error of CPA delineation has no significant influence on the AGB/ carbon estimation.
   Ha: The error of CPA delineation has a significant influence on the AGB/ carbon estimation.

1.6. Conceptual Diagram

The conceptual diagram was developed after identifying and defining the problem of the study. The relevant systems, sub-systems, elements and potential interactions among them were identified and illustrated using **Figure 1**.
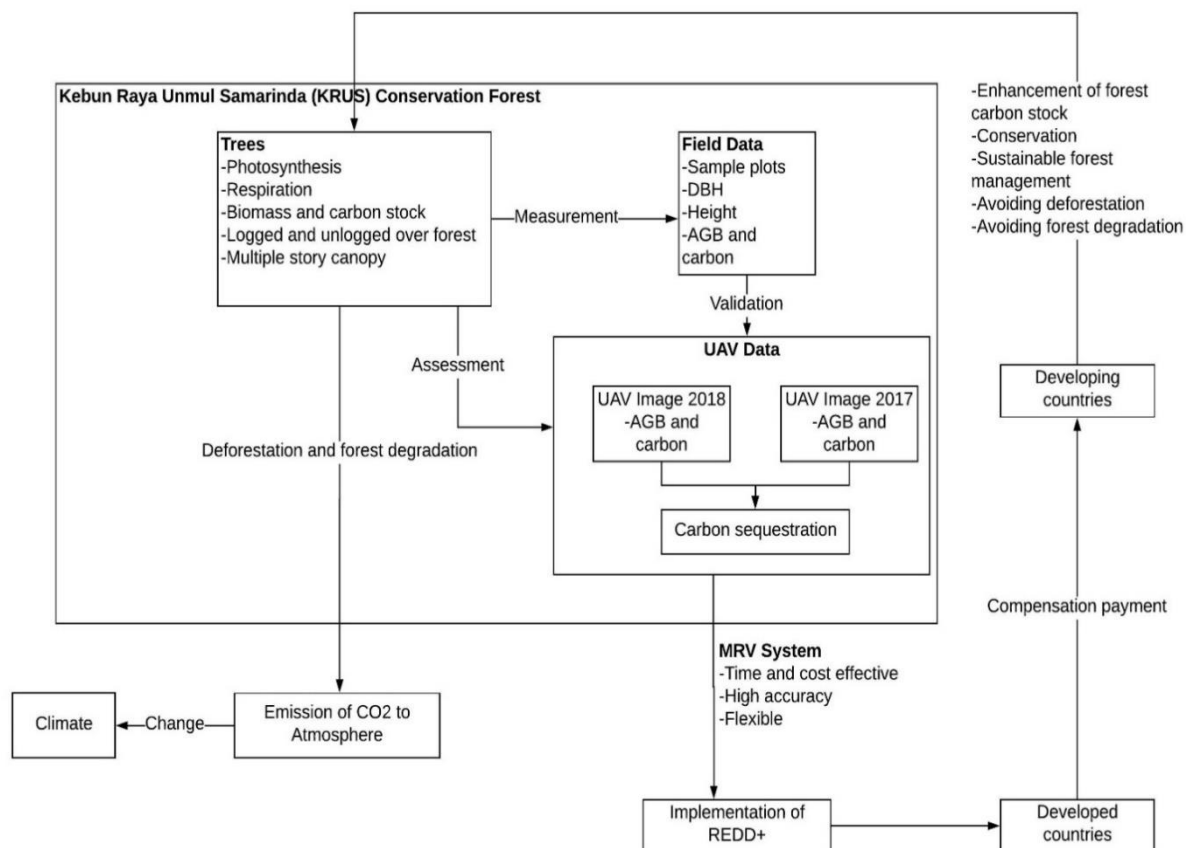
Figure 1: Conceptual diagram

2. STUDY AREA, MATERIALS, AND METHODS

2.1. Study Area

UNMUL Samarinda botanical garden also known as 'KRUS' located in the Samarinda City of East Kalimantan province, Indonesia which was belonging to CV. Mahakam wood before 1974. CV. Mahakam wood handed over an area of 300 hectares to the rector of Mulawarman University in 1974. Then the area was used as a conservation forest area and a suitable place for conducting research and educational activities on tropical forest. On 9 July 1974, the area was inaugurated as educational forests. In 2001, 300 hectares was reduced by 62 hectares because the area was allocated for a recreational botanical garden tourist spot (Wikipedia, 2015). The map of the study area is shown in **Figure** 2.
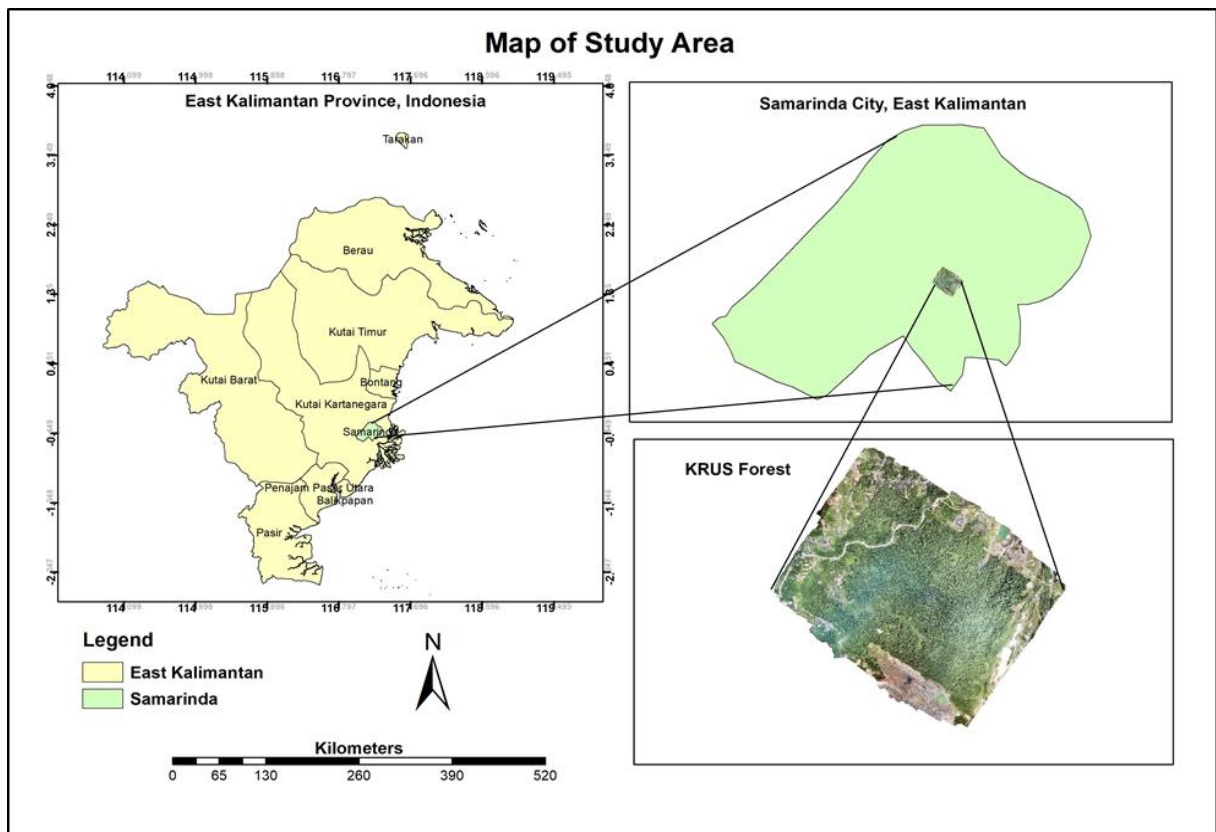
Figure 2: Map showing the study area

2.1.1. Geographical Location

Kebun Raya Unmul Samarinda education forest is located between 117° 12' 15.388" E - 117° 13' 35.786" E and 0° 26' 17.435" N - 0° 27' 32.769" N. The study area is located in urban villages namely Laterite and Mugirejo under the North Samarinda and Sungai Pinang administrative districts respectively (Faculty of Forestry, University of Mulawarman, 2018).

2.1.2. Climate and Topography

The average annual rainfall is 2000 mm while the rainfall is observed slightly lower from June to October. The daily maximum temperature is observed 33.20^0 C while 24.50^0 C is observed as the daily minimum temperature (Faculty of Forestry. University of Mulawarman, 2018). Very dry years occasionally occur due to the effect of the Southern Oscillation phenomenon and El Niño (Guhardja et al., 2000). The soils of the

study area are Podzolic Kandic, Podromolic Chromic, and Cambisol. The 60-70% of the study area consists of forest areas with ramps up rather steep slope.

2.1.3. Vegetation

The study area is largely a forest area with vegetation cover logged secondary dry forest (logged-over areas), and thickets with an area covering around 209 hectares while 29% of the area is the non-forested area. Among the 70% of secondary forests, the dominant species are Artocarpus spp, Macaranga spp, Eusideroxylon zwageri, Pentace spp, etc. (Faculty of Forestry. University of Mulawarman., 2018).

2.2. Materials

2.2.1. Field Equipment

The tools and equipment mentioned in **Table** 1 were used in the study to measure and collect the required data from the field.

Table 1: List of field equipment and its uses

Name of tools/ equipment	Uses
UAV Phanton4 DJI	2-D image capturing
Measuring tape (50m)	Identification of the outer boundary of plots
Diameter tape (5m)	Measurement of tree DBH
Handheld GPS (Garmin)	Navigation and X, Y coordinate reading
Field data sheet and pencil	Data recording
Range finder/ Haga altimeter	Measurement of tree height
Leica DISTO D5	Height measurement
Tablet	Navigation
Santo Clinometer	Slope measurement
DGPS	GCPs and plot center location

2.2.2. Data Processing Software

The different types of software were used to process and analyze the collected data from the study area. The list of software and their uses are mentioned in
Table 2.

Table 2: List of software and uses

Name of software	Uses
ArcMap 10.6.1	Data processing and visualization
Pix4D	Photogrammetry processing
Erdas Imagine	Resampling of ortho-mosaic image
Microsoft Excel	Data analysis
Cloud compare	3-D point cloud visualization
Microsoft Word	Reports and thesis writing
Mendeley Desktop	Citation and references
Lucidchart	Flowchart drawing
Microsoft power point	Presentation of thesis

2.3.   Research Methods

The research method encompasses the fieldwork design, spatial and statistical analysis and estimating the AGB/AGC and carbon sequestration and lastly evaluating the influence of height and CPA delineation error on assessing AGB. The research method of this study was comprised of five parts (see **Figure** 3):

(i)   The first part was the biometric data collection, processing, and analysis. It involved the field observation and acquiring required tree parameters using the above-mentioned instruments in Table-1;

(ii)   The second part was capturing digital images using a UAV platform. Then the data was processed by Pix4D software to generate DSM, DTM and orthophoto;

(iii)   The third part was the extraction of tree height from CHM generated from DSM and DTM;

(iv)   In the fourth part, aboveground biomass (AGB)/ carbon stock and carbon sequestration were assessed using tree height and predicted DBH extracted from UAV data in the third part.

(v)   In the fifth and the last part, the effect of the height and CPA delineation error on aboveground biomass was assessed.

2.3.1.   Workflow of the Methods
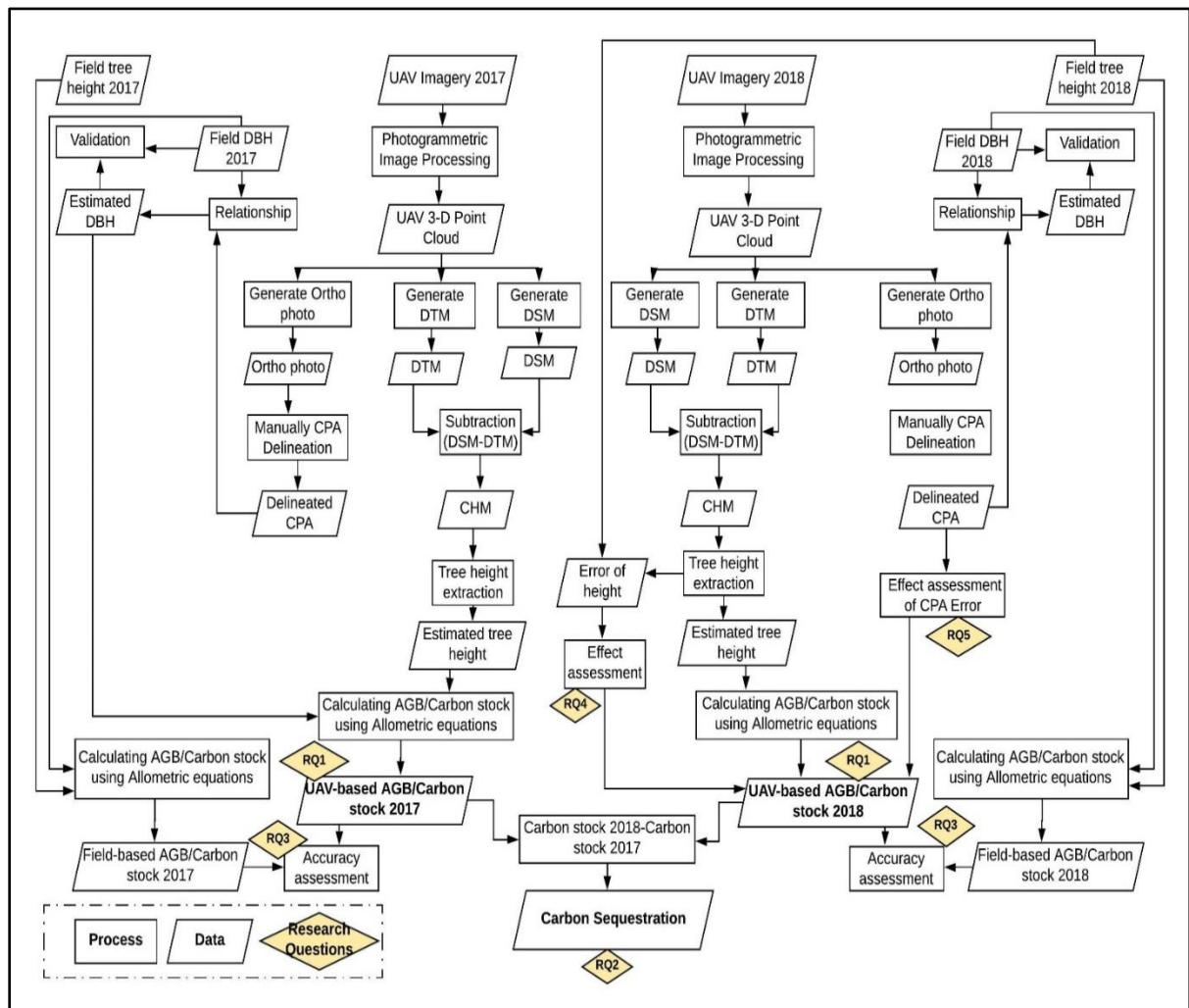
Figure 3: Workflow of the method

2.3.2. Pre-field Work

The pre-fieldwork activities such as preparing data collection sheet (see **Appendix 1**), black and white paint marker and plastic tubes to set the ground control points (GCPs) (see **Appendix 2**), tree tag, testing of equipment and tools to be used in the field, checking GPS and batteries condition of UAV were done before going to field. Possible plots were identified in the orthomosaic images of 2017 and loaded in the tablet to ease the identification of the plots as well as navigation.

2.3.3. Plot Size

Circular plots with an area of 500 m² (radius 12.62m) were used in flat terrain to collect the biophysical parameters of trees. Circular plots are preferred compared to square and rectangular plots because of delineating the outline of the plots is relatively easy and less error-prone (Mauya et al., 2015). A study conducted by Ruiz et al. (2014) brought to light that no significant difference in results could be found if the plot size is increased beyond 500 m². The radius of the plots was adjusted using a slope correction table (see **Appendix 3**) if any slopes existed inside the plots. **Figure** 4 shows a sampling of plots with an area of 500m² and radius 12.62m as an example.
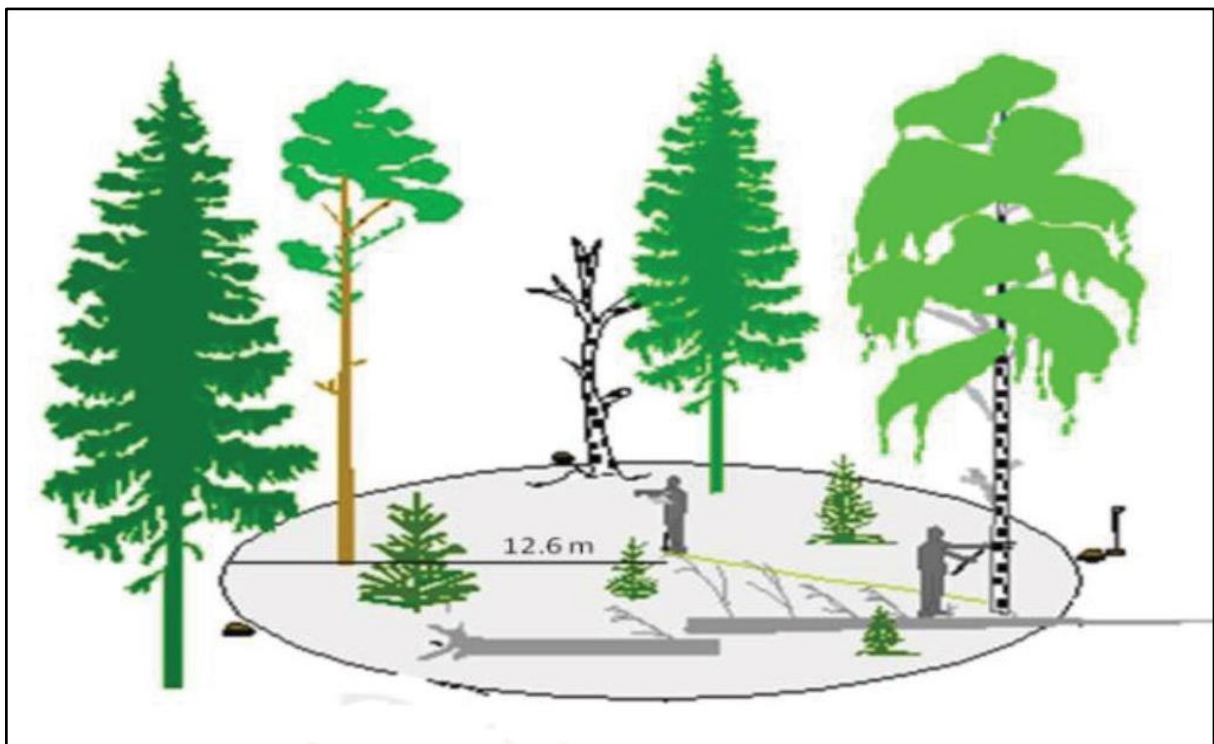
Figure 4: Circular plot with 12.62m radius
Source: Asmare (2013)

2.3.4. Sampling Design

In this study, a purposive sampling method was used to collect the field data. This sampling method is a non-probability method based on the judgment of researchers. The purposive sampling method was chosen considering the time limitation, inaccessibility in the forest, covering the variation of all forest structure, terrain conditions, UAV flight planning, etc. The total of 41 plots was selected to collect the biometric data. The distribution of sampling plots is shown in Figure 5.
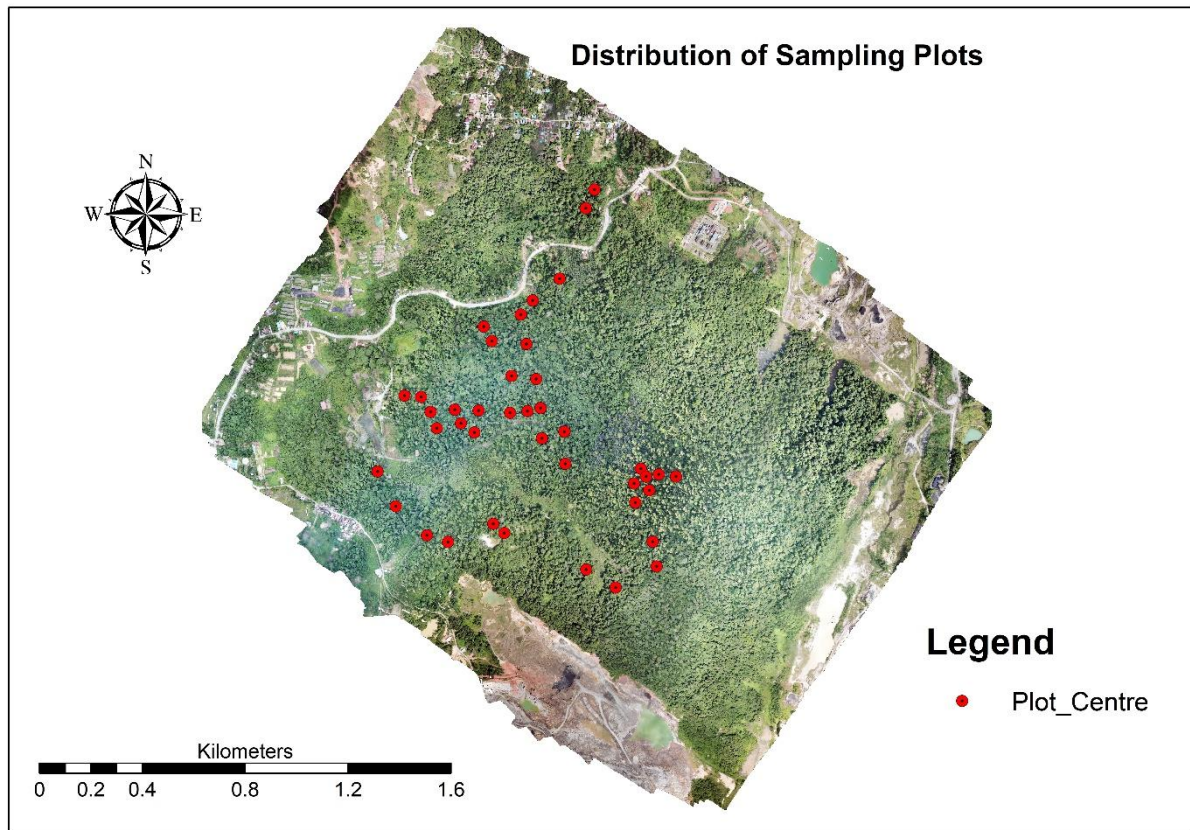
Figure 5: Distribution of sampling plots in the study area

2.4. Data Collection

In this study, the primary, as well as secondary data were used to achieve the objectives of the research. The UAV images for 2017 obtained by the University of Mulawarman, Indonesia were used as secondary data. The following sub-sections illustrate the procedures and methods of field data as well as UAV data collection including the recording of the ground control point (GCP) using differential global positioning system (DGPS).

2.4.1. Biometric Data Collection

Fieldwork was conducted from 01 October 2018 to 25 October 2018. First, the center of the plot was fixed; then the measuring tape was used to delineate the outline of the plot with a 12.62m radius which covers 500 m². The XY coordinate of the center of the plots and the tree location was recorded by Garmin GPS. The diameter of breast height (DBH) was measured using diameter tape at 1.3m above ground. The height of the trees was measured using a Leica DISTO D510. The tree is having DBH equal to or greater than 10 cm was considered because the trees that have DBH less than 10 cm cannot contribute a role significantly in assessing aboveground biomass (Sandra, 2002). The tree height and DBH were recorded for 943 trees from the 41 plots. All the measured tree parameters were documented in a datasheet that was prepared before going to the field and later the data were transferred into the excel sheet for analysis. The captured photograph during the collection of biometric data is shown in **Figure** 6.

Figure 6: Biometric data collection

2.4.1.1.   Calculation of Biometric Data 2017

The biometric data was collected as ground truth to be used as an accuracy assessment. To assess the accuracy of UAV-derived AGB for the year 2017, it was also needed biometric data for the year 2017. But the biometric data was not available for the year 2017. Few researchers and students of Mulawarman university collect data every year for their research. They used the tag in the tree mentioning the tree recorded parameters. During the collection of biometric data of 2018, the DBH data available for 134 trees from the tagged was collected. Based on the difference in size of DBH between 2017 and 2018, the annual increment of DBH was calculated. The annual growth of DBH was deducted from the size of DBH 2018 and calculated the DBH for the year 2017. The height of the tree was calculated based on the mean annual growth of trees in the tropical forest. The study conducted in Lambir, Sarawak, Malaysia revealed that the 11 species of Macaranga has the lowest average growth rate of 0.18 m while the highest growth rate is 1.80 m (Davies & Apr, 2007). Another study conducted by Affendy et al. (2009) in secondary forest in a tropical area revealed that the highest height increment is 1.38m y^{-1} while the lowest height increment is 0.77 my^{-1}. In the study area, different tree species were found, and there was no generic annual increment of height was not possible to apply. Different tree size has a different growth rate. Based on different literature regarding increment of tree height in the tropical area, the tree was classified by the size of DBH and the tree height was calculated for the year 2017. The calculated DBH and height of the tree was also modeled height and DBH which was used to assess the field-based modeled AGB 2017.

2.4.2.   UAV Flight Planning

In this study, the UAV imagery was collected from the Kebun Raya UNMUL Samarinda (KRUS) education forest. The flight areas were selected based on the availability of enough open space to set the ground control points (GCPs) as well as landing and taking off UAV. The images were collected using Phantom-4 DJI UAV/ Drones. The mission planning was done setting flight parameters using Pix4D capture app. The spatial quality of the images acquired from the UAV platform depends on flight height and front and side

overlap. There is a significant relationship between flight height, overlap, weather conditions and the quality of the point clouds (Dandois et al., 2015). **Table** 3 shows the image acquisition parameters that were set-up to obtain the high-quality photogrammetric output.

Table 3: UAV flight planning

Parameter	Value
Speed	Moderate
Angle	90^0 (Nadir)
Front Overlap	75%
Side Overlap	65%
Flight Height	160 m -180 m

2.4.3. Ground Control Point

The UAV flight areas were selected in such a way that enough open spaces were available to place the ground control points. The ground control points were used for georeferencing. The number and distribution of GCPs influence image orientation. So, the GCPs were evenly distributed using black and white spray paint in the study area. The minimum number of GCPs would be 3 and the larger the number of GCPS the better the accuracy (Agüera et al., 2017). The total 12 ground control point (GCP) were put in the study area. The coordinates of the GCPs were recorded using a differential global positioning system (DGPS). The distribution of GCP is shown in **Figure 7.**
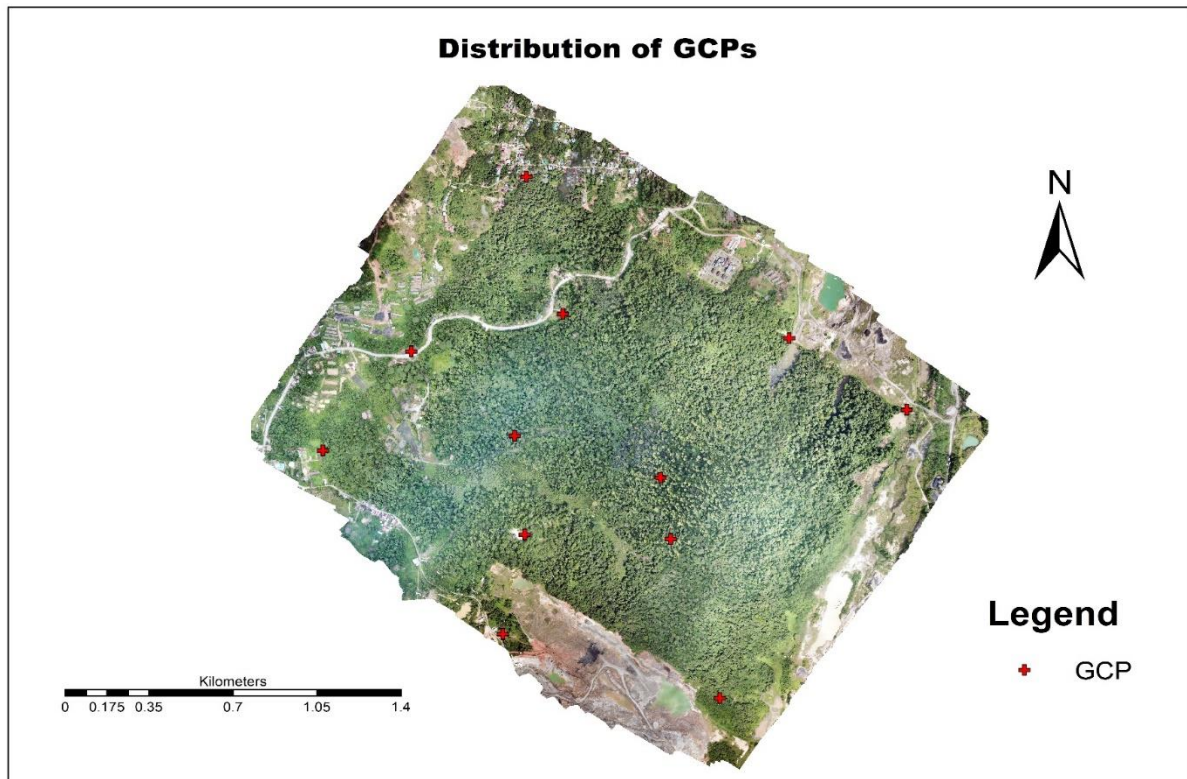
Figure 7: Distribution of ground control points (GCPs)

2.4.4. UAV Image Acquisition

Based on the defined parameters (flight height, overlap, speed) during flight planning, UAV captured digital images. All the images were stored in a memory card of UAV, and the quality of images was assessed after extracting the images from the memory card.

2.5.   Data Processing

The biometric and UAV data were processed after returning from the field using different types of software. This section illustrates the procedures and methods of processing biometric data as well as UAV data.

2.5.1.   Biometric Data

The data collected from the field was entered the Microsoft Excel Sheet for the analysis (see **Appendix 4**). The collected field data such as plot number, tree number, coordinate of the center of the plot, coordinate of every single tree, tree height, DBH, plot radius was given entry in the Excel. The biometric information of 943 trees from 41 plots was collected and recorded. The photograph of one plot and trees with a label within the plots are shown in Figure 8.

Figure 8: Plot with trees and tree tag

2.5.2.   UAV Image Processing

The photogrammetric software Pix4D was used to generate 3-D dense point cloud, DSM, DTM and orthophoto from UAV-derived images. This software used SfM and stereo-matching algorithms for 3-D reconstructions. Structure for motion (SfM) represents the process to obtain a three-dimensional structure of a scene of an object as well as the camera motion from a series of two-dimensional digital images. SfM used a sequence of overlapping images which has a minimum number of common matching points to produce a sparse 3D model of the scene and camera parameters (Westoby et al., 2012). In the initial processing, the Pix4D software executed the computation of key points, image matching, and camera calibration. The key points are the common points between the two images that are matched. In the figure, the light green images are already matched and calibrated, and the software is being tried to calibrate and match the dark green images. The blue points indicated the location of the GCP. After loading the images in the Pix4D software, the processing options were set up; then the GCPs were loaded for the georeferencing. In the first stage, the software computed the key points of different images of the same scene, and then image matching was performed based on key points. In the second stage, the software generated the sparse point clouds along with camera calibration. The high-quality point cloud was generated based on the estimated camera positions where the software computed depth information also. The point cloud was used to develop a digital surface model (DSM), digital terrain model (DTM), and orthophoto. The canopy height model (CHM) was extracted by subtracting DTM from DSM. The process of producing

DSM, DTM, orthomosaic and CHM were described in the following two sub-sections. The processing of UAV images in Pix4D software is shown in **Figure 9.**
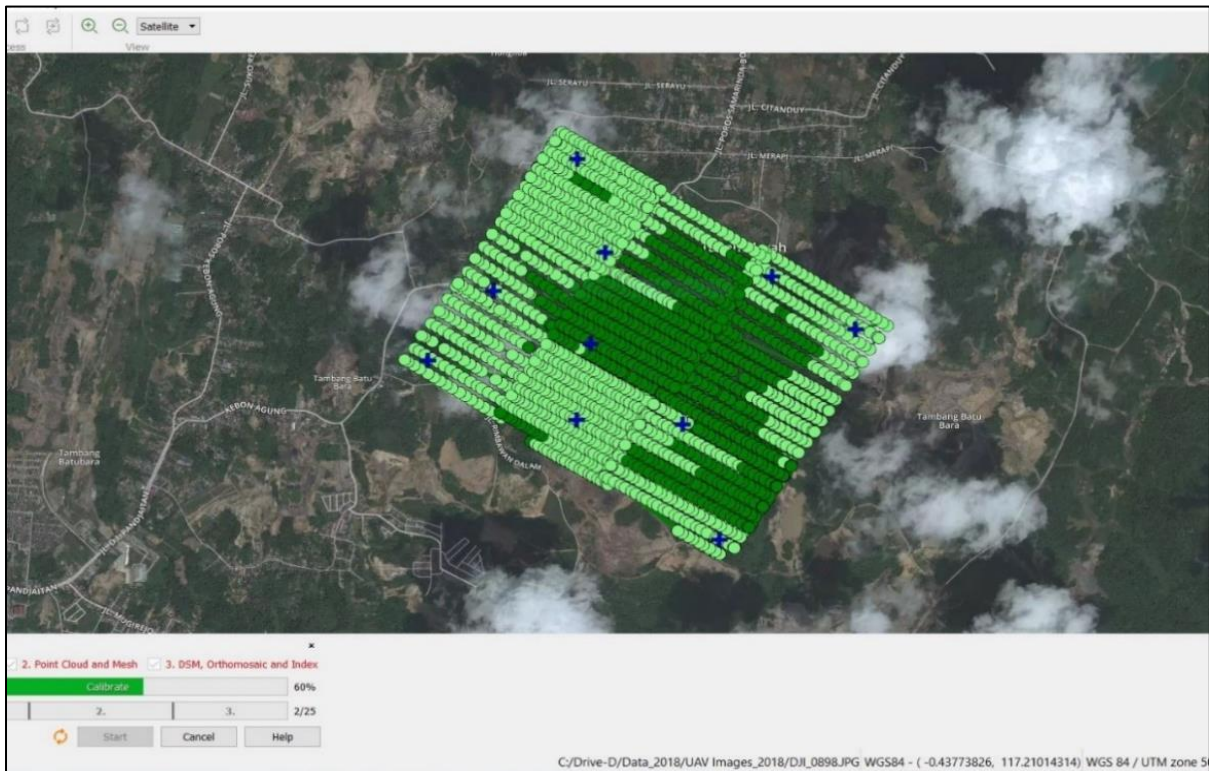
Figure 9: Image processing in Pix4D software

2.5.3. **DSM, DTM, and Orthophoto Generation**

The digital surface model (DSM) is a representation of the terrain relief that includes the topography and all natural (trees etc.) and man-made (buildings, bridges, etc.) objects. On the other hand, the digital terrain model (DTM) is a representation of the terrain relief in a digital form without any objects on the earth surface (Nex, 2018). A canopy height model (CHM) is generated from the difference between DSM and DTM (Zarco et al., 2014). Digital terrain model, digital surface model, and orthomosaic were generated automatically after producing dense point clouds using the Pix4D software. The software generated the DTM based on ground pixels only using an algorithm. A DSM represents the surface model as a regular grid that contains the height values. A DSM can be generated from the dense point cloud, sparse point cloud or a mesh. The quality of DSM is also dependent on the quality of the point cloud. The DSM was generated by interpolation using a delaunay triangulation method. Delaunay triangulation is a geometric structure that generates meshes and maximizes the minimum angles (Cheng & Shewchuk, 2012). This method is recommended because of considering the suitability in the forestry applications. Finally, the orthomosaic was produced from the mosaicking of the geometrically corrected images. The schematic representation of DSM and DTM is shown in **Figure** 10.
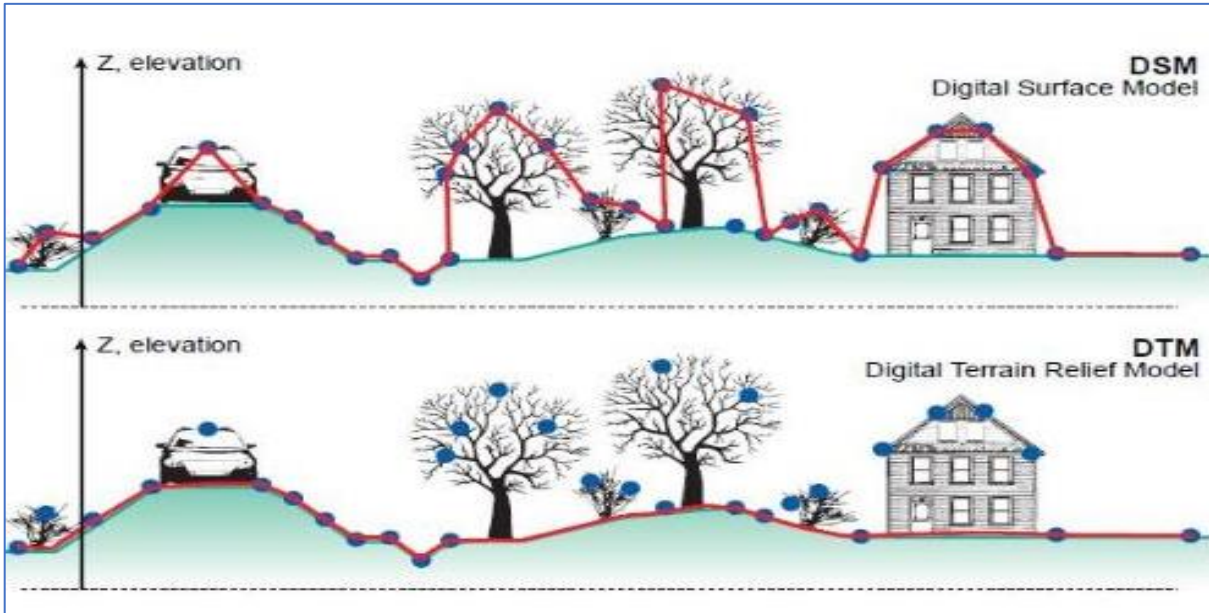
Figure 10: Difference between DSM and DTM
Source: http://www.charim.net/datamanagement/32

2.5.4. Generation of Canopy Height Model

The canopy height model (CHM) is required to extract the tree height. The CHM was generated by subtracting the DTM from the DSM using the raster calculator tool in ArcMap software. The CHM represented the tree height values as continuous surface while DTM and DSM were used as input data. The individual tree height was extracted from the CHM by removing the negative values and values more than tree height was collected from the field (Magar, 2014). The tree height and DBH as input parameters are required to estimate aboveground biomass using allometric equations (Chave et al., 2014). The shapefile of the segmented tree, the recorded coordinates from the field, the center of the plot and circular plot were overlaid on the CHMs, and the highest pixel value of the CHM within the segmented individual tree crown was extracted as the tree height. The schematic representation of CHM is shown in **Figure** 11.
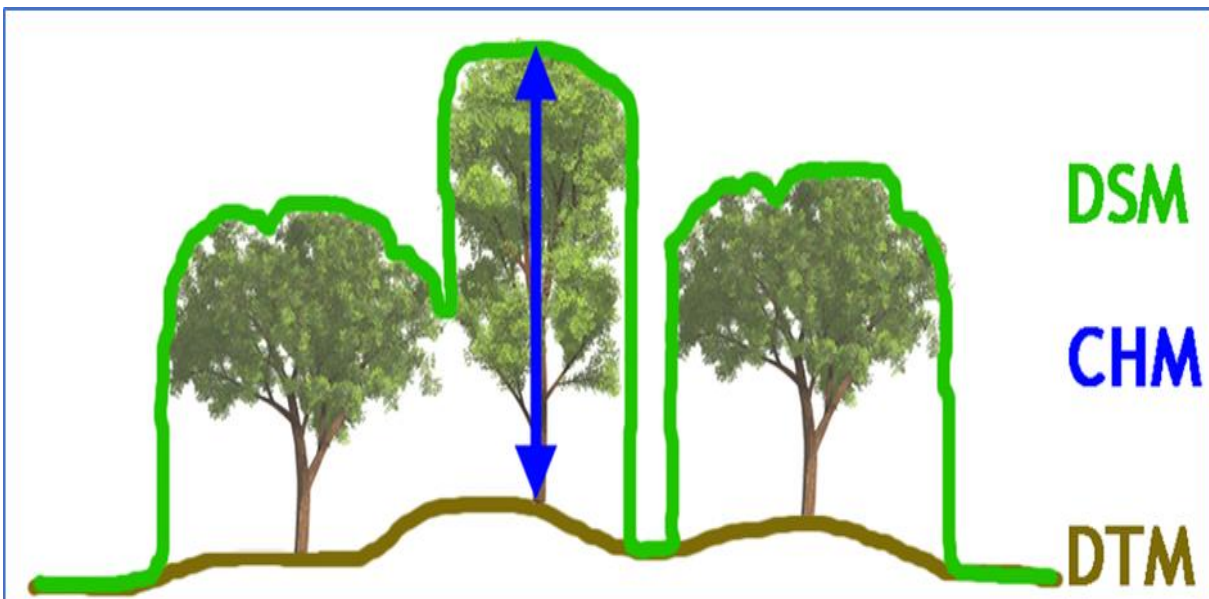
Figure 11: Canopy height model

Source: Perko et al. (2011)

2.5.5. Validation of tree height from UAV-CHM

The tree height extracted from the UAV-CHM was compared with the tree height collected from the field using a scatter plot, F-test, and t-test. The performance was presented in terms of the model fit coefficient (R^2), and root means square error (RMSE). Furthermore, Pearson's correlation test was used to assess how the tree height is related to each other.

2.6. Data Analysis

Data analysis was accomplished using a suitable statistical analysis to achieve the objectives and test the hypothesis. The important statistical methods such as descriptive statistics, regression analysis, correlation, RMSE, the percentage of RMSE, F-test and t-test for two samples, and ANOVA test were applied in this study. The RMSE and percentage of RMSE were calculated using the equations developed by Sherali et al. (2003) to test the closeness of two parameters of the tree.

Equation 1: RMSE Computation

$$\text{RMSE} = \sqrt{\sum_{i=1}^{n}\left(Y_i - \hat{Y}\right)^2 / n} \dots\dots\dots\dots\dots\dots\dots\dots\dots\dots\dots\dots\dots\dots\dots\dots\dots\dots\dots\dots\dots \text{ (1)}$$

Equation 2: Percentage of RMSE Computation

$$\% \text{ RMSE} = \text{RMSE} * n* 100/ \Sigma \text{ Yi} \dots\dots\dots\dots\dots\dots\dots\dots\dots\dots\dots\dots\dots\dots\dots\dots\dots\dots\dots\dots\dots\dots \text{ (2)}$$

Where,
RMSE is the root mean squared error
% RMSE is the percentage of root mean squared error
Yi is the original value of the dependent variable
$\hat{Y}$ is the predicted value of the dependent variable and
 n is the number of observations.

2.6.1. Relationship between DBH and CPA

For model development the CPA obtained from manual digitization was used as input to predict DBH. In this study, the linear, power, quadratic and logarithmic model was tested to choose the suitable model for establishing the relationship between CPA and DBH. To perform this, the area of a delineated shapefile was calculated using ArcMap software. The DBH of matched trees was regressed with the corresponding CPA using quadratic relationship. The scatter plot was plotted while the trend line was fitted. The RMSE and %RMSE were calculated to observe and evaluate the relationship between CPA and DBH.

2.6.2. Estimation of Aboveground Biomass (AGB) for 2017 and 2018

The allometric equation is the commonly used method to estimate forest biomass in a non-destructive way. Various researchers have developed allometric equation based on a destructive method to estimate biomass and carbon in the different forest ecosystem and different tree species (Curtis, 2008). The region or site-specific allometric equations must be considered to assess the biomass accurately as the equations consider the site effects (Basuki et al., 2009). Application of regionally or locally developed allometric equations are not recommended due to high species-diversity in tropical forest (Gibbs et al., 2007). The generic allometric equations developed by Chave et al. (2014) was considered a suitable equation to estimate above ground biomass in a tropical forest. The allometric equation developed by Chave et al. (2014) is shown in ***Equation 3***.

Equation 3: Allometric Equation for AGB Calculation

$$AGB_{est} = 0.0673 \times (\varrho D^2 H)^{0.976} \ldots\ldots\ldots\ldots\ldots\ldots\ldots\ldots\ldots\ldots\ldots. \text{ (3) (Source: Chave et al., 2014)}$$

Where AGB_{est} is the estimated above ground biomass in kilograms (kg),
D is the diameter at breast height (DBH) in centimeter (cm),
H is the tree height in meter (m),
and ϱ is wood density in gram per cubic centimeters (gcm^{-3}),
0.0673 and 0.976 are constant.

The aboveground biomass (AGB) was estimated for the year 2017 and 2018 using this allometric equation. The AGB was calculated and assessed for each plot.

2.6.3. Estimation of Aboveground Carbon for 2017 and 2018

The carbon stock was calculated from the estimated AGB. 50% of the estimated biomass is considered as carbon (Houghton & Hackler, 2000; Burrows et al., 2002; & Drake et al., 2002). The carbon stock was calculated using **Equation 4**.
.

Equation 4: AGC Calculation from AGB

$$AGC = AGB \times CF \ldots\ldots\ldots\ldots\ldots\ldots\ldots\ldots\ldots\ldots\ldots\ldots\ldots\ldots\ldots\ldots\ldots\ldots\ldots\ldots\ldots\ldots\ldots\ldots \text{ (4)}$$
Where,
AGC is aboveground carbon stock (Mg),
CF is the carbon fraction (0.5)
The total amount of sequestered carbon was assessed from the difference between the estimated amount of carbon for 2017 and 2018.

2.6.4. Comparison of UAV-based AGB and Field-based AGB

The height derived from UAV-CHM and predicted DBH based on UAV CPA were used as an input parameter to estimate the UAV-based AGB. The field-derived tree height and DBH were used as input parameter for estimation of field-based AGB. The UAV-based AGB and Field-based AGB were compared using a scatter plot and RMSE. Furthermore, the F-test and t-test were performed to test if there is a significant difference between UAV-based AGB and Field-based AGB. Lastly, the mean difference between the UAV-based AGB and Field-based AGB was assessed and evaluated.

2.7. Error Sources

Almost all related researches usually concentrate on accuracy assessment in each step they take in assessing biomass and carbon stock and rarely consider the error propagation in final results carefully (Chave et al., 2005). Error propagation assessment needs to be evaluated perfectly and properly to make correct inferences. Measurement of error is expressed in terms of accuracy. It is essential to identify and assess the influence of various sources of error on biomass and carbon estimation (Lo, 2005).

2.7.1. Main Sources of Error in AGB/ Carbon Estimation

The error and uncertainty originated from the multiple sources can influence the final biomass estimation such as tree parameter measurement errors, errors in the allometric equation, data processing error, etc. Chave et al. (2004) identified four types of error that could lead to statistical error in assessing biomass and carbon: (i) tree measurement error; (ii) selection of allometric equations; (iii) choosing the size of the sampling plot; (iv) landscape-scale representation. Nguyet (2012) stated five types of error namely: (i) field-based carbon error; (ii) height extraction error; (iii) CPA extraction error; (iv) tree detection error; (v)

classification error. Samalca (2007) identified two sources of uncertainty in his research like: (i) error in selecting sampling plots (ii) selection of sampling trees. Holdaway et al. (2014) developed quantitative statistical methods for propagating uncertainty in carbon estimation. They described the measurement error, model uncertainty, and sampling uncertainty. Moreover, when assessing the sequestration of carbon between two consecutive years, the error in measurement and assessed carbon sequestration might be greater than the actual sequestration of carbon. There were very limited researches conducted on the influence of height error and CPA delineation error on biomass and carbon estimation. In this research, DBH and height were the input parameters for biomass assessment. For this reason, the effect of height and CPA delineation error on AGB estimation was analyzed and discussed in this study.

2.7.1.1. Effects of Error of Height on AGB Estimation

The error of UAV-derived height is affected by the number of sources such as UAV quality data (point density, seasonality), CHM generation process (interpolation algorithm), co-registration error, flight height, number and distribution of GCPs. RMSE and percentage of RMSE of the estimated height were calculated from the difference between height measurement from the field and height extracted from CHM. The height derived from UAV-CHM was used to evaluate the variation of biomass due to the changes in height. How much AGB is underestimated or overestimated was assessed by using height from the percentage of RMSE calculated from UAV CHM height and field height for 2018. The single factor/ one-way ANOVA test was performed to evaluate the significance of the difference between UAV-based AGB without inflated/ deflated height and the UAV-based AGB with inflated and deflated height for 2018. The influence of the error of height on AGB estimation for the year 2017 was not analyzed because the biometric height for the year 2017 was a modeled height calculated based on annual increment. It was assumed that the effect of the error of height on AGB estimation would be the same. The percentage of error of estimated biomass was assessed and analyzed based on calculating the percentage of the mean difference between original biomass without inflation/deflation of height and the height inflated/deflated mean biomass values. The formula for calculation of the average biomass is shown in **Equations-5-9**.

Equation 5: Mean AGB (without height inflation and deflation) calculation

Mean AGB (without height inflation and deflation) = {(ΣAGB of 41 plots)/Number of Plots} ………..………... (5)

Equation 6: Mean AGB (with height inflation) calculation

Mean AGB (with height inflation) = {(ΣAGB with height inflation of 41 plots)/Number of Plots} ………………(6)

Equation 7: Mean AGB (with height deflation) calculation

Mean AGB (with height deflation) = {(ΣAGB with height deflation of 41 plots)/Number of Plots} ..……...…… (7)

Equation 8: Biomass difference calculation

Biomass Difference = (Mean AGB with inflated height - Mean AGB with deflated height)/2.………...…………. (8)

Equation 9: Percentage of the biomass difference calculation

Percentage of Biomass Difference= {Biomass Difference/Mean AGB (without height inflation and deflation)}…….
×100…………………………………………………………………...……………………… (9)

2.7.1.2. Effects of CPA Delineation Error on AGB Estimation

The range of variation of biomass due to CPA delineation error was quantified and assessed by 1%, 5%, and 10% inflated and deflated CPA delineation error. In this study, the CPA was delineated manually for both years. It was assumed that the manually delineated CPA is more accurate and precise compared to the automatic segmented CPA. However, due to the quality of orthomosaic and man-made error in visual interpretation, the manually delineated CPA might have a certain level of inaccuracy. In this study, the manually delineated CPA was inflated and deflated by 1%, 5%, and 10% and accordingly plot-based AGB was calculated to evaluate the range of variation of biomass. After plot-based estimation of AGB with inflated and deflated CPA, the range of variation of biomass was calculated based on **Equations-10-14.**

Equation 10: Mean AGB without CPA inflation and deflation calculation
Mean AGB (without CPA inflation and deflation) = {(ΣAGB of 41 plots)/Number of Plots} ………………... (10)

Equation 11: Mean AGB with inflated CPA calculation
Mean AGB (with CPA inflation) = {(ΣAGB with CPA inflation of 41 plots)/Number of Plots} ……..…………(11)

Equation 12: Mean AGB with deflated CPA calculation
Mean AGB (with CPA deflation) = {(ΣAGB with CPA deflation of 41 plots)/Number of Plot} ..……...……… (12)

Equation 13: Biomass difference calculation
Biomass Difference = (Mean AGB with inflated CPA - Mean AGB with deflated CPA)/2.………….……….. (13)

Equation 14: Percentage of the biomass difference calculation
Percentage of Biomass Difference= {Biomass Difference/Mean AGB (without CPA inflation and deflation)}……... ×100……………………………………………………………………………………………………. (14)

3.   RESULTS

3.1.   Biometric Data 2018

Diameter at breast height (DBH) and height were recorded for 943 trees collected from 41 plots in the study area. The analyzed results of the biometric data for the year 2018 in the form of descriptive statistics were presented in **Table** 4**.**

Table 4: Descriptive statistics of field-measured tree DBH and height

Descriptive Statistics for DBH and Height		
Nature of Statistics	**DBH (cm)**	**Height (m)**
Mean	28.11	15.51
Standard Error	0.54	0.16
Median	23.6	15.4
Mode	10	11.5
Standard Deviation	16.45	4.86
Sample Variance	270.51	23.62
Kurtosis	2.07	-0.55
Skewness	1.38	0.19
Range	101.3	25.2
Minimum	10	6.8
Maximum	111.3	30.2
Sum	26506.9	14624.68
Count	943	943

From the results as mentioned above, the average DBH was 28.11 cm while the minimum and maximum DBH were 10 cm and 111.3 cm respectively. The standard deviation of height was 16.45 cm. On the other hand, the average height was 15.51m, whereas the minimum and maximum height were 6.8 m and 30.2m respectively. The standard deviation of height was 4.86m. The graphical analysis was conducted for the distribution of field-measured DBH and height in **Figure** 12 and **Figure** 13.
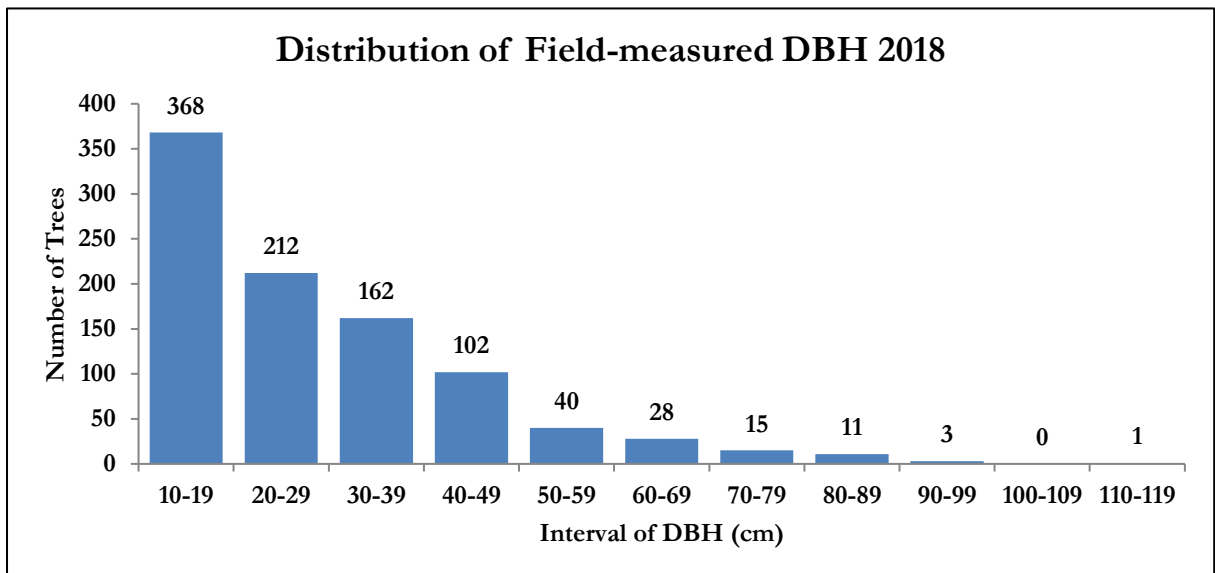
Figure 12: Distribution of field-measured DBH 2018

It can be mentioned from the histogram that the positive skewness is observed for the field-measured DBH. Considering the contribution to the total biomass, only trees with DBH of ≥10 cm was recorded in the field. Within the range of DBH between 10 and 19 cm, a total of 368 trees was found out of 943 trees. The number of trees decreased with an increase in the size of DBH.
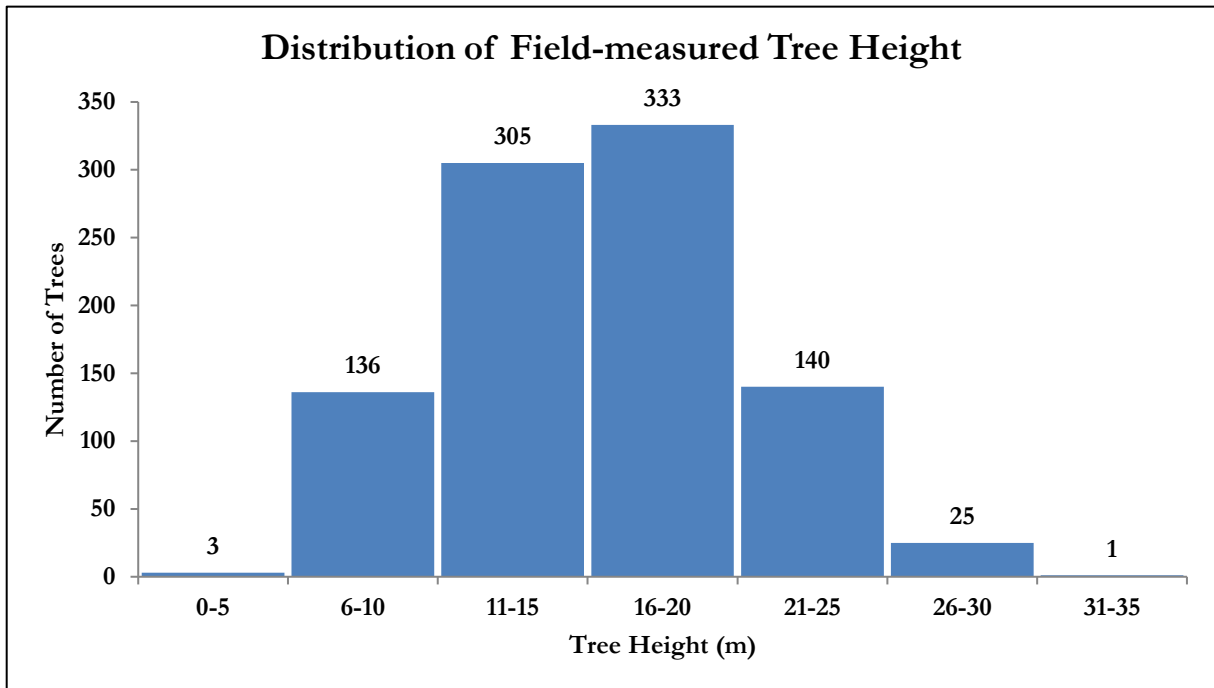
Figure 13: Distribution of field-measured height 2018

It can be recapitulated from the histogram that the maximum number of trees are shown in the height range between 16m and 20m while the lowest number of trees was found in the height range between 31m and 35m. Only three trees were also found within the height range 0-5 m.

3.2. Biometric Data 2017

The biometric data (DBH and Height) for the year 2017 was calculated from the biometric data 2018 based on an annual increment of DBH and height. Diameter at breast height (DBH) and height of 943 of trees were calculated based on a yearly increase of DBH and height. The analyzed results of the calculated biometric data for the year 2017 in the form of descriptive statistics were presented in **Table** 5.

Table 5: Descriptive Statistics for DBH and Height

Descriptive Statistics for DBH and Height		
Nature of Statistics	**DBH (cm)**	**Height (m)**
Mean	27.11	14.41
Standard Error	0.55	0.17
Median	22.71	14.22
Mode	8.63	8.92
Standard Deviation	16.75	5.08
Sample Variance	280.49	25.82
Kurtosis	1.96	-0.56
Skewness	1.35	0.21
Range	102.32	26.35

Nature of Statistics	DBH (cm)	Height (m)
Minimum	8.63	6.3
Maximum	110.95	29.97
Sum	25565.65	13588.22
Count	943	943
Confidence Level (95.0%)	1.07	0.32

From the results mentioned above, the average DBH was 27.11 cm while the minimum and maximum DBH were 8.63 cm and 110.95 cm respectively. The standard deviation of height was 16.75 cm. On the other hand, the average height was 14.41m, whereas the minimum and maximum heights were 6.3 m and 29.97 m respectively. The standard deviation of height was 5.08m.

3.3. Generation of DSM, DTM, Orthomosaic and CHM 2017

The DSM, DTM and orthomosaic image were generated using Pix4D software through the structure from motion (SfM) and photogrammetric image matching techniques. Total 8 ground control points (GCPs) were used to provide spatial referencing for the 3D model and final output produced from UAV images. Total of 949 UAV images was used to produce DSM, DTM and orthomosaic. A total of 5.253 km² area was covered by the 9 flight blocks while the average ground sampling distance was 9.99 cm. 97% of images were calibrated to produce dense point clouds. The mean RMS error was 0.046 m. The average point density was 31.85 m³. The generated DSM, DTM and orthomosaic are shown in **Figure** 14 and **Figure** 15.
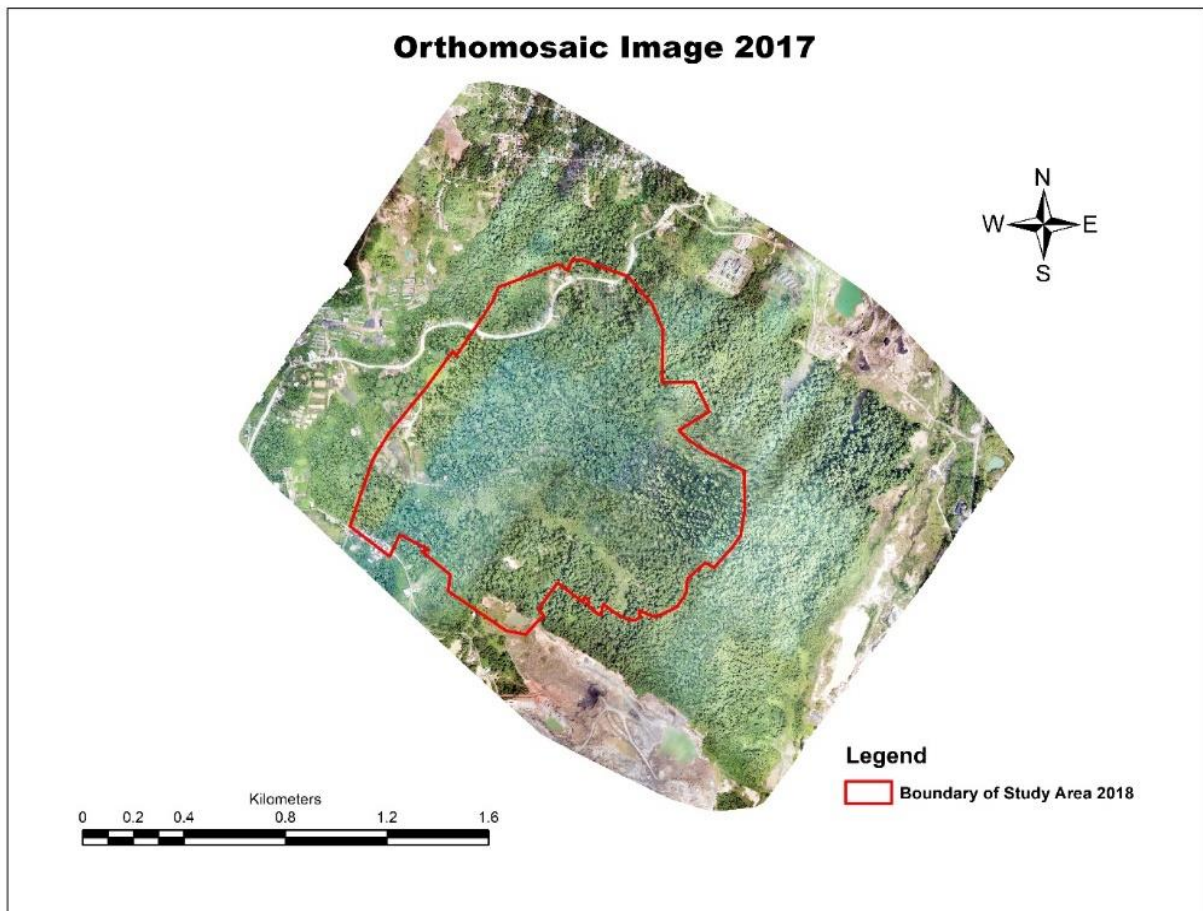
Figure 14: Generated orthomosaic 2017
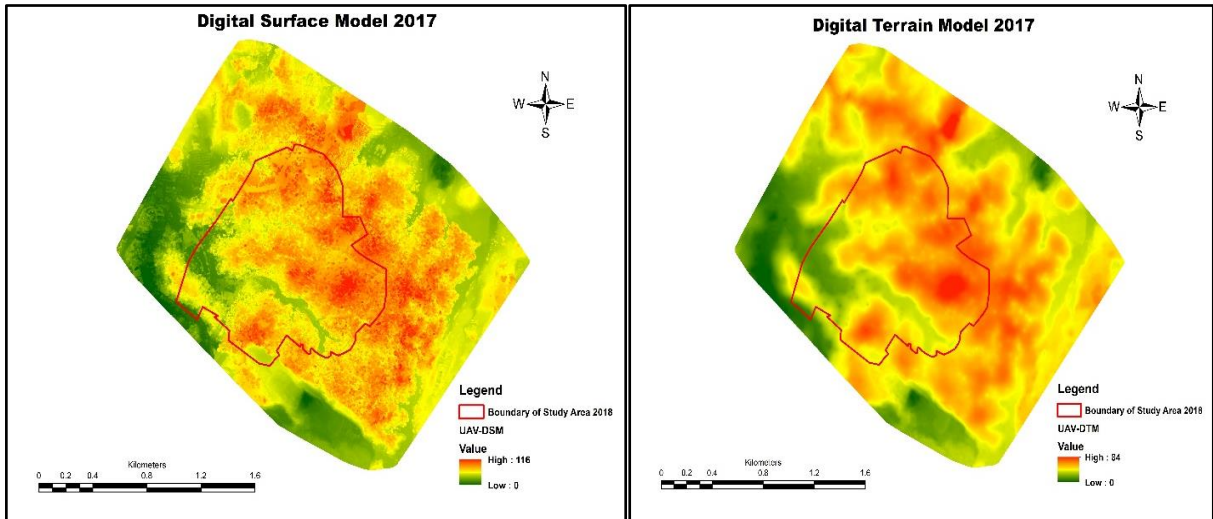
Figure 15: Generated DSM and DTM 2017

3.3.1. CHM Generation from 2017 Data

The CHM was generated by subtracting the DTM from the DSM. The pixel value of DTM was subtracted from the corresponding DSM by using the raster calculator of ArcMap 10.6.1 software to produce the UAV-CHM. The minimum value of CHM was 0 (zero) while the highest value was 55 (fifty-five). The produced CHM are shown in
Figure 16.
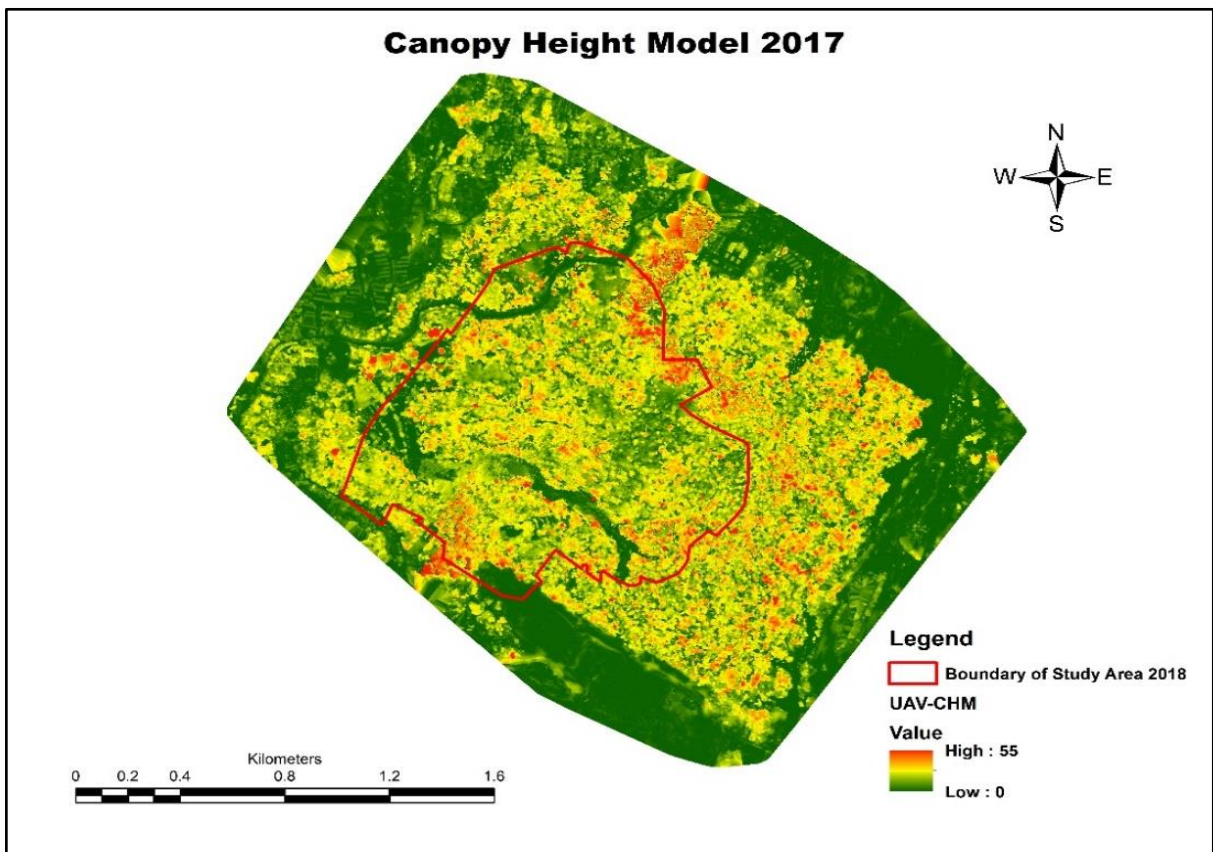
Figure 16: Generated CHM 2017

3.3.2. Extraction of Tree Height from CHM 2017

A total of 569 upper canopy trees were identified from the UAV images out of 943 trees which were located within the 41 plots in the study area. UAV can only observe the upper canopy and lower canopy trees were out of AGB estimation. Individual tree height was extracted from the generated CHM.

3.3.3. Comparison of Field-measured and UAV-derived Tree Height 2017

Descriptive statistics analysis was performed for UAV-derived height and field-measured height. The mean tree height from CHM was 17.52 m while the average height from the field-derived tree was 14.41 m. The standard deviation for UAV-derived height and field-measured height was 4.21 m and 4.01 m respectively. The minimum tree height was recorded 6.3 m in the field while the minimum tree height from the UAV-CHM was 6.70 m. On the other hand, the maximum tree height in the field was found 29.97 m whereas the maximum tree height extracted from UAV-CHM was 31.18 m. The height difference of two maximum height was only 1.21 m. The distribution of UAV-derived tree height from CHM and descriptive statistics are presented in **Figure** 17 and **Table** 6.
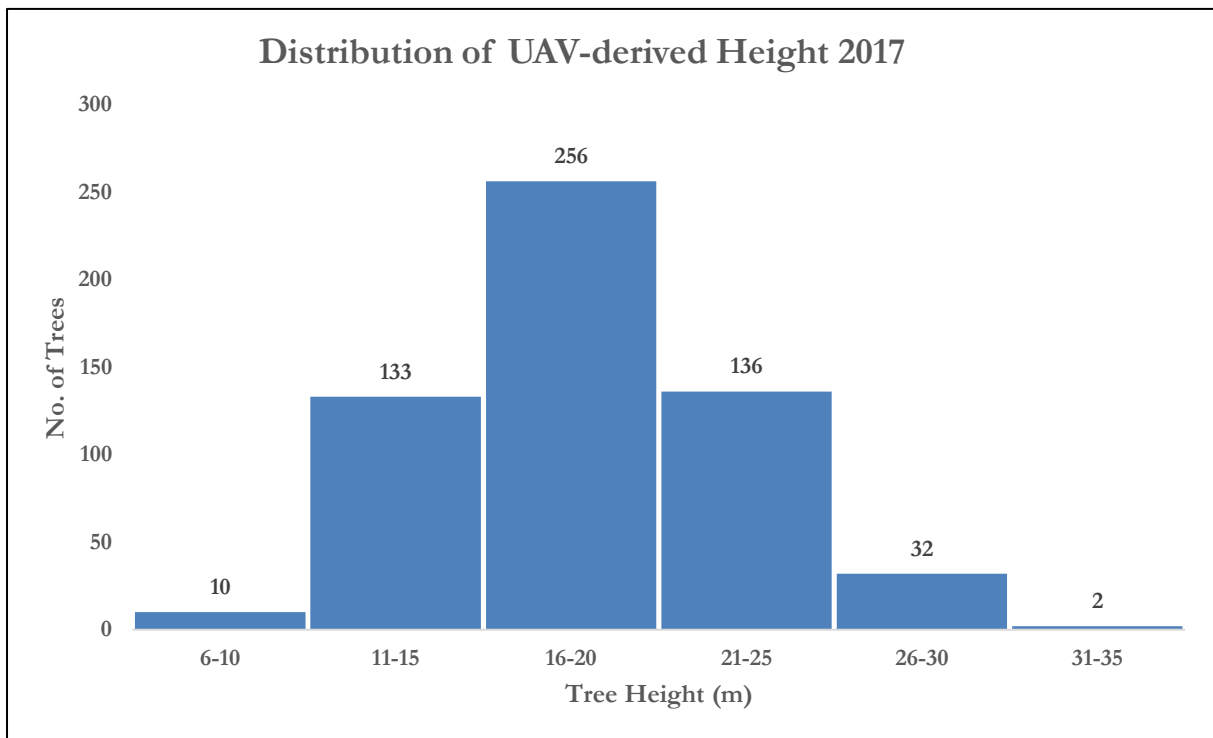
Figure 17: Distribution of UAV-derived height 2017

Table 6: Descriptive statistics of UAV-derived tree height

Descriptive Statistics of UAV-derived Tree Height 2017	
Nature of Statistics	**UAV-derived Tree Height (m)**
Mean	17.52
Standard Error	0.18
Median	17.48
Mode	14.82
Standard Deviation	4.21
Sample Variance	17.70
Kurtosis	-0.22

Nature of Statistics	UAV-derived Tree Height (m)
Skewness	0.20
Range	23.46
Minimum	6.70
Maximum	31.18
Sum	10148.35
Count	569
Confidence Level (95.0%)	0.35

3.3.4. Accuracy of UAV-derived Tree Height with Field-derived Tree Height 2017

A total of 569 identified trees were used to compare the UAV-derived height and field-measured height. The scatter plot demonstrated the relationship between UAV-derived height and field-measured height and showed a strong correlation of 0.92 and coefficient of determination (R^2) of 0.89. The root mean square error (RMSE) was ±1.57 m which is equivalent to 9.24 % of the measured tree height from the field. The scatter plot and regression statistics are shown in **Figure** 18 and **Table** 7.
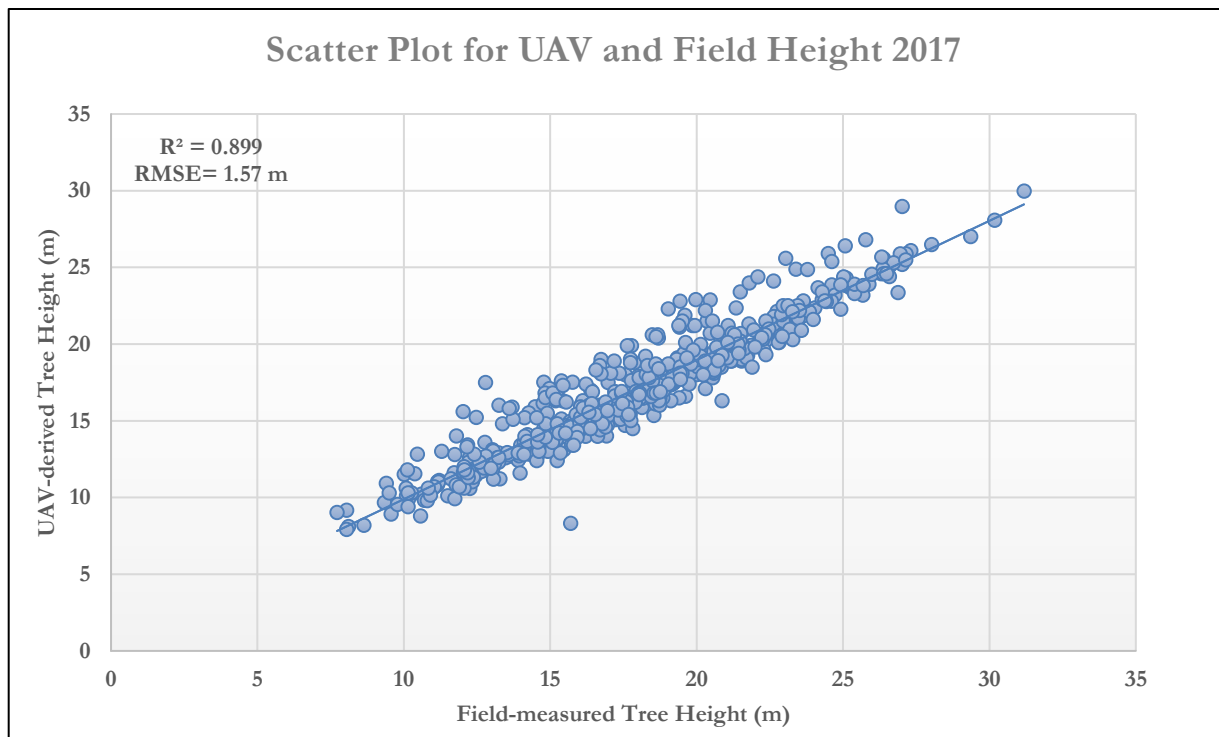
Figure 18: Scatter plot of field-measured and UAV-derived tree height

Table 7: Regression statistics for UAV-CHM estimated tree height and field-measured tree height

Regression Statistics	
Multiple R	0.95
R Square	0.90
Adjusted R Square	0.90
Standard Error (m)	1.33
RMSE (m)	1.57
Observations	569

3.4. Generation of DSM, DTM, Orthomosaic and CHM 2018

The Pix4D software was also used in 2018 to produce DSM, DTM and orthomosaic. Total 12 evenly distributed ground control points (GCPs) were used to provide spatial referencing. The total 2250 images were captured by UAV, and the selected better-quality images were processed separately to get better DSM, DTM, and orthomosaic. While processing all images together, the quality of the produced DSM, DTM and orthomosaic was not good. The captured images were processed in four cluster according to the flight plan. The four set of orthomosaic, DSM and DTM were produced to extract reasonable height from the CHM and better CPA from orthomosaic. The tree height and CPA were extracted from the four set of produced output. In one block which covers maximum plots, a total of 666 UAV images was used to produce DSM, DTM and orthomosaic. A total of 1.48 km² area was covered by that blocks while the average ground sampling distance was 4.92 cm. 87% of images were calibrated to produce dense point clouds. The mean RMS error was 0.006 m. The RMSE is quite good enough than the RMSE of 2017. The number of GCP was greater than the GCP of 2017, and the distribution of GCP was evenly in 2018 compared to the GCP of 2017. The average point density was 51.57 m³ which was almost double of the point density of 2017 because the altitude of the UAV flight for the year 2017 was 350-370m while in 2018 the flight height was only 160-180m. The maximum and minimum value of the DSM and DTM for 2018 was different compared with the DSM and DTM generated from 2017 UAV images due to the quality of the images. The tilted images were not calibrated and produced distorted area in the edge of the orthomosaic, DSM and DTM. The raster value of DSM, DTM, and CHM was high for the data 2018 compared with the raster value of DSM, DTM, and CHM of 2017. The high value caused for some distorted portion of the DSM and DTM. Despite the highest value for some portion, it gave the reasonable CHM value for each tree. The generated DSM, DTM and orthomosaic in one set are shown in **Figure** 19 and **Figure** 20.
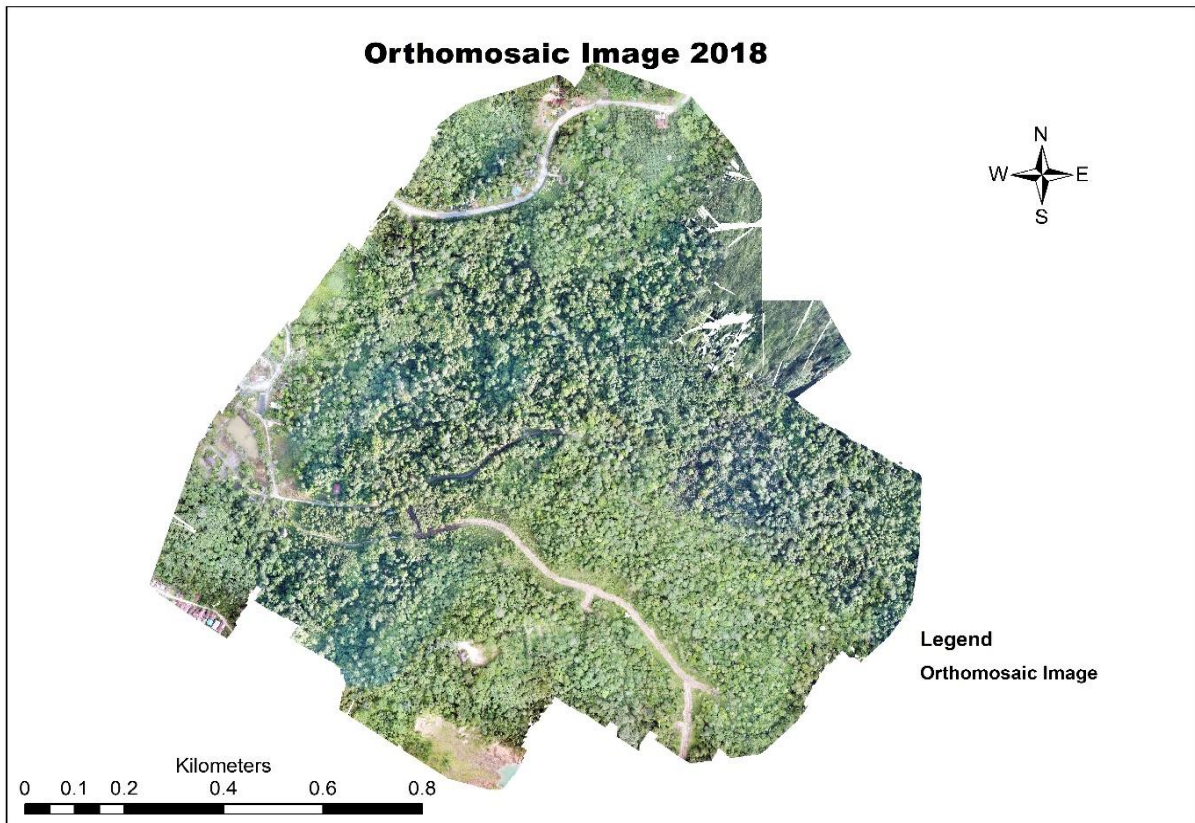
Figure 19: Generated orthomosaic 2018
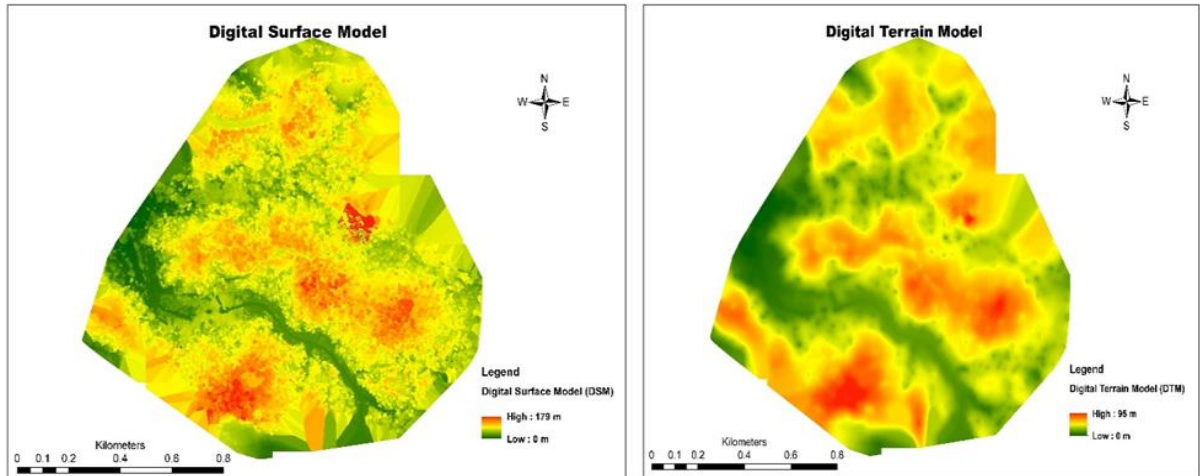
Figure 20: Generated DSM and DTM 2018

3.4.1. CHM Generation from 2018 Data

The CHM was also generated from the produced DSM and DTM of 2018. The minimum value of CHM was 0 (zero) while the highest value was 60 (sixty). The produced CHM are shown in **Figure** 21. The value of CHM is different from the value of CHM generated for 2017. The reason for variation for the growth of trees as well as the effect of point cloud density and the quality of images.
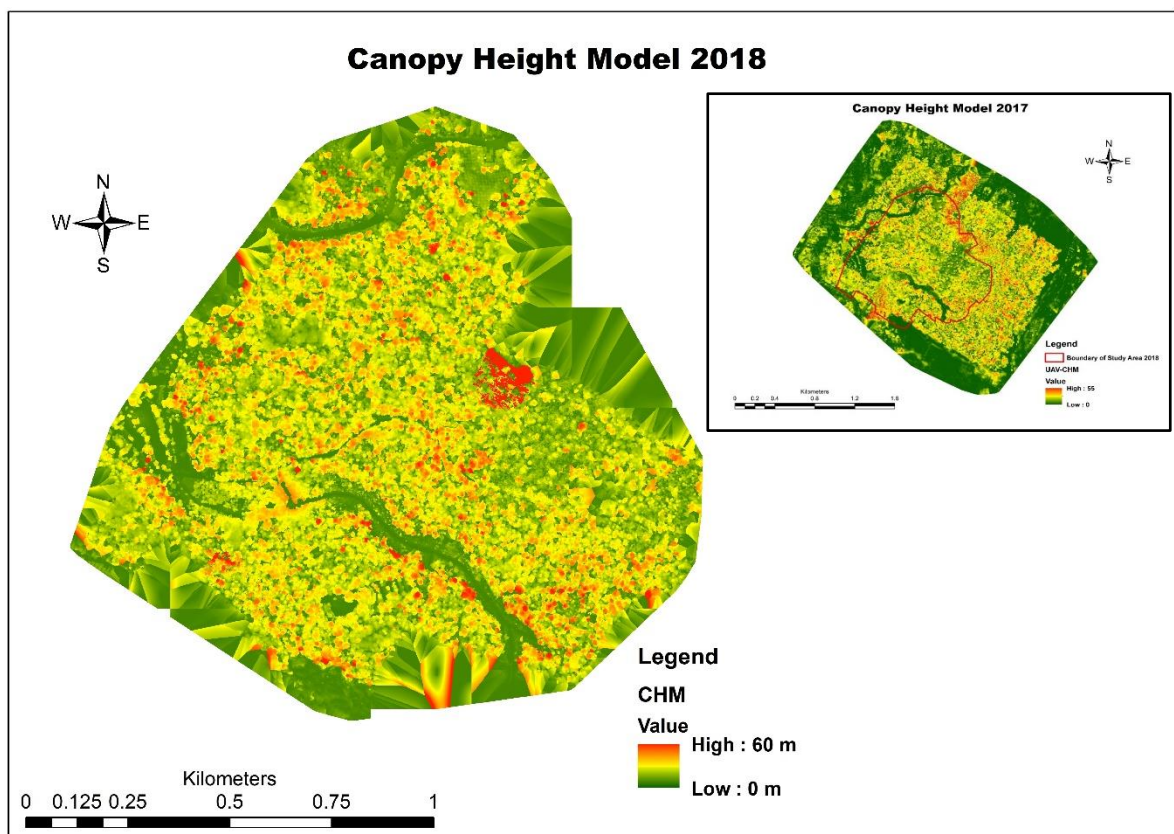
Figure 21: Generated CHM 2018

3.4.2. Extraction of Tree Height from CHM 2018

A total of 590 upper canopy trees were identified from the orthomosaic of 2018 while 569 trees were identified from the orthomosaic of 2017. The additional only 21 trees were identified in 2018 because these trees were not visible in 2017 due to their lower height. The difference of the number of trees between 2017 and 2018 was only 21 because of the only one-year duration.

3.4.3. Comparison between UAV-derived Tree Height and Field-based Tree Height 2018

The average tree height from CHM was 17.75 m while the mean field-measured tree height was found 15.51 m. The difference between the two average height was calculated at 2.24 m while the field-measured tree height was lower than UAV-derived tree height. The minimum and maximum extracted tree height from CHM were 7.10 m and 31.50m. The height difference of two maximum height was only 1.30 m. The distribution of UAV-derived tree height for the year 2018 was shown by descriptive statistics and histogram (see **Figure** 22 and **Table** 8).
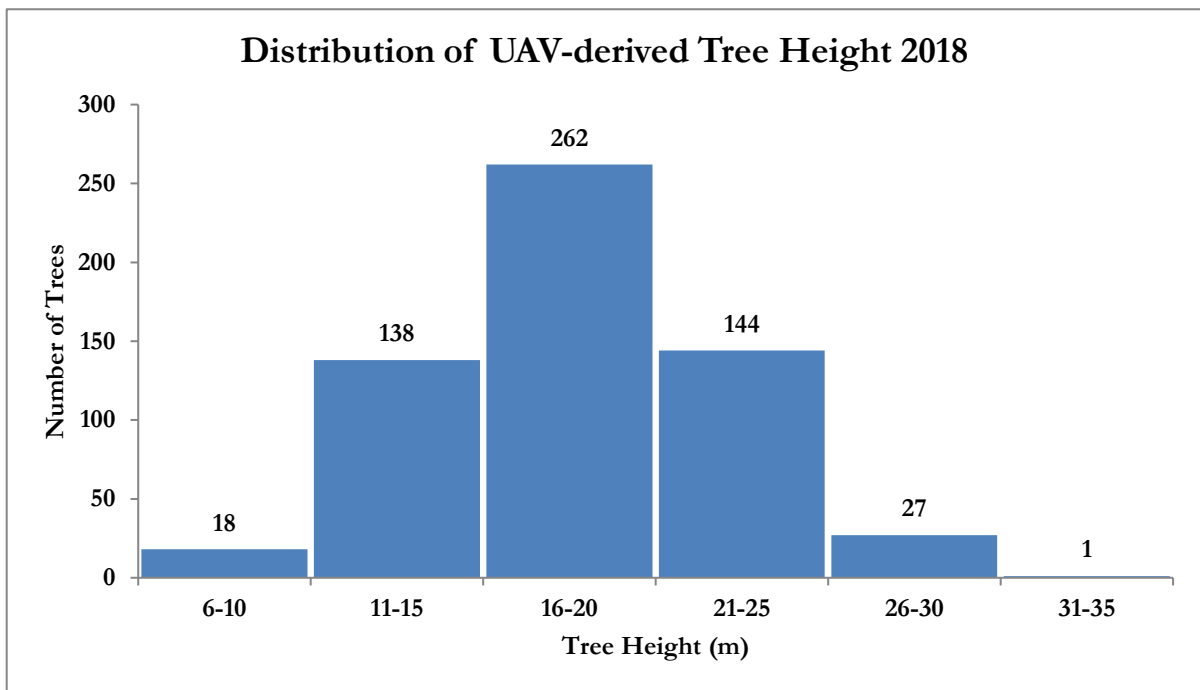
Figure 22: Distribution of UAV-derived tree height 2018

Table 8: Descriptive statistics of UAV Height 2018

Descriptive Statistics of UAV Height 2018	
Nature of Statistics	**UAV-derived Tree Height (m)**
Mean	17.75
Standard Error	0.18
Median	17.65
Mode	18.5
Standard Deviation	4.29
Sample Variance	18.36
Kurtosis	-0.33
Skewness	0.08
Range	24.4

Nature of Statistics	UAV-derived Tree Height (m)
Minimum	7.1
Maximum	31.5
Sum	10473.47
Count	590
Confidence Level (95.0%)	0.35

3.4.4. Accuracy of UAV-derived Tree Height with Field-derived Tree Height 2018

A total of 590 identified trees were used for descriptive statistics as well as making a comparison with field-measured tree height. The same number of trees was considered to compare the UAV-derived tree height and field-measured tree height. The scatter plot demonstrated the relationship between UAV-derived height and field-measured height and showed a strong correlation of 0.93 and coefficient of determination (R^2) of 0.86. The root mean square error (RMSE) was ±1.58 m which is equivalent to 8.94 % of the measured tree height from the field.
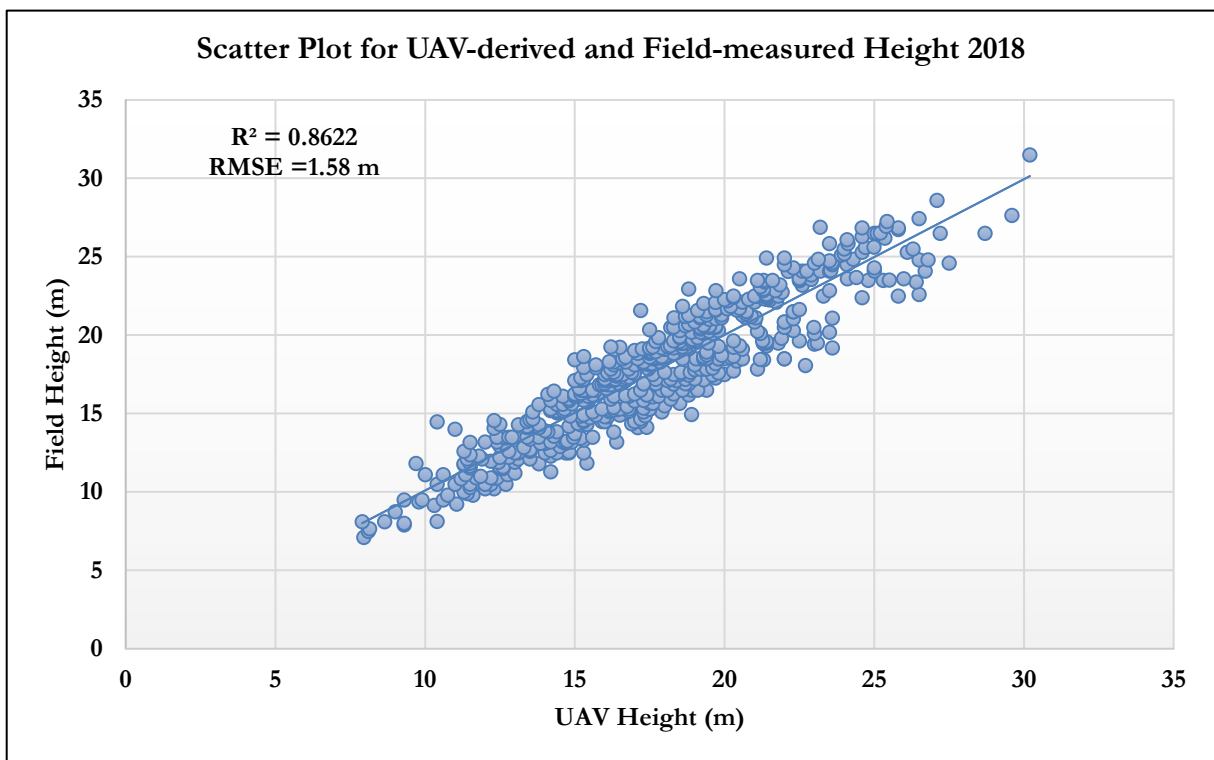
Figure 23: Scatter plot of UAV-derived and field-measured tree height 2018

Table 9: Regression statistics for UAV and field height in 2018

Regression Statistics	
Multiple R	0.93
R Square	0.86
Adjusted R Square	0.86
Standard Error (m)	1.59
Observations	590

Moreover, F-test was performed to determine if the estimated tree height from the UAV-CHM had an equal variance or unequal variance. The results are shown in the **Table** 10.

Table 10: F-test Two-sample for Variances between UAV-CHM tree height and field-measured tree height

Statistics	UAV-CHM tree height	Field-measured tree height
Mean	17.75	17.72
Variance	18.36	16.07
Observations	590	590
df	589	589
F	1.14	
P(F<=f) one-tail	0.06	
F Critical one-tail	1.15	
Decision: F-Statistics < F-Critical (P >0.05): Equal Variance		

From the results of the F-test, it can be recapitulated that there was an equal variance between estimated tree height from UAV-CHM and field-derived tree height, because the P-value (0.06) was greater than 0.05 at $\alpha = 0.05$ and F-Statistics < F-Critical.

Based on the results of the F-test, the t-test assuming equal variance was conducted to determine if there was a statistically significant difference or not between estimated tree height from UAV-CHM and field-derived tree height. The results are shown in **Table** 11.

Table 11:t-Test: Two-Sample equal variances for estimated tree height from UAV-CHM and field-height

Statistics	UAV-CHM tree height	Field-measured tree height
Mean	17.75	17.72
Variance	18.36	16.07
Observations	590	590
Pooled Variance	17.22	
Hypothesized Mean Difference	0	
df	1178	
t Stat	0.14	
P(T<=t) one-tail	0.44	
t Critical one-tail	1.65	
P(T<=t) two-tail	0.89	
t Critical two-tail	1.96	
Decision: t-Statistics < t-Critical (P > 0.05): The null hypothesis was accepted. So, there was no significant difference between two means.		

From the results of the t-test, it can be concluded that there was no statistically significant difference between estimated tree height from UAV-CHM and field-derived tree height because the P-value is greater than 0.05 at $\alpha = 0.05$ and t-Statistics < t-Critical.

3.5. Model Development Using CPA and DBH

To develop the relationship between CPA and field-measured DBH, the crowns of the trees were delineated on the ortho-mosaic image based on visual image interpretation. From the 41 plots, the trees were randomly selected to develop and validate the model. Out of total randomly selected trees, 60% of trees were used to establish the model while 40% of the chosen trees were used to validate the model. CPA of trees which had one to one match with field-derived DBH were used to develop the model as well as to validate the model. The developed four models (linear, logarithmic, quadratic and power) were compared based on RMSE and coefficient of determination (R^2).

3.5.1. Model Development between CPA and DBH for the Data of 2017

The manually delineated CPA and corresponding field DBH of 75 trees were chosen from the randomly selected 123 trees which were picked from the 41 plots to model the relationship between CPA and DBH. The trees were also selected in such a way that covers all size classes of CPA and DBH. The results of the developed model are shown in **Table** 12 and **Figure** 24.

Table 12: Model Development for the Predicted DBH

Model	Equation	R^2	RMSE
Linear	DBH (cm)= 0.5134*CPA+ 13.872	0.8503	8.90
Logarithmic	DBH (cm)= 20.853*ln (CPA)-33.774	0.7493	11.52
Power	DBH (cm)= 4.5835* $CPA^{0.5636}$	0.7996	9.39
Quadratic	DBH (cm)= -0.0009* CPA^2+0.6349*CPA+11.465	0.8543	8.78
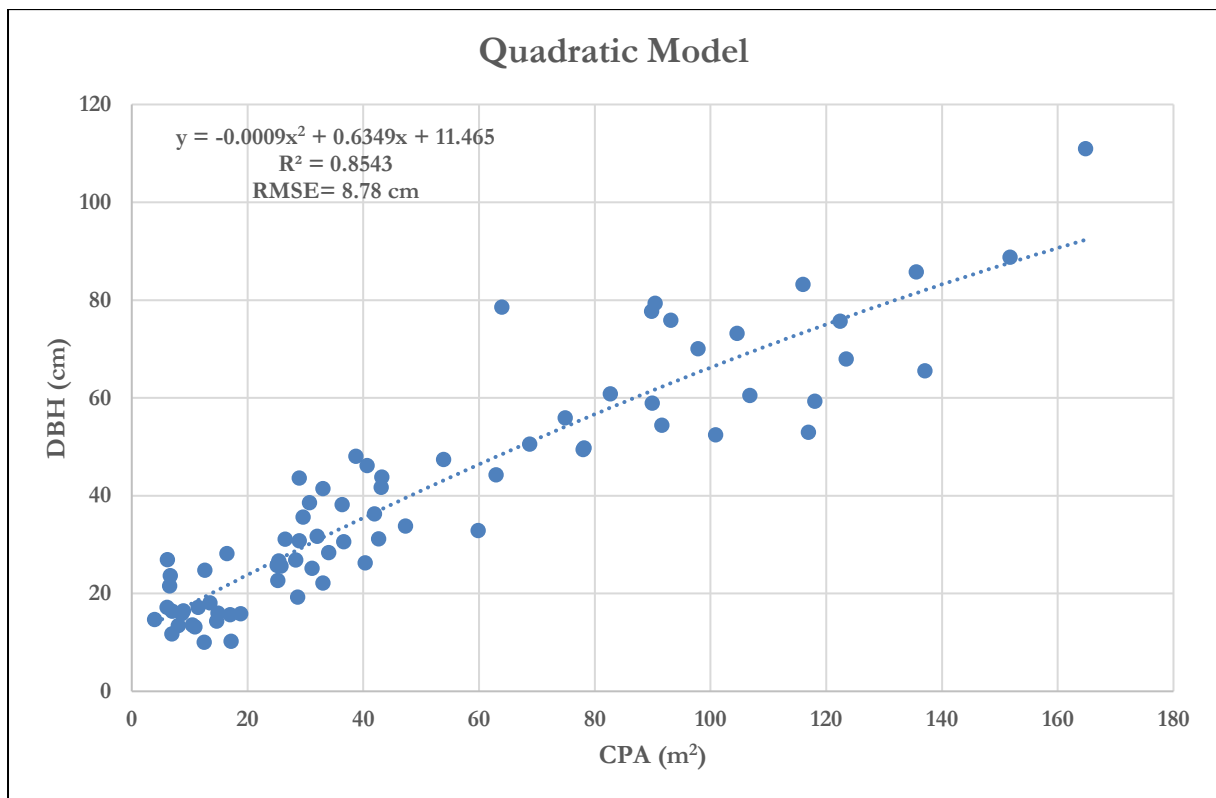
Figure 24: Quadratic model between CPA and DBH, 2017

From the results of the model development between CPA and DBH, it can be recapitulated that among all models, the linear and quadratic models had the very nearest predictive power and errors. Among all models, the quadratic model had the highest predictive power and the least errors. Considering the highest predictive power and lowest RMSE, the quadratic model was selected for the prediction of DBH.

3.5.2. Model Validation for the Data 2017

The predicted DBH was validated using observed DBH by scatter plot. The model was validated using 48 (40% of selected trees) predicted and observed DBH those were chosen randomly from 123 trees from 41 plots. The value of the coefficient of determination (R^2) was found at 0.89 (see **Figure 25**). The value of R^2 means that 89% of the field DBH was explained by the quadratic model. The test of goodness of fit was performed using RMSE that value was 8.22 cm.
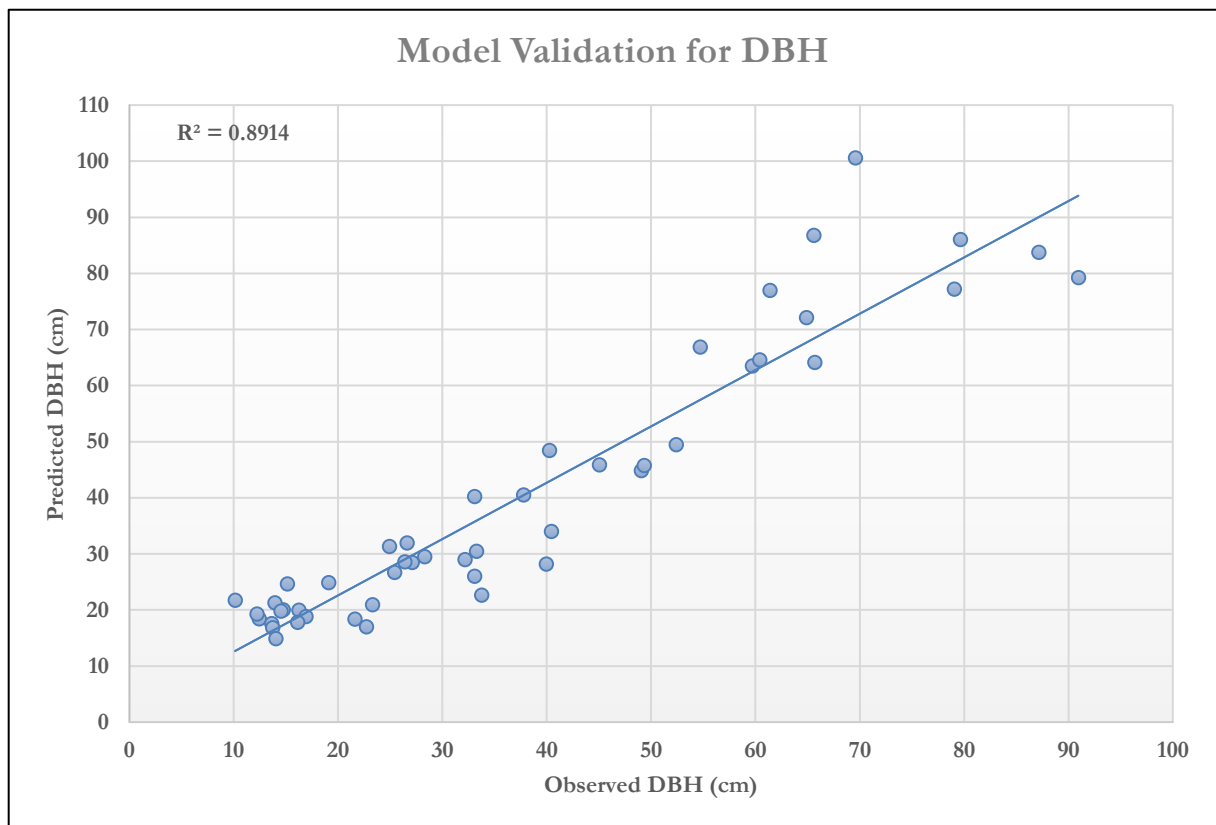
Figure 25: Scatter plot for model validation 2017

3.5.3. Model Development between CPA and DBH for the Data 2018

The CPA and corresponding DBH of 70 trees were chosen from the randomly selected 123 trees from the 41 plots to model the relationship between CPA and DBH. The results of the developed model are shown in the **Table** 13 and **Figure** 26.

Table 13: Model Development for the predicted DBH

Model	Equation	R^2	RMSE
Linear	DBH (cm)= 0.5263*CPA+ 15.669	0.7768	8.29
Logarithmic	DBH (cm)= 18.693*ln (CPA)-27.037	0.7423	8.71
Power	DBH (cm)= 4.9912* $CPA^{0.5497}$	0.7339	8.03
Quadratic	DBH (cm)= -0.0023* CPA^2+0.7705*CPA+11.531	0.7872	8.05
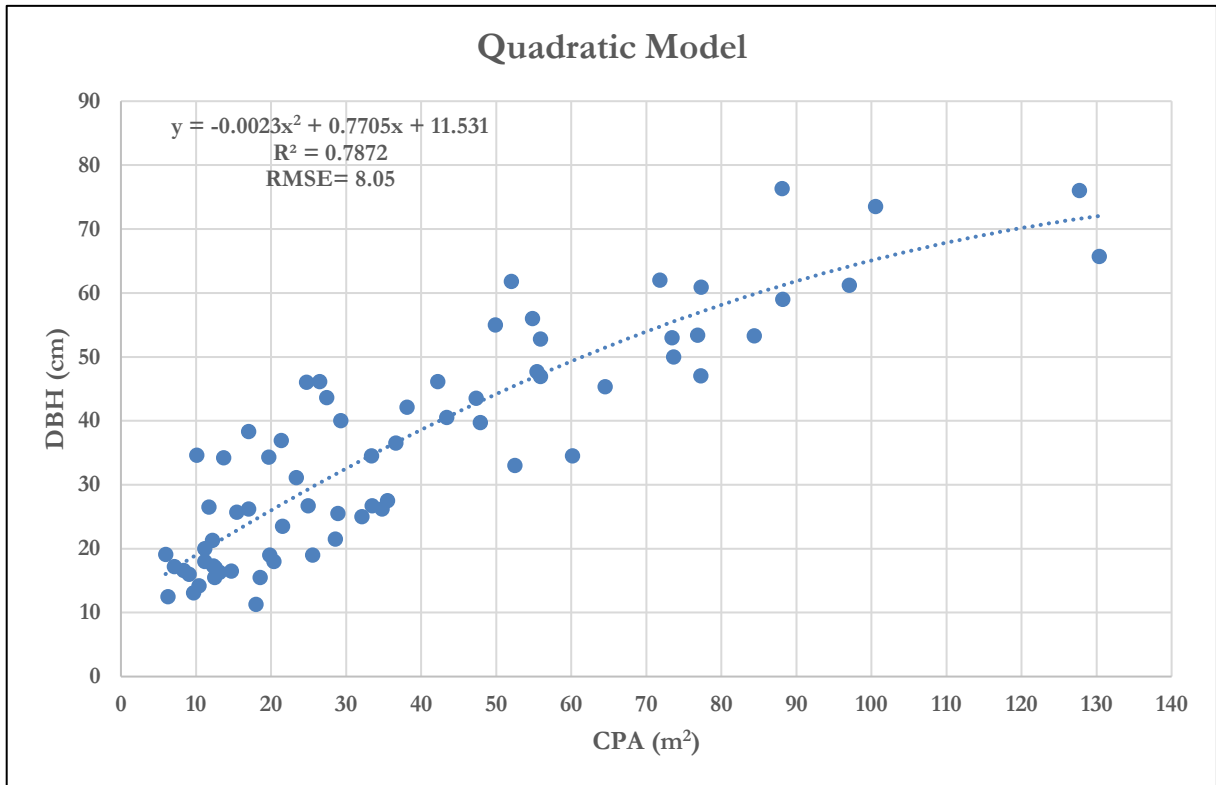
Figure 26: Quadratic model between CPA and DBH, 2018

From the results of the model development between CPA and DBH, it can be recapitulated that the linear and quadratic models had the closest predictive power and errors like an established model for 2017. Among all models, the quadratic model had the highest predictive power and reasonable errors. Considering the highest predictive power and reasonable RMSE, the quadratic model was selected for the prediction of DBH.

3.5.4.   Model Validation for the Data 2018

The predicted DBH was validated using observed DBH by scatter plot. The model was validated using 48 (40% of selected trees) predicted and observed DBH those were selected randomly from 118 trees from 41 plots. The value of the coefficient of determination (R^2) was found at 0.86 (see **Figure 27**). The value of R^2 means that 86% of the field DBH was explained by the quadratic model. The test of goodness of fit was performed using RMSE that value was 8.65 cm.
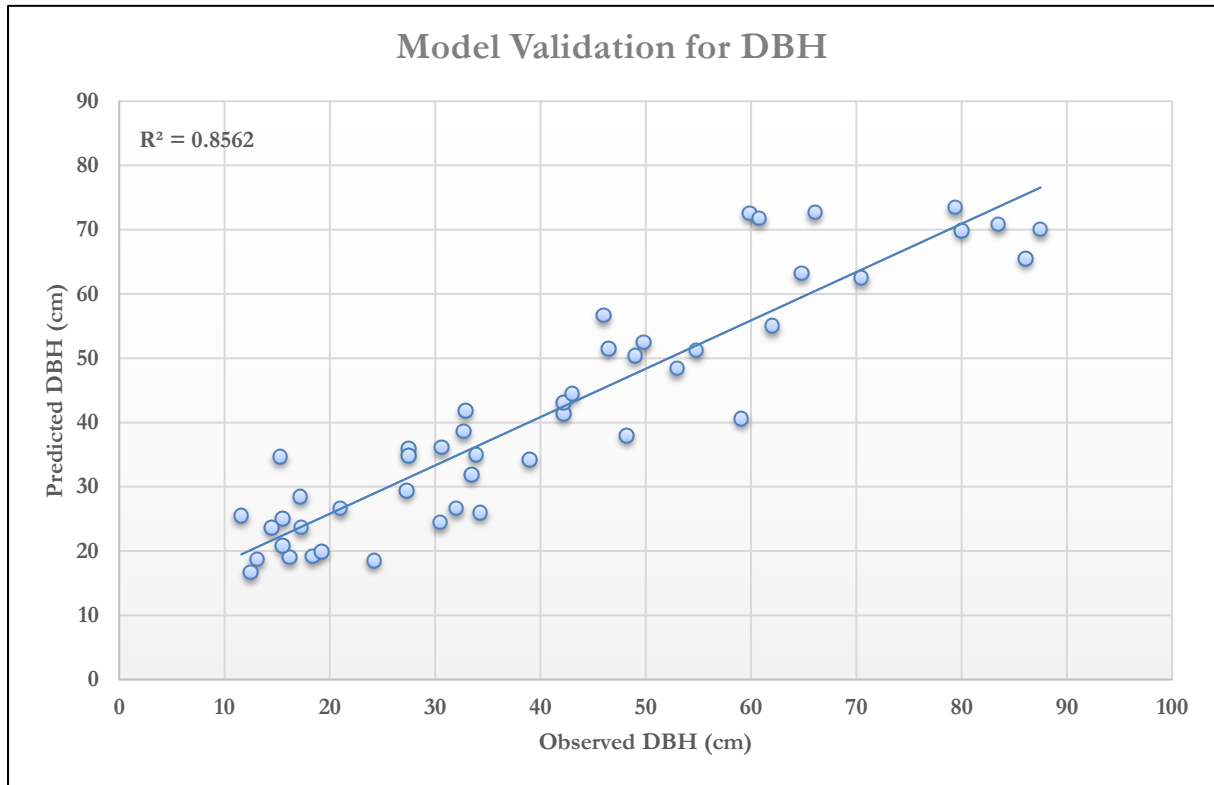
Figure 27: Model validation for observed DBH and predicted DBH 2018

3.5.5. Estimation of AGB and AGC

UAV-based and field-based aboveground biomass (AGB) and aboveground carbon (AGC) were calculated for the year 2017 and 2018. The tree height and DBH recorded in 2018 were used as input in the allometric equation to assess biomass and carbon for the year 2018. On the other hand, the modeled tree height and DBH of 2017 based on annual increment were used as input in the allometric equation for the calculation of field-based modelled AGB and AGC for the year 2017. The UAV-CHM and predicted DBH based on the model were used as input for the assessment of UAV-based AGB and AGC. The biometric data was collected from 41 plots covering every variation in the study area. The allometric equation developed by Chave et al. (2014) was used to estimate the AGB.

3.5.5.1. Plot-wise Estimation of Field-based/Modelled AGB/ AGC and UAV-based AGB/ AGC 2017

Based on the field measured parameters, the average plot-based AGB was assessed 258.71 Mg ha^{-1} while the UAV-based AGB was estimated at 235.37 Mg ha^{-1}. The difference between two means of field-based and UAV-based AGB was found 23.34 Mg ha^{-1}. The minimum and maximum field-based AGB was found 71.23 Mg ha^{-1} and 585.46 Mg ha^{-1}respectively. On the other hand, the average field-based carbon was estimated 129.36 Mg ha^{-1} whereas, the lowest and highest carbon was assessed 35.62 Mg ha^{-1} and 292.73 Mg ha^{-1} respectively. The minimum and maximum UAV-based AGB was assessed 129.49 Mg ha^{-1} and 349.27 Mg ha^{-1} respectively. On the other hand, the average UAV-based carbon was estimated 117.69 Mg ha^{-1} whereas, the lowest and highest carbon was assessed 64.75 Mg ha^{-1} and 174.64 Mg ha^{-1} respectively.

3.5.5.2. Comparison of Field-based/Modelled AGB/AGC and UAV-based AGB/AGC 2017

The field-based AGB was found higher than the estimated UAV-based AGB because the number of trees was higher to calculate the field-based AGB than the number of trees for estimating UAV-based AGB. All trees within the plots were considered to assess field-based AGB while some of the trees were missing in every plot to estimate UAV-based AGB because the UAV can only observe the upper canopy. Out of 41 plots, the UAV-based AGB was higher than field-based AGB in 18 plots. The amount of UAV-based AGB is dependent on the predicted DBH that was calculated based on CPA using the quadratic model. The comparison between field-based AGB/AGC and UAV-based AGB/AGC are presented in **Figure** 28 and **Appendix 5**.
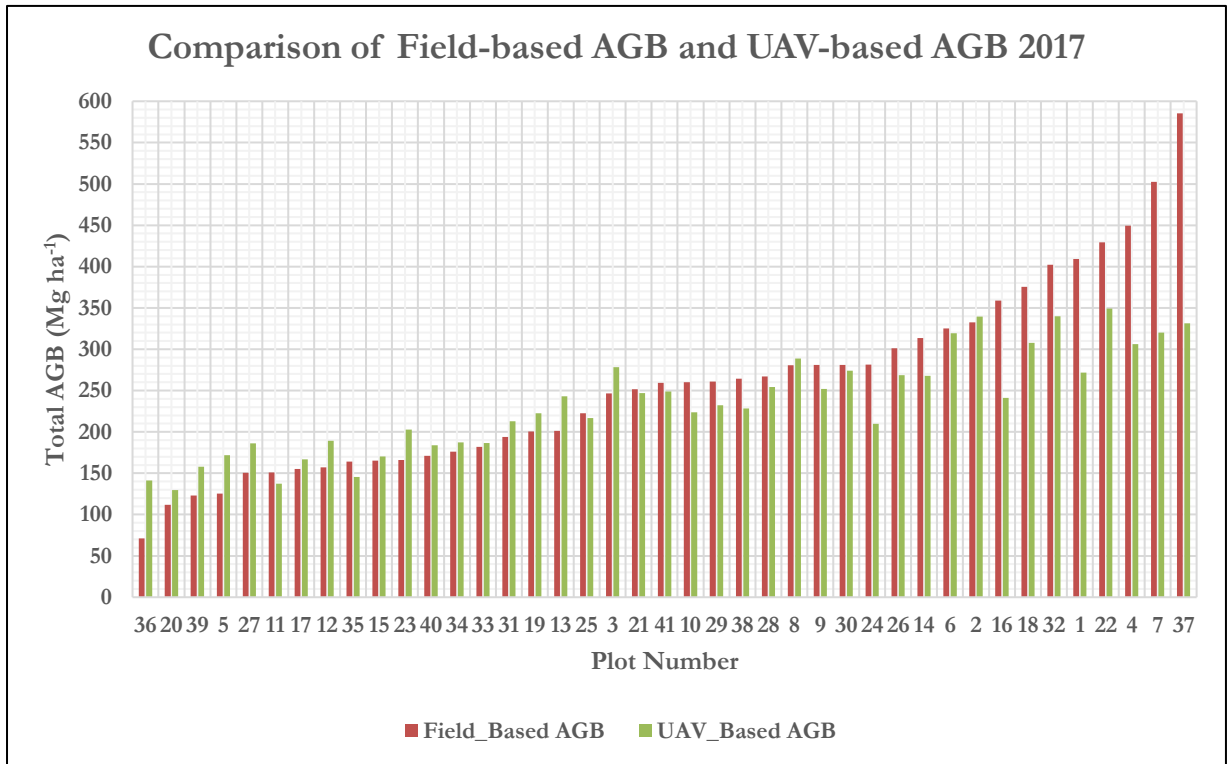
Figure 28: Comparison between field-based and UAV-based AGB 2017

3.5.5.3. Accuracy Assessment of UAV-based AGB 2017

The accuracy assessment was performed for UAV-based AGB 2017 while the field-based AGB with the same number of trees which were identified from the UAV images for the year 2017 was used as reference AGB. The scatter plot, regression and correlation statistics, F-test and t-test were performed to assess the significance of the relationship between field-based AGB and UAV-based AGB. The scatter plot demonstrated the relationship between UAV-based AGB and Field-based AGB and showed a strong correlation of 0.92 and coefficient of determination (R^2) of 0.85. The root mean square error (RMSE) was 42.35 Mg ha^{-1} which are equivalent to 18.27 % of the field-based AGB. The scatter plot, regression statistics, F-test and t-test are shown in **Table 14, 15,16** and **Figure** 29.
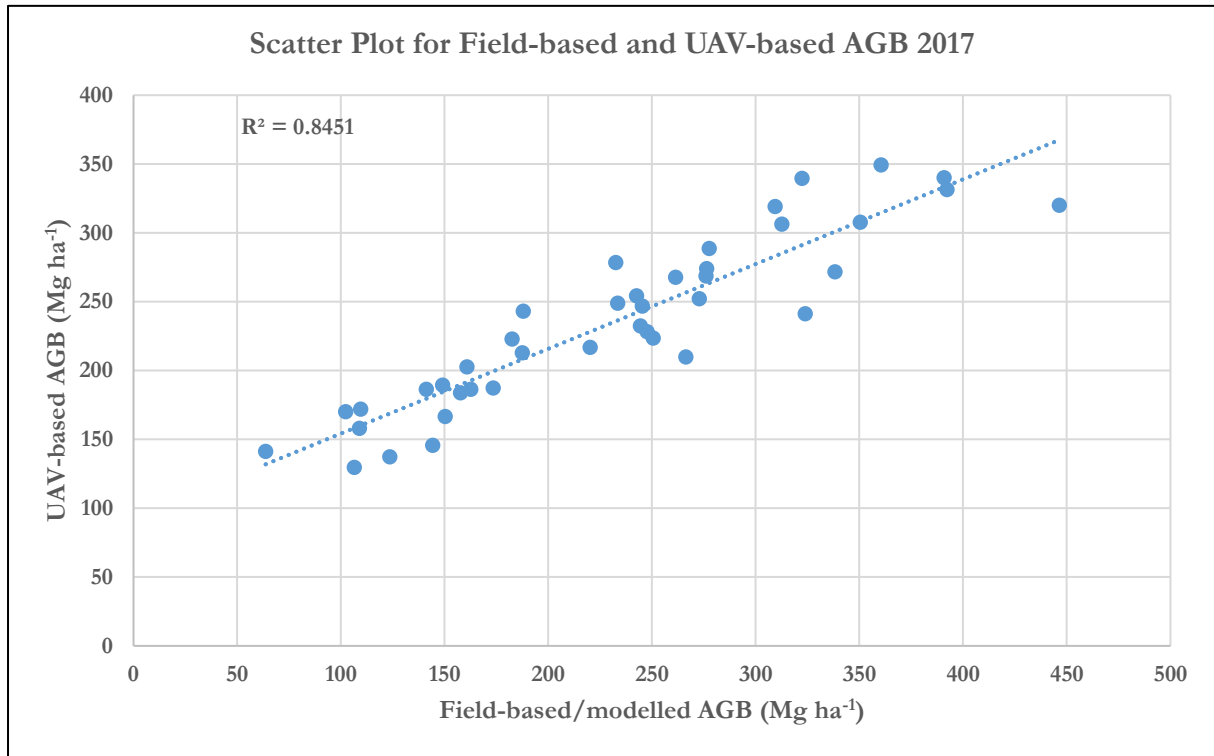
Figure 29: Scatter plot for accuracy assessment between field-based/modelled and UAV-based AGB 2017

Table 14: Regression statistics for UAV-based AGB and Field-based AGB 2017

Regression Statistics	
Multiple R	0.92
R Square	0.85
Adjusted R Square	0.84
Standard Error	24.47
Observations	41

Moreover, F-test was performed to determine if the estimated AGB from the UAV had an equal variance or unequal variance. The results of F-test are shown in **Table** 15.

Table 15: F-Test Two-Sample for Variances for UAV-based AGB and Field-based/modeled AGB

Statistics	Field-based AGB	UAV-based AGB
Mean	231.81	235.37
Variance	8404.10	3768.29
Observations	41	41
df	40	40
F	2.23	
P(F<=f) one-tail	0.01	
F Critical one-tail	1.69	
Decision: F-Statistics > F-Critical (P <0.05): Unequal Variance		

From the results of the F-test, it should be recapitulated that there was an unequal variance between UAV-based AGB and field-derived/modelled AGB because the P-value was smaller than 0.05 at α= 0.05 and F-Statistics > F-Critical.

Table 16:t-Test: Two-Sample Assuming Unequal Variances for UAV-based AGB and Field-based AGB

Statistics	Field-based AGB	UAV-based AGB
Mean	231.81	235.37
Variance	8404.10	3768.29
Observations	41	41
Hypothesized Mean Difference	0	
df	70	
t Stat	-0.21	
P(T<=t) one-tail	0.42	
t Critical one-tail	1.67	
P(T<=t) two-tail	0.84	
t Critical two-tail	1.99	
Decision: t-Statistics < t-Critical (P > 0.05): The null hypothesis was accepted. So, there is no significant difference between two means.		

From the results of the t-test, it can be concluded that there was no statistically significant difference between estimated AGB from UAV data and field-derived/modelled AGB because the P-value was greater than 0.05 at α= 0.05 and t-Statistics < t-Critical. Therefore, there was no significant difference between AGB/ carbon stock estimated from UAV imagery and modelled AGB calculated from modeled DBH and height.

3.5.5.4. Plot-wise Estimation of Field-based and UAV-based AGB and AGC 2018

The average field-based AGB was assessed 278.93 Mg ha^{-1} while the minimum and maximum AGB was 84.44 Mg ha^{-1} and 612.01 Mg ha^{-1} respectively. On the other hand, the average field-based carbon was estimated 139.47 Mg ha^{-1} whereas, the lowest and highest carbon was assessed 42.22 Mg ha^{-1} and 306.00 Mg ha^{-1} respectively. The average UAV-based AGB was estimated 248.01 Mg ha^{-1} while the minimum and maximum AGB was 142.55 Mg ha^{-1} and 369.00 Mg ha^{-1} respectively. On the other hand, the average UAV-based AGC was estimated 124.00 Mg ha^{-1} whereas, the lowest and highest carbon was assessed 71.28 Mg ha^{-1} and 184.50 Mg ha^{-1} respectively.

3.5.5.5. Comparison of Field-based AGB and UAV-based AGB 2018

Like the comparison of 2017, the field-based AGB was generally higher than the estimated UAV-based AGB because the number of trees was higher to calculate field-based AGB than the UAV-based AGB. In 14 plots, the UAV-based AGB was higher than the field-based AGB out of 41 plots. The variation of the amount of UAV-based AGB is dependent on the predicted DBH that was calculated based on CPA using the quadratic model. The detailed results of the comparison between field-based AGB/AGC and UAV-based AGB /AGC are illustrated in **Figure** 30 and **Appendix 6**.
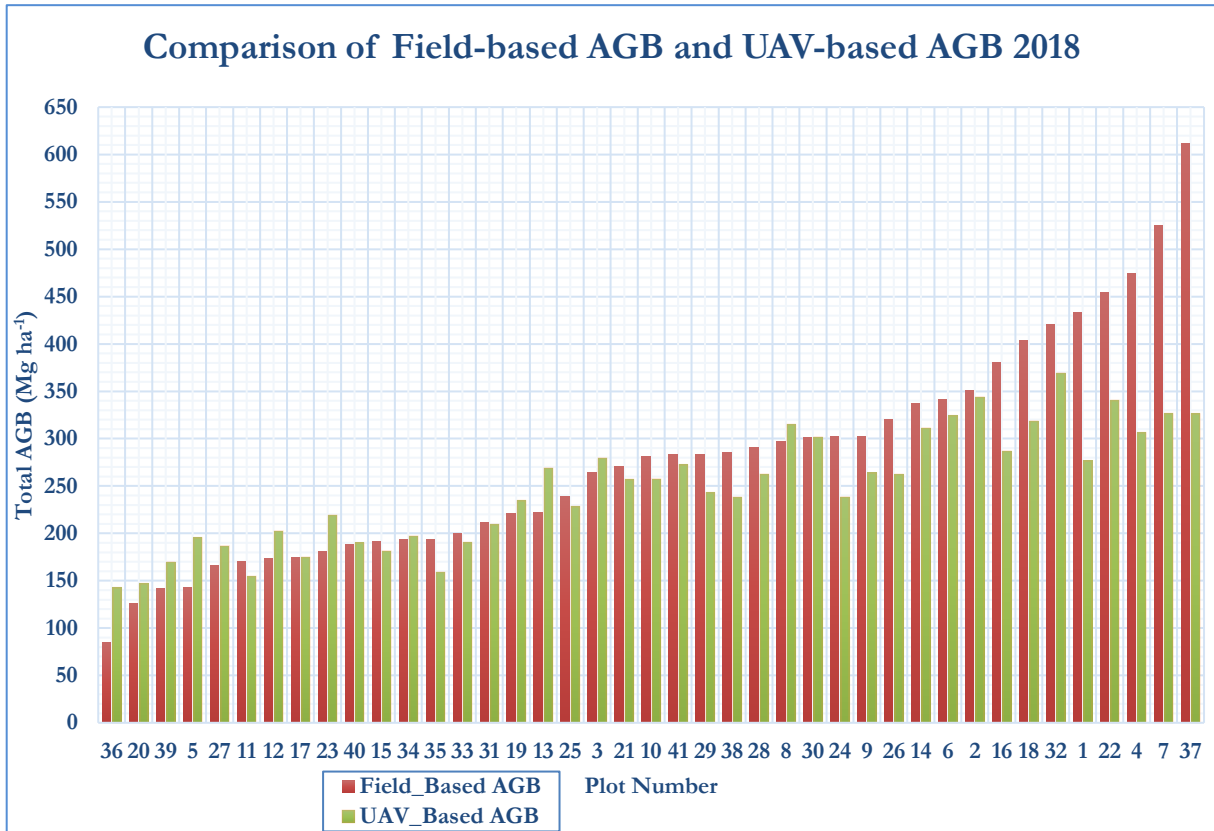
Figure 30: Comparison between field-based and UAV-based AGB 2018

3.5.5.6. Accuracy Assessment of UAV-based AGB 2018

The accuracy assessment was performed for UAV-based AGB 2018 while the field-based AGB with the same trees which were identified from the UAV images for the year 2018 was used as reference AGB. The scatter plot, regression and correlation statistics, F-test and t-test were performed to assess the significance of the relationship between field-based AGB and UAV-based AGB. The scatter plot demonstrated the relationship between UAV-based AGB and Field-based AGB and showed a strong correlation of 0.90 and the coefficient of determination (R^2) of 0.82. The root mean square error (RMSE) was 50.00 Mg ha^{-1} which are equivalent to 19.84 % of the Field-based AGB. The scatter plot, regression statistics, F-test and t-test are shown in **Table 17, 18,19** and **Figure 31**.
.
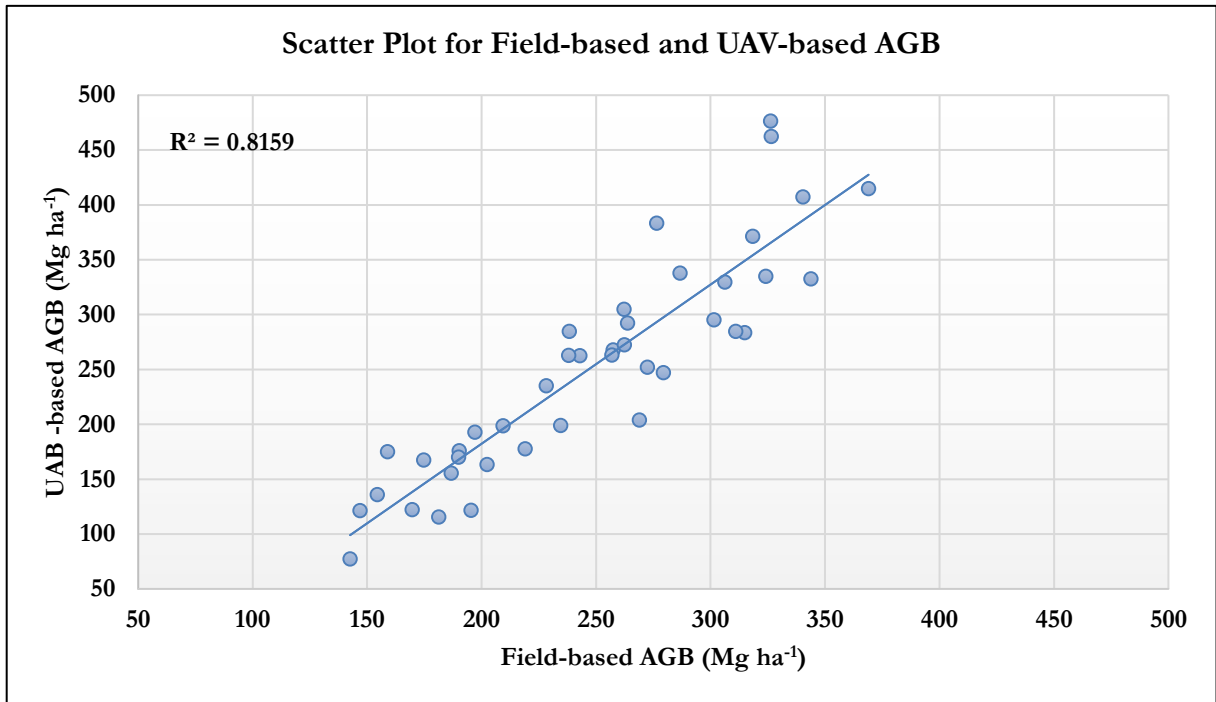
Figure 31: Scatter plot for field-based AGB and UAV-based AGB 2018

Table 17: Regression statistics for field-based AGB and UAV-based AGB 2018

Regression Statistics	
Multiple R	0.90
R Square	0.82
Adjusted R Square	0.81
Standard Error	26.64
Observations	41

Moreover, f-test was performed to determine if the estimated AGB from the UAV had an equal variance or unequal variance. The results of F-test are shown in **Table** 18.

Table 18: F-test assuming variances between field-based and UAV-based AGB 2018

Statistics	Field-based AGB	UAV-based AGB
Mean	251.98	248.01
Variance	9689.89	3757.46
Observations	41	41
df	40	40
F	2.58	
P(F<=f) one-tail	0.002	
F Critical one-tail	1.69	
Decision: F-Statistics > F-Critical (P <0.05): Unequal Variance		

From the results of the F-test, it can be recapitulated that there was an unequal variance between estimated AGB from UAV and field-derived AGB, because the P-value was smaller than 0.05 at α= 0.05 and F-Statistics > F-Critical.

Table 19: t-Test: Two-Sample Assuming Unequal Variances between Field-based AGB and UAV-based AGB 2018

Statistics	*Field-AGB*	*UAV-AGB*
Mean	251.98	248.01
Variance	9689.89	3757.46
Observations	41	41
Hypothesized Mean Difference	0	
df	67	
t Stat	0.22	
P(T<=t) one-tail	0.41	
t Critical one-tail	1.67	
P(T<=t) two-tail	0.83	
t Critical two-tail	2.00	
Decision: t-Statistics < t-Critical (P > 0.05): The null hypothesis was not rejected. So, there is no significant difference between two means.		

From the results of the t-test, it can be concluded that there was no significant difference between estimated AGB from UAV and field-based AGB, because the P-value was greater than 0.05 at α= 0.05 and t-Statistics < t-Critical. Therefore, there is no significant difference between AGB/ carbon stock estimated from UAV imagery and AGB calculated from field-derived data.

3.5.6.   **Comparison of UAV-based AGB 2017 and UAV-based AGB 2018**

The UAV-based AGB for the year 2017 and 2018 were estimated and assessed for the 41 plots. The average UAV-based AGB for 2017 was estimated 235.37 Mg ha^{-1} while the mean UAV-based AGB for the year 2018 was assessed 248.01 Mg ha^{-1}. The difference between two means of UAV-based AGB for the year 2017 and 2018 was 12.64 Mg ha^{-1}. For the year 2017, the minimum 129.49 Mg ha^{-1} AGB was assessed while the UAV-based AGB for the year 2018 was estimated 142.55 Mg ha^{-1}. On the other hand, the maximum 349.27 Mg ha^{-1} AGB was estimated for the year 2017 whereas the UAV-based maximum 369.00 Mg ha^{-1} AGB was assessed for the year 2018. The plot-wise comparison of UAV-based AGB 2017 and UAV-based AGB 2018 is presented in **Figure 32.**
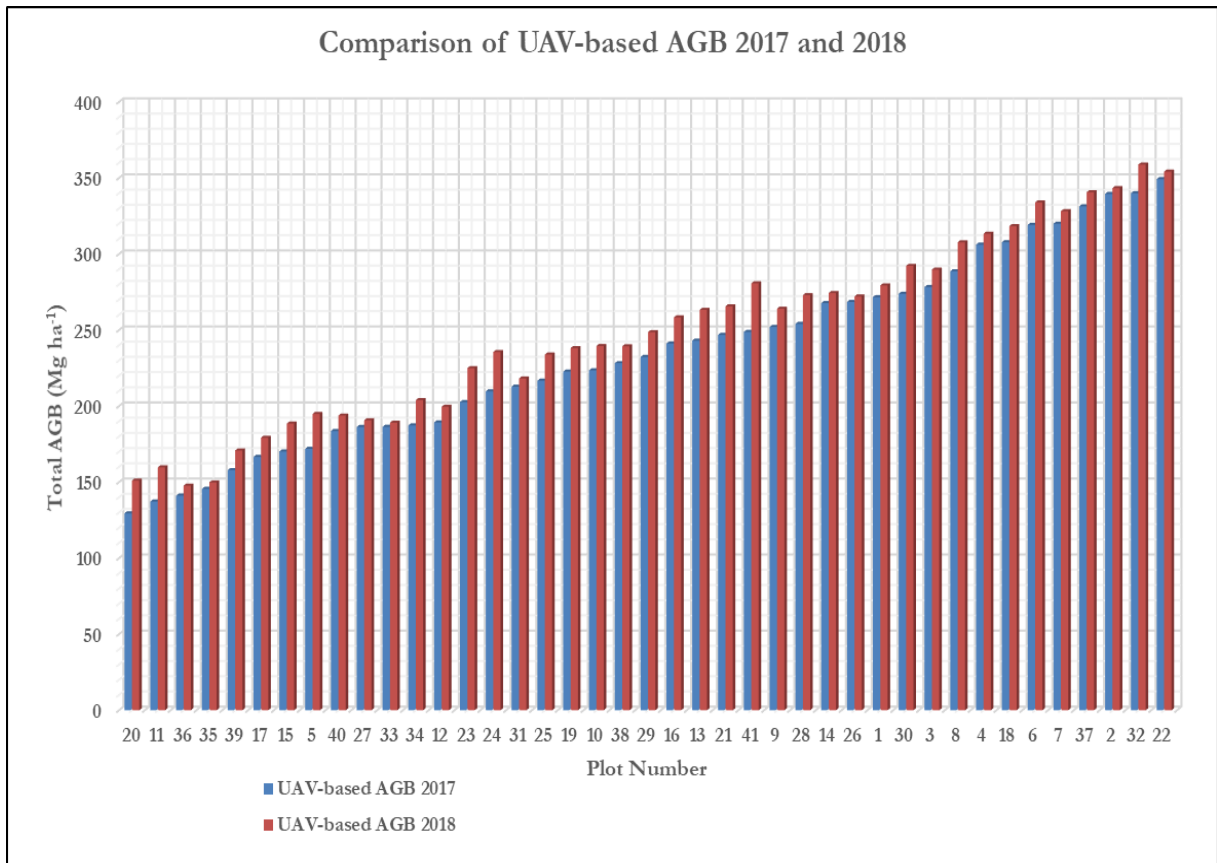
Figure 32: Comparison between UAV-based AGB 2017 and 2018

3.5.7. **Assessment of Carbon Sequestration**

The UAV-based aboveground carbon for the year 2017 and 2018 was estimated and assessed for the 41 plots. The average UAV-based AGC for 2017 was estimated 117.68 Mg ha^{-1} while the mean UAV-based AGC for the year 2018 was assessed 124.00 Mg ha^{-1}. The difference between two means of UAV-based AGC for the year 2017 and 2018 was 6.32 Mg ha^{-1}. For the year 2017, the minimum 64.74 Mg ha^{-1} AGC was assessed while the UAV-based AGC for the year 2018 was estimated 71.28 Mg ha^{-1}. On the other hand, the maximum 174.64 Mg ha^{-1} AGC was estimated for the year 2017 whereas the UAV-based maximum 184.50 Mg ha^{-1} AGC was assessed for the year 2018. The total amount of sequestered carbon for one year was 6.32 Mg ha^{-1}. The plot-wise distribution of carbon stock is shown in **Figure 33.**
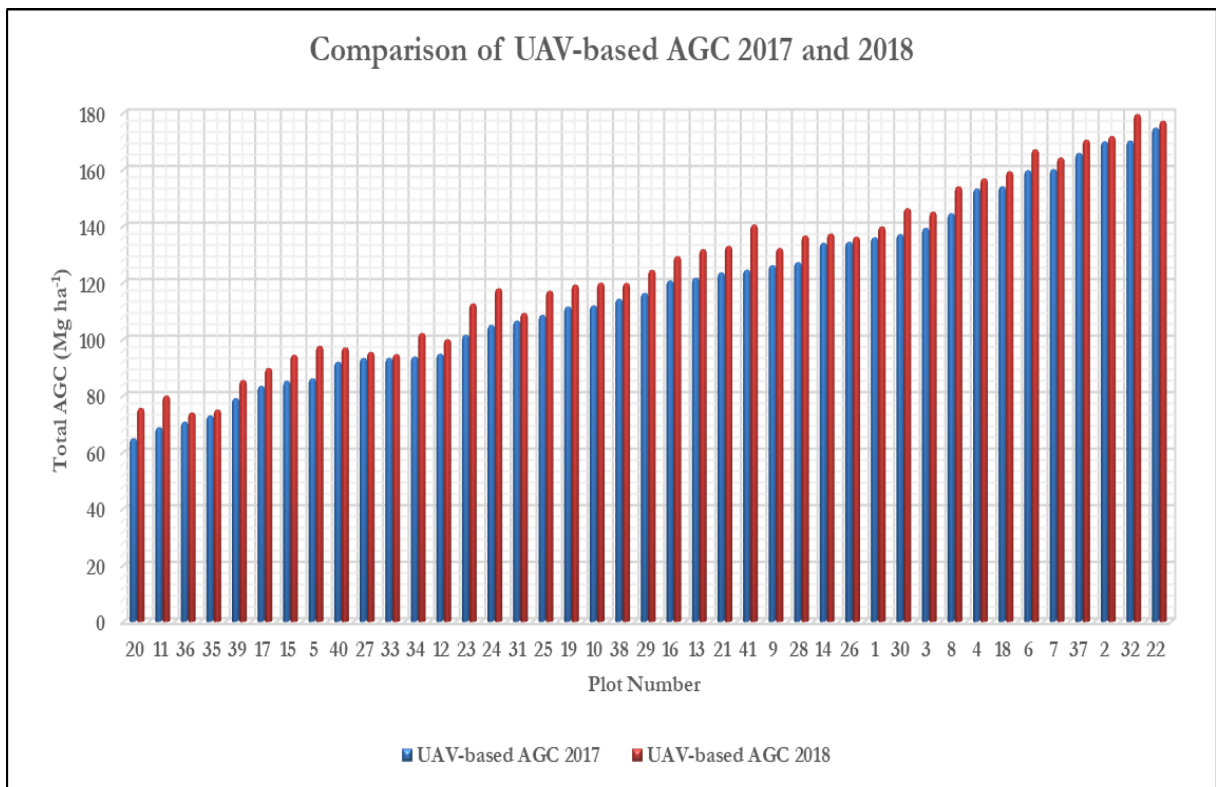
Figure 33: Comparison between UAV-based AGC 2017 and 2018

3.6.   Effect of Error of Height on AGB Estimation for 2018

The height obtained from the field was used as a reference height to assess the effect of the error of height on aboveground biomass estimation. The root mean square error (RMSE) was ±1.58 m, and the percentage of RMSE was calculated 8.94 % of the measured tree height from the field. The calculated average UAV-based AGB was 248.01 Mg ha^{-1} while the minimum and maximum AGB were 142.55 Mg ha^{-1} and 369.00 Mg ha^{-1} respectively without inflation and deflation of height. Based on the results of the percentage of RMSE, UAV-based AGB was assessed with inflated and deflated height. Firstly, 8.94% of CHM height was inflated with the original height for each tree, and then plot-wise AGB was estimated keeping the same DBH and wood density value. The calculated mean AGB was 269.83 Mg ha^{-1} while the minimum and maximum were 154.98 Mg ha^{-1} and 401.17 Mg ha^{-1} respectively. Secondly, 8.94% height was deflated with the UAV-CHM original height and then plot-wise AGB was estimated. The mean UAV-based AGB was assessed 226.51 Mg ha^{-1}, and the minimum and maximum UAV-based AGB were 130.10 Mg ha^{-1} and 336.77 Mg ha^{-1} respectively. The difference of two means of estimated AGB with inflated height and AGB without inflated/deflated height was 21.82 Mg ha^{-1}. On the other hand, the difference of two means of estimated AGB with deflated height and AGB without inflated/deflated height was 21.50 Mg ha^{-1}. The average difference between AGB without inflated/deflated height and with inflated/deflated height was found 21.66 Mg ha^{-1} which is equivalent to 8.73% of UAV-based AGB without inflation/deflation of height. The comparison of UAV-based AGB with and without inflation and deflation of height is shown in **Figure** 34.
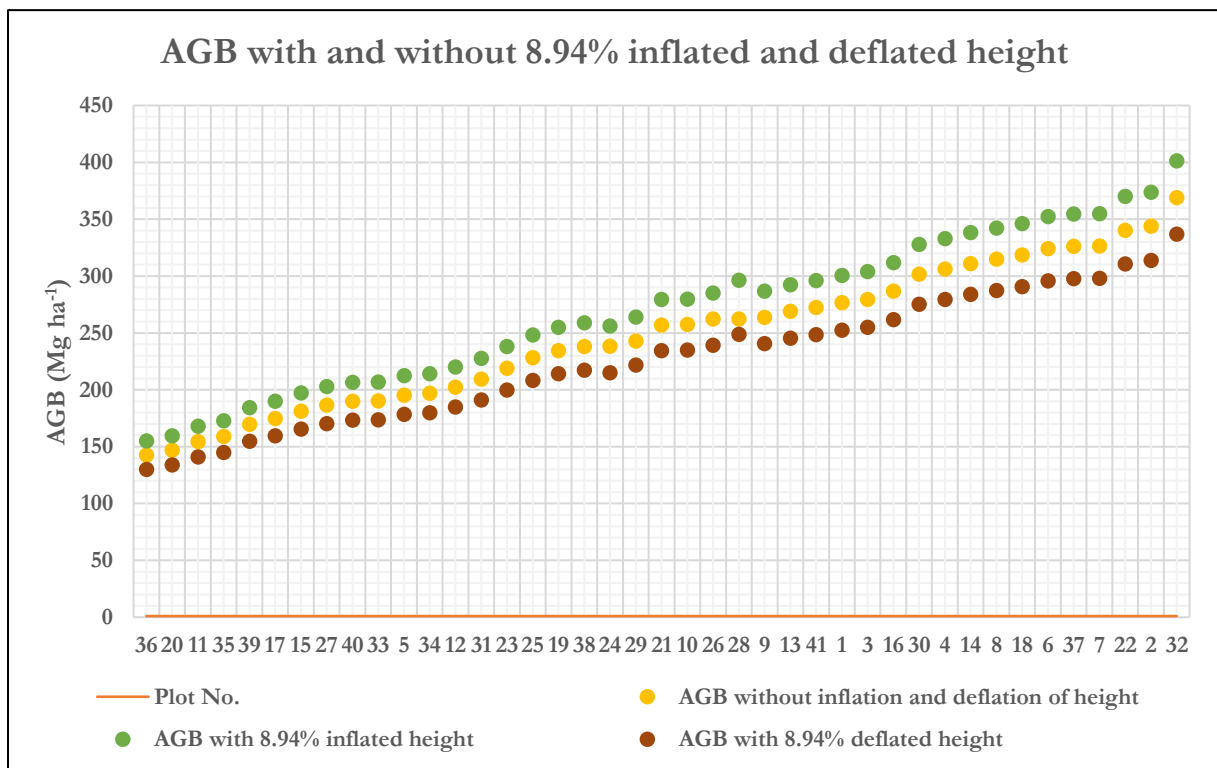
Figure 34: UAV-AGB with and without height inflation and deflation

Single factor/ one-way ANOVA test was performed to determine if there was a significant difference or not among original estimated AGB from the UAV, AGB estimated with inflated height, and the AGB estimated with deflated height. The results of the ANOVA test are shown in **Table** 20.

Table 20: Single factor/ one-way ANOVA test among AGB with and without inflated and deflated height

SUMMARY					
Groups		*Count*	*Sum*	*Average*	*Variance*
AGB without inflation and deflation of height		41	10168.37	248.01	3757.46
AGB with 8.94% inflated height		41	11062.85	269.83	4454.54
AGB with 8.94% deflated height		41	9287.01	226.51	3139.21
ANOVA					
Source of Variation	*SS*	*df*	*MS*	*F*	*P-value*	*F crit*
Between Groups	38459.29	2	19229.64	5.08	0.01	3.07
Within Groups	454048.17	120	3783.73			
Total	492507.46	122				

From the results of the single factor/ one-way ANOVA test, it can be concluded that there was a statistically significant difference among original estimated UAV-based AGB, UAV-based AGB with inflated height, and UAV-based AGB with deflated height because the P-value (0.01) was smaller than 0.05 at $\alpha = 0.05$ and F-Statistics > F-Critical.

In conclusion, it could be mentioned that there was a significant effect of the error of height on aboveground biomass and carbon estimation using UAV-CHM in a tropical forest.

3.7. Effect of CPA Delineation Error on AGB Estimation

The range of variation of biomass due to CPA delineation error was evaluated based on 1%, 5%, and 10% inflation and deflation of delineated CPA. The range of variation of AGB due to 1%, 5%, and 10% inflated and deflated CPA delineation is presented in **Table** 21.

Table 21: Range of variation of AGB due to CPA delineation error

Percentage of CPA delineation error	**Range of Variation of AGB (Mg/ha)**	**Average variation from original AGB without inflation/deflation AGB (Mg/ha)**	**Percentage of Variation**
1%	2.36 – 7.66	2.47	0.99%
5%	11.79 – 38.27	12.37	5.05%
10%	23.56 – 76.45	24.70	9.96%

Moreover, the single factor/ one-way ANOVA test was conducted for estimated AGB by 1%, 5%, and 10% inflated and deflated CPA to evaluate the significance of difference among the estimated AGB with and without inflated and deflated CPA. The results of the ANOVA test and the estimated amount of AGB with and without inflated and deflated CPA are presented in **Table** 22**, 23, 24** and **Figure** 35**, 36, 37.**

Table 22: Single factor/one-way ANOVA test among AGB without and with 1% inflated and deflated CPA

SUMMARY					
Groups		Count	Sum	Average	Variance
AGB without inflated/deflated CPA		41	10168.37	248.01	3757.46
AGB with 1% inflated CPA		41	10269.63	250.48	3825.60
AGB with 1% deflated CPA		41	10066.76	245.53	3689.48
ANOVA					
Source of Variation	SS	df	MS	F	P-value	F crit
Between Groups	501.9018014	2	250.95	0.07	0.94	3.07
Within Groups	450901.6757	120	3757.51			
Total	451403.58	122				

From the results of the single factor/ one-way ANOVA test, it can be concluded that there was no statistically significant difference among the original estimated UAV-based AGB, UAV-based AGB with 1% inflated CPA, and UAV-based AGB with 1% deflated CPA because the P-value (0.94) was greater than 0.05 at α= 0.05 and F-Statistics < F-Critical.
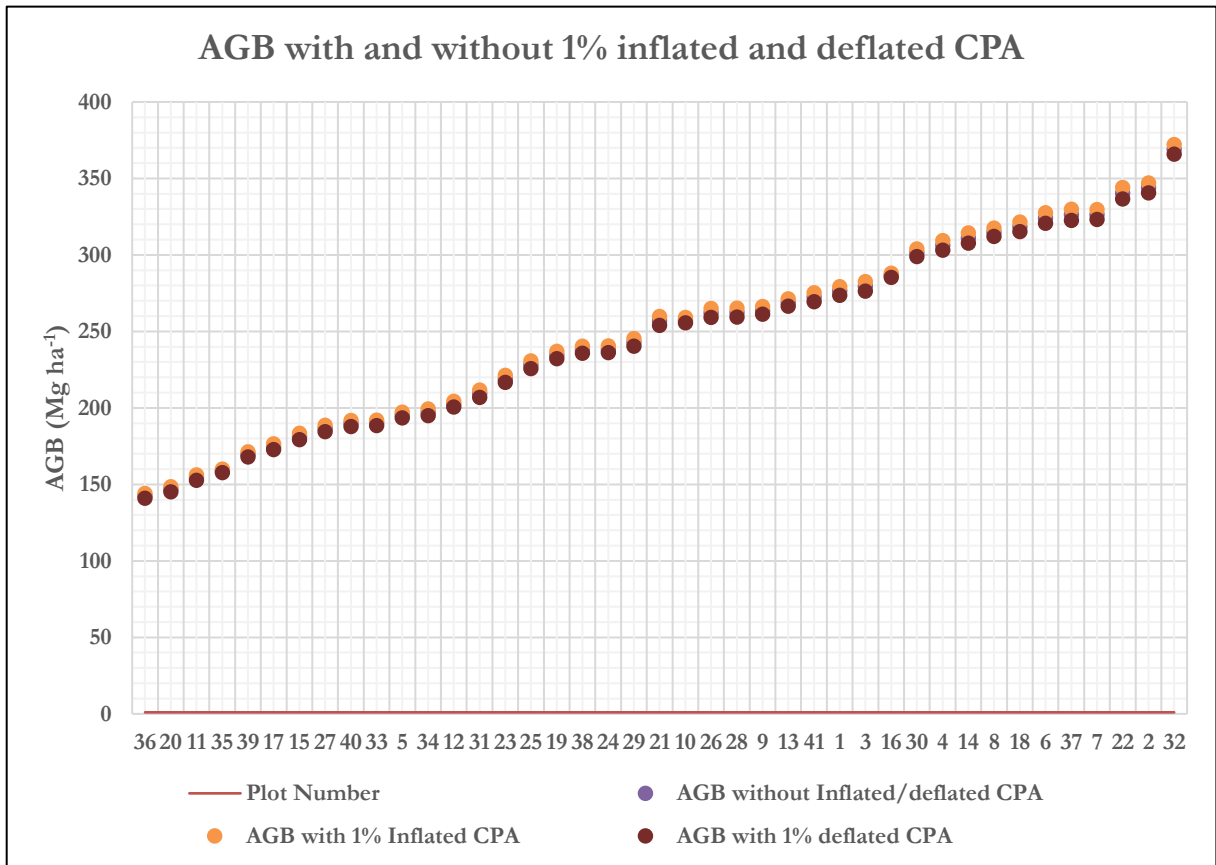
Figure 35: Estimated AGB with 1% inflated and deflated CPA

Table 23: Single factor/one-way ANOVA test among AGB without and with 5% inflated and deflated CPA

SUMMARY					
Groups		*Count*	*Sum*	*Average*	*Variance*
AGB without inflated/deflated CPA		41	10168.37	248.01	3757.46
AGB with 5% inflated CPA		41	10671.20	260.27	4099.61
AGB with 5% deflated CPA		41	9657.24	235.54	3419.43
ANOVA					
Source of Variation	*SS*	*df*	*MS*	*F*	*P-value*	*F crit*
Between Groups	12538.40	2	6269.20	1.67	0.19	3.07
Within Groups	451060.14	120	3758.83			
Total	463598.54	122				

From the results of the single factor/ one-way ANOVA test, it can be recapitulated that there was no statistically significant difference among the original estimated UAV-based AGB, UAV-based AGB with 5% inflated CPA, and UAV-based AGB with 5% deflated CPA because the P-value (0.19) was greater than 0.05 at α= 0.05 and F-Statistics < F-Critical.
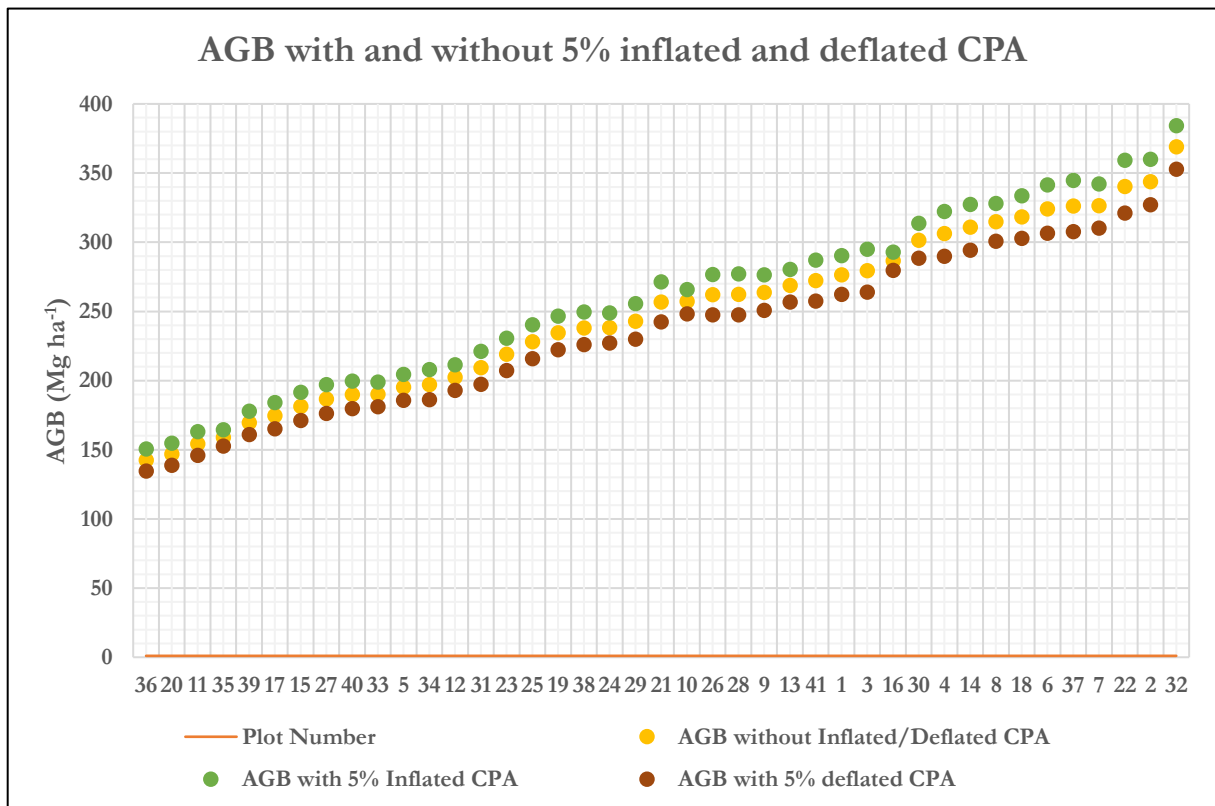
Figure 36: Estimated AGB with and without % inflated and deflated CPA

Table 24: Single factor/one-way ANOVA test among AGB without and with 10% inflated and deflated CPA

SUMMARY					
Groups		*Count*	*Sum*	*Average*	*Variance*
AGB without inflated/deflated CPA		41	10168.37	248.01	3757.46
AGB with 10% inflated CPA		41	11164.64	272.31	4444.73
AGB with 10% deflated CPA		41	9139.08	222.90	3086.90
ANOVA					
Source of Variation	*SS*	*df*	*MS*	*F*	*P-value*	*F crit*
Between Groups	50039.40	2	25019.70	6.65	0.002	3.07
Within Groups	451563.70	120	3763.03			
Total	501603.10	122				

From the results of the single factor/ one-way ANOVA test, it can be concluded that there was a statistically significant difference among the original estimated UAV-based AGB, UAV-based AGB with 10% inflated CPA, and UAV-based AGB with 10% deflated CPA because the P-value (0.002) was smaller than 0.05 at $\alpha= 0.05$ and F-Statistics > F-Critical.
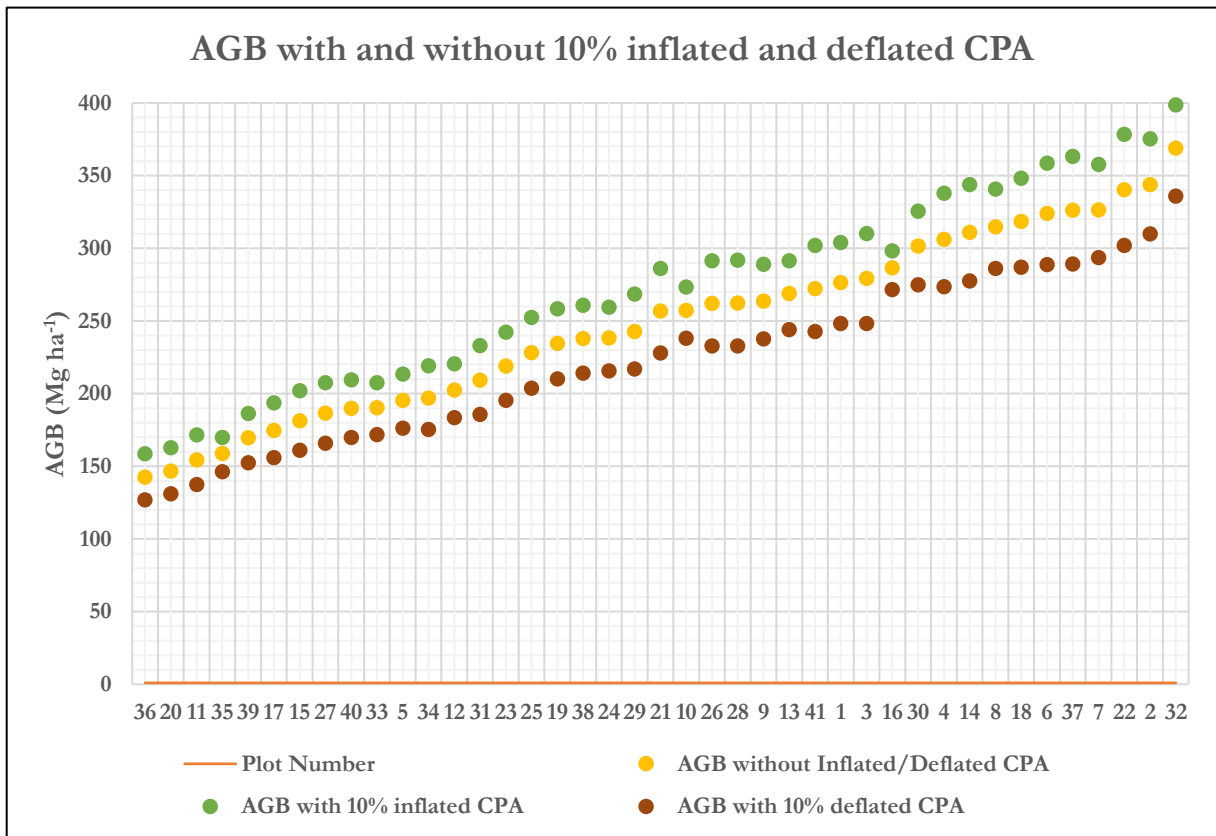
Figure 37: Estimated AGB with and without 10% inflated and deflated CPA

4. DISCUSSION

4.1. Descriptive Analysis of Tree Height and DBH

In this study, the tree height was recorded using Leica DISTO 510 which uses laser technology to measure the range up to 200m. This equipment has ±1mm accuracy to measure distance up to 200m. However, it has also a measurement error in the multi-layer complex tropical forest. Sadadi (2016) stated in his study that the handheld Leica DISTO 510 has the threshold accuracy of ±50 cm while the Airborne Lidar has the threshold accuracy of ±10cm. The data collection by airborne Lidar is expensive. On the other hand, Leica DISTO is very handy to collect data. Despite having the error in tree height measurement by Leica DISTO, it is measurement, but the UAV CHM is just estimation. 50 cm error does not affect much on AGB estimation. Considering the cost-effectiveness, the Leica DISTO can become the best alternative. The DBH was measured using DBH tape that was precise and accurate. The results show that the field-measured DBH was not normally distributed and was positively skewed because the trees with DBH equal to or greater than 10 cm were considered only. The similar study was done by Mtui (2017) in tropical forest at Ayer-Hitam in Malaysia found that the DBH was not normally distributed and it was positively skewed. The trees with DBH is less than 10 cm cannot contribute much to the total aboveground biomass assessment (Brown, 2002). Within the size of DBH between 10 and 20 cm, the maximum number of trees were found out of all recorded trees. The frequency distribution curves of field-measured DBH was L-shaped, and the pattern of the frequency was exponentially toward the larger DBH classes. The result of this study is similar to the result of the study conducted by Terakunpisut et al. (2007). The number of trees was decreased with the increase in the size of DBH meaning the number of big trees was minimal compared to the trees with small size of DBH. The results of the field-measured tree height showed that the curve was almost normally distributed, and the skewness value was 0.19 because the maximum trees were fallen under the height class 16-20 m that was mid-level class amongst of all height class. The results of the tree height derived from UAV-CHM for the year 2017 and 2018 appeared to follow the normal distribution curve while the value of skewness was 0.20 and 0.08 respectively (see **Figure 38 and Figure 39**). The similar study was done by Mtui (2017) in tropical forest at Ayer-Hitam in Malaysia found the normal distribution of the field-measured tree height and UAV-derived tree height.
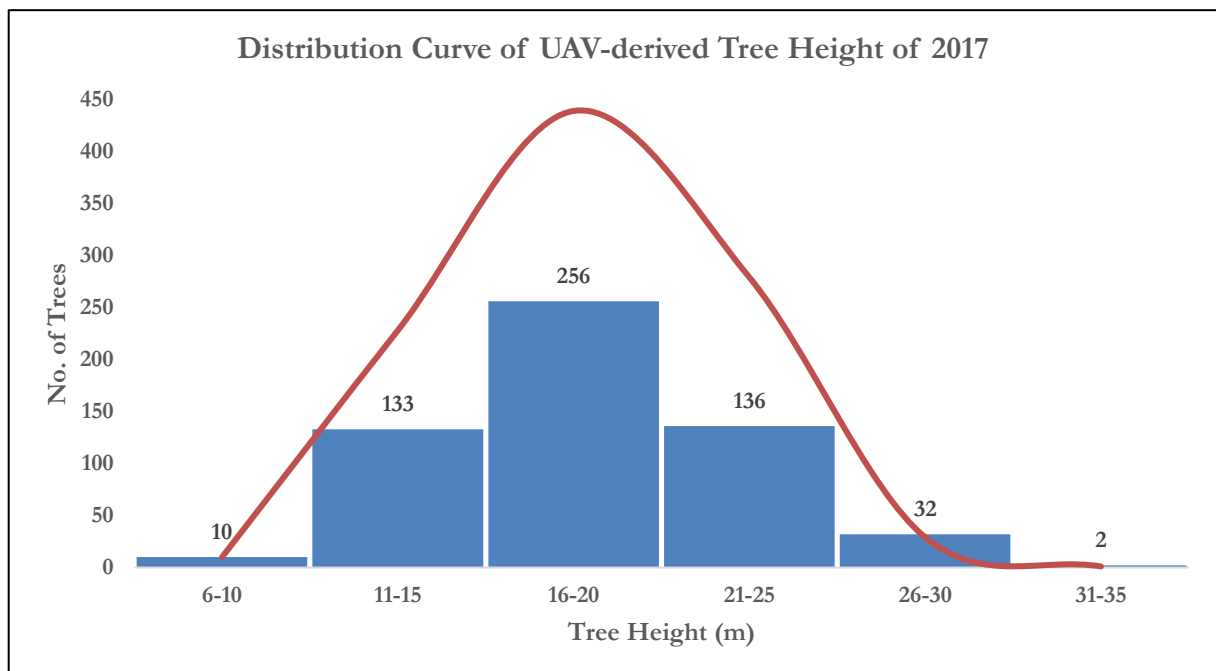
Figure 38: Distribution curve of UAV-derived tree height 2017
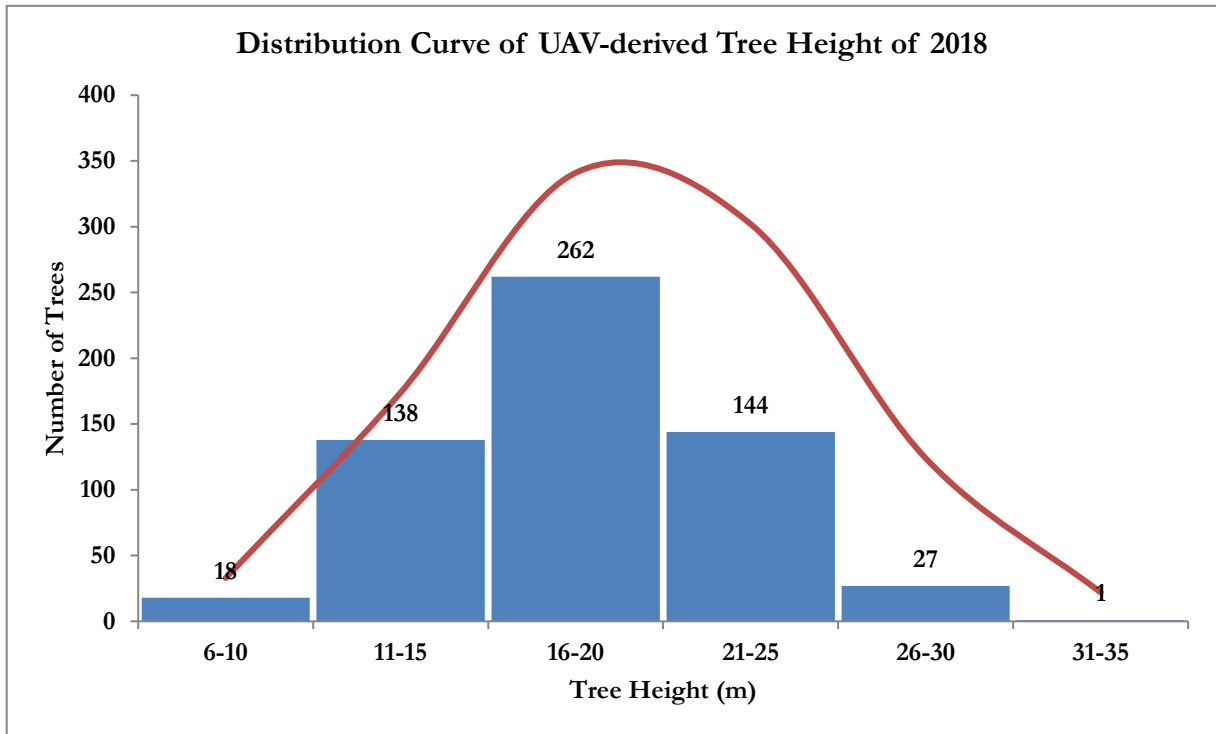
Figure 39: Distribution curve of UAV-derived tree height 2018

4.2. Model Development and Validation Between CPA and DBH

The positive and significant relationship was found between crown projection area and diameter at breast height in this study like other similar studies conducted in the tropical forest. The quadratic model was chosen among four models due to its highest predictive power and lowest RMSE. In the dominant forest, the non-linear regression (quadratic) model was preferred because the growth pattern of CPA and DBH does not follow the linear relationship between CPA and DBH (Kuuluvainen, 1991; Köhl et al., 2006). The non-linear relationship is found between CPA and DBH in the forest with natural conditions where high competitions exist among the species as the growth of CPA slow down compared to the growth of DBH (Shimano, 1997). In the dense forest ecosystem, the non-linear relationship between CPA and DBH are found where the trees possessed DBH larger than 40 cm (Hemery et al., 2005). The study conducted by Odia (2018) in the tropical forest of Malaysia found the highest coefficient of determination (R^2) and lowest RMSE for the quadratic model to establish the relationship between CPA and DBH. It was observed from the distribution of DBH class in the study area, around 20% of total recorded trees having the DBH more than 40cm. The growth of the CPA of these trees is slow compared to the growth of DBH of the same tree. The study area is a dense natural forest having a large diversity of species and CPA grows slowly. This was one of the reasons for finding a non-linear relationship between CPA and DBH. The research done by Odia (2018) found that almost 20% of trees having DBH more than 40cm in the tropical forest. In this study, the model was also validated and found a strong correlation and coefficient of determination for both years like the study conducted Odia (2018) in three sites of tropical forest.

4.3. Estimation of AGB and AGC

The field-based and UAV-based aboveground biomass (AGB) and aboveground carbon (AGC) were calculated and estimated for the year 2017 and 2018. There was a difference between field-based AGB and UAV-based AGB for both years, and there were many reasons for the difference. One of the reasons was identified that the UAV could only observe the upper canopy. 943 trees were measured in the field, but only 569 trees were found on the orthomosaic of 2017 and 590 trees on the one for 2018. 374 trees were not considered in the estimation of the UAV-derived biomass for the year 2017 while the 353 trees were missing in 2018 for biomass. Although many trees are missing from the overall estimation of biomass, the difference between field-based AGB and UAV-based AGB was not significant because all the missing trees contain small DBH and height, so they contributed less in overall biomass assessment.

4.3.1. Reason for Variation of Amount of AGB Across the Plots

The plot-wise AGB was estimated for the 41 plots. Among 41 plots, the difference between the highest and lowest AGB was 226.45 Mg ha^{-1}. In plot with lowest AGB, the maximum height was estimated 17.84m while the average height was found 14.43 m. The highest CPA was found 59.68 Sq.m² while the average CPA was 28.46 Sq.m². On the other hand, the plot with the highest AGB had the highest height 26.50 m while the mean height was estimated at 18.51 m. The highest CPA was calculated 129.33 Sq.m² whereas the average size of the CPA was found 44.86 Sq.m². The difference in average height between the two plots was 4.08m. On the other hand, the difference in the average CPA between the two plots was 16.4 Sq.m². The variation of the amount of AGB across the plots depends on the tree height, CPA and the number of trees also. Among all factors, the CPA influence more on biomass variation across the plots because the predicted DBH was calculated based on CPA. The predicted DBH was the input in the allometric equation developed by Chave et al. (2014) that used square power on DBH. Tree height also influences the variation of AGB estimation. The photographs and screenshot of the plots are presented in **Figure** 40 **(a)-(b)** and **Figure** 41 **(a)-(b)**.

Figure 40: (a) Plot with big tree and (b) Plot with small tree
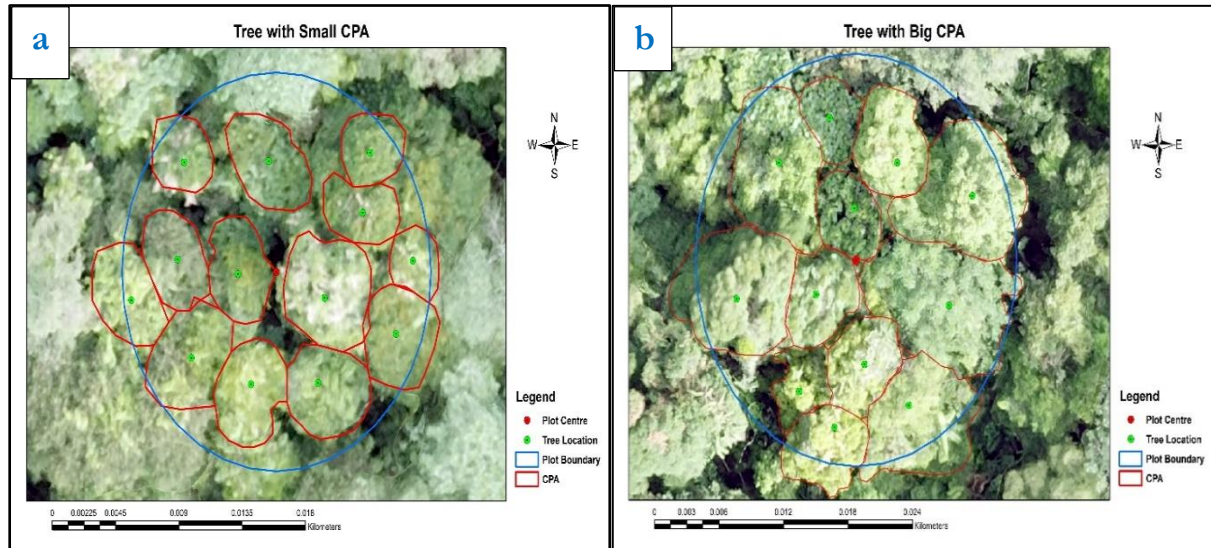
Figure 41: (a) Tree with small CPA and (b) Tree with big CPA

4.3.2. Comparison of AGB and AGC Assessment with Other Studies

The estimation of aboveground biomass and carbon stock is varied in the tropical forest due to the variation of environmental conditions, allometric equation, type of sensor used, methods applied, management strategy of the forest, species types, size of trees, etc. (Sium, 2015). According to the assessment of IPCC (2006), the range of the estimated amount of aboveground biomass in the tropical forest of Asia is 120-680 Mg ha^{-1}. The result of this study was within the estimated range of the IPCC. The results of the different studies conducted in different forests by different researcher are presented in **Table** 25.

Table 25: Aboveground biomass and carbon stock in different forests

Country/Region	Tropical rainforest		Dry evergreen forest		Mixed deciduous forest	
	AGBM (Mg ha^{-1})	C-stock (Mg ha^{-1})	AGBM (Mg ha^{-1})	C-stock (Mg ha^{-1})	AGBM (Mg ha^{-1})	C-stock (Mg ha^{-1})
Source: Adapted from Terakunpisut et al., (2007)						
Thailand	275.46	137.73	140.58	70.29	96.28	48.14
Malaysia	225 - 446	112.5- 223	-	-	-	-
Cameron	238- 341	119- 170.5	-	-	-	-
Sri Lanka	153- 221	76.5- 110.5	-	-	-	-
Source: Toma et al., (2017)						
East Kalimantan, Indonesia	279	139.5	-	-	-	-
Source: This study						
East Kalimantan, Indonesia (2017)	235.37	117.69	-	-	-	-
East Kalimantan, Indonesia (2018)	248.01	124.00	-	-	-	-

From the table mentioned above, it can be concluded that the estimated amount of AGB in this study was within the range of AGB assessed by other studies.

4.4. Assessment of Carbon Sequestration

The UAV-based aboveground carbon for the year 2017 and 2018 was estimated and assessed for the 41 plots. The total amount of sequestered carbon for one year was 6.32 Mg ha^{-1}. Sedjo (1989) applied a universal average rate of 6.24 Mg C/ha/yr in his study which was very much close to the result of this study. A study conducted by Diana et al. (2002) found the amount of sequestered carbon for the species *Acacia mangium, Eucalyptus pelitta,* and *Gmelina arborea* were 5.9-9.9, 7.1-7.2, 8.3-12.3 Mg ha^{-1}y^{-1}. The result of this study was similar to and within the range of AGB of these three species. A study conducted on the tropical forest by Brown, (1992) produced a table mentioning the amount of sequestering carbon assessed by the different researcher in different types of tropical forest (see **Table** 26).

Table 26: Carbon sequestration in different tropical forests

Forest Type	Dry Matter Mg/ha/year	Carbon Mg/ha/year	Studied By	Source
Tropical rainforest	7.75- 10.19	3.88- 5.10	Bolin et al. (1986) (various sites)	Source: Adapted from Brown, (1992)
Seasonal tropical forest	5.50- 7.20	2.75- 3.60		
Rainforest (Manaus)	15.00	7.50	Cannell (1982)	
Rainforest (Ivory Coast)	12.73- 24.60	6.36- 12.30		
Amazonian rainforest (mean)	12.66	6.33	Jordan (1989)	
Slash and burn (after 3 years)	5.26	2.62		

From the table, it can be mentioned that the estimated amount of sequestered carbon in this study was very much close to the estimated amount of sequestered carbon in Amazonian rainforest and rainforest of Ivory Coast. The assessed sequestered carbon in this study was higher than the range of sequestered carbon estimated for tropical rainforest and seasonal tropical rainforest by Bolin et al. (1986) in various sites. This variation occurred due to different forest structure, different tree species and the size of the trees, etc.

4.5. Effect of Tree Parameters Error on AGB Estimation

The tree parameters extracted from the UAV images influence the biomass estimation. The inflated and deflated tree height and CPA were used to evaluate the variation of biomass. The difference of UAV-based AGB with and without inflated/deflated height was found 21.66 Mg ha^{-1} which was equivalent to 8.73% of original estimated UAV-based AGB without inflation and deflation of height. The single factor/ one-way ANOVA test revealed that there was a statistically significant difference between estimated UAV-based AGB with 8.94% inflation and deflation of height and UAV-based AGB without inflation/deflation of height. The study conducted by Okojie (2017) found that the estimation of biomass was significantly influenced by the variation of height. The study conducted by Hunter et al. (2013) also found that the influence of height imprecision on biomass assessment is approximately 6%. In this study, the difference of UAV-based assessed carbon with and without height inflation and deflation was bigger than the total amount of sequestered carbon for one year. In this study, the field-based tree height measured by Leica DISTO 510 was used as a reference height that has ±50 cm inaccuracy. This level of inaccuracy has uncertainty in assessing AGB. This level of inaccuracy was not considered in this study because there was no other best alternative that was cost-effective to collect tree height. Despite the certain level of inaccuracy in Leica DISTO 510, this height is measurement, but the CHM is an estimation. The accuracy of the CHM depends on the density of the point clouds.

The average variation of biomass due to 1% inflation and deflation of CPA was 2.47 Mg ha^{-1} which was equivalent to 0.99%, and it does not influence more on biomass estimation. For 5% inflation and deflation of CPA, the average variation of biomass was estimated 12.37 Mg ha^{-1}. It had no statistically significant difference from original biomass, but the amount of AGB was close to the estimated amount of sequestered biomass for one year. On the other hand, the average variation of biomass 24.70 Mg ha^{-1} was estimated due to 10% inflated and deflated CPA that showed a statistically significant difference, and it affected 9.96% variation of biomass from the original biomass. The estimated amount of carbon caused inflation and deflation of CPA was observed double compared to the amount of sequestered carbon for one year. The missing tree was also responsible for the variation of AGB that was finally influenced the estimation of carbon sequestration. Due to the missing tree, 11.05% of AGB was underestimated in the year 2018, and 9.02% of AGB was underestimated in the year 2017 compared with the field-based AGB. This has also influence on estimating carbon sequestration.

The combined error from the tree height and the CPA delineation might be affected more on biomass estimation. The variance of the estimated amount of carbon with height and CPA inflation/deflation and the estimated amount of carbon without inflation and deflation might be high. This variation would be larger while considering error for both years. The effect of tree height and CPA delineation error on biomass estimation was bigger than the estimated amount of sequestered carbon. The estimated amount of sequestered carbon might be the reason for error of tree height and CPA delineation. The carbon sequestration assessment for one year might be influenced more by the error originated from the tree parameters extraction. The total amount of sequestered carbon might be more than the estimated carbon sequestration variation for the different type of error. The influence of different errors on carbon sequestration estimation would be less while assessing sequestered carbon for more than one year because the amount of sequestered carbon would be large.

4.6.   Limitations

The conducted research has limitations. Some of the significant limitations are mentioned below that would be helpful to construct recommendations for similar studies in the future.

- ✓ The handheld GPS named Garmin has a certain level of inaccuracy, and it was quite challenging to identify the correct location of the respective trees and plot centers;

- ✓ Enough open space is needed to place the GCP marker inside the forest. In a tropical forest, it is a very challenging task to find enough open space to put the GCP as if they are evenly distributed in the study area;

- ✓ In this study, Leica DISTO 510 laser ranger was used to record the tree height. In a dense tropical forest, it is quite challenging to measure the tree height of tall trees using Leica DISTO 510 because of existing understory, intermingling situation, etc. It was also experienced in this study;

- ✓ It was not possible to select sampling plots that covered large area due to inaccessibility for mining activities and rugged terrain with steep slopes;

5.   CONCLUSION AND RECOMMENDATIONS

5.1.   Conclusion

Quantification and monitoring of carbon sequestration in the tropical rainforest is essential for understanding the role of the tropical rainforest on the global carbon cycle. This study explored the potentialities of using UAV to assess aboveground biomass/carbon stock and carbon sequestration of KRUS education forest of East Kalimantan, Indonesia. The study also investigated the influence of height and CPA delineation error on biomass and carbon sequestration estimation. To address the research objectives and questions, the following conclusions were made based on results.

5.1.1.   What is the estimated amount of the AGB/carbon stock for 2017 and 2018?

In 2017, the average UAV-based AGB was assessed 235.37 Mg ha^{-1} while the mean UAV-based AGB was estimated at 248.01 Mg ha^{-1} for 2018. The difference between the two means of AGB was 12.64 Mg ha^{-1}. On the other hand, the average UAV-based carbon was estimated 117.69 Mg ha^{-1} for the year 2017 whereas, the average UAV-based carbon was estimated 124.00 Mg ha^{-1} for the year 2018.

5.1.2.   What is the estimated amount of sequestered carbon?

The amount of sequestered carbon for one year was estimated at 6.32 Mg ha^{-1}. The total area of the KRUS educational forest is 238 hectares. Therefore, the annual amount of sequestered carbon was estimated 1504.16 Mg.

5.1.3.   What is the accuracy of aboveground biomass measured from UAV images?

For the year 2017, the scatter plot demonstrated the relationship between UAV-based AGB and field-based AGB and the root mean square error (RMSE) was 42.35 Mg ha^{-1} which are equivalent to 18.27 % of the field-based AGB. For the year 2018, the root mean square error (RMSE) was 50.00 Mg ha^{-1} which are equivalent to 19.84 % of the field-based AGB. For both years, there was no significant difference between estimated AGB from UAV and field-based AGB, because the P-value was greater than 0.05 at α= 0.05 and t-Statistics < t-Critical.

5.1.4.   What is the error of UAV-derived tree height and how does that affect the AGB estimation?

The effect of height error on biomass estimation was conducted based on the percentage of the root mean square error (RMSE). The percentage of RMSE was calculated at 8.94% for the UAV- derived tree height compared to the field-measured tree height. The mean difference of UAV-based AGB without inflated/deflated height and the UAV-based AGB with inflated/deflated height was 21.66 Mg ha^{-1}. The 8.73% biomass variation was found due to height error, and it was proved to be a significant effect on overall plot-based biomass assessment. The resultant estimated amount of carbon stock due to height error was greater than the amount of sequestered carbon for one year.

5.1.5.   How much the CPA delineation error affect the AGB estimation?

The average variation of biomass due to 1% inflation and deflation of CPA was 2.47 Mg ha^{-1} which was equivalent to 0.99%. The range of variation of biomass for 1% inflated and deflated CPA was 2.36 to 7.66 Mg ha^{-1}, and it showed statistically insignificant influence on biomass estimation. For 5% inflation and deflation of CPA, the average variation of biomass was estimated 12.37 Mg ha^{-1} while the range of variation was observed 11.79- 38.27 Mg ha^{-1}. On the other hand, the average variation of biomass 24.70 Mg ha^{-1} was estimated due to 10% inflated and deflated CPA that showed a statistically significant difference, and it affected 9.96% variation of AGB from the original biomass. The range of variation was calculated 23.56- 76.45 Mg ha^{-1}. The estimated amount of carbon due to CPA error was double compared to the amount of sequestered carbon for one year.

5.2.   Recommendations

✓   The handheld Garmin GPS has 5-10 m inaccuracy. It is quite challenging to identify the right tree in the right location. Even if the center of the plot is recorded correctly, it is easy to identify the tree location by tracing the direction of trees from the center. Therefore, Differential Global Positioning System (DGPS) should be used to record the coordinate of the plot center to ease the identification of individual trees within the plot because the DGPS has few centimeters error only.

✓   A large number of UAV images need more processing time. The software namely Pix4D produce point clouds to generate DSM, DTM, and orthomosaic based on image matching technique. If some of the images are tilted and distorted among all images, the software takes a long time to find the tie points. The distorted DSM, DTM, and orthomosaic are produced due to the poor quality of images. If the some of the portions of the DSM, DTM, and orthomosaic are distorted, the average density of point clouds would be small, and the value of DSM and DTM would be higher or lower compared to the normal range. The processing of a small number of images is better to produce good quality DSM, DTM, and orthomosaic. Therefore, the study area should be small, and the number of images should be reasonable to produce high-density point clouds and eventually to generate good quality DSM, DTM, and orthomosaic.

✓   The high speed of UAV produces tilted images. Therefore, the slow or moderate speed should be chosen as a parameter for flying UAV to get a better UAV output.

✓   Sometimes, the UAV images look good visually, but at the time of processing images, the software does not find the tie points. It may happen for overlapping, altitude, speed, etc. of UAV flight planning. Therefore, if the study area is located far from the origin of the researcher, the UAV images should be processed before leaving the study area.

✓   The software namely Avanza Map should be used to identify the individual tree within the plots during biometric data collection because it's very easy to operate

LIST OF REFERENCES

Affendy, H., Aminuddin, M., Razak, W., Arifin, A., Mojiol, A. R. (2009). Growth increments of indigenous species planted in secondary forest area. *Research Journal of Forestry,* 3(1), 23-28.doi.org/10.3923/rjf.2009.23.28

Agüera-Vega, F., Carvajal-Ramírez, F., & Martínez-Carricondo, P. (2017). Assessment of photogrammetric mapping accuracy based on variation ground control points number using unmanned aerial vehicle. *Measurement: Journal of the International Measurement Confederation*, *98*, 221–227. https://doi.org/10.1016/j.measurement.2016.12.002

Anderson, S. C., Kupfer, J. A., Wilson, R. R., & Cooper, R. J. (2000). Estimating forest crown area removed by selection cutting: A linked regression-GIS approach based on stump diameters. *Forest Ecology and Management*, *137*(1–3), 171–177. https://doi.org/10.1016/S0378-1127(99)00325-4

Asmare, M. F. (2013). Airborne LiDAR data and VHR WORLDVIEW satellite imagery to support community based forest certification in Chitwan, Nepal (MSc Thesis). *University of Twente, Faculty of Geo-Information Science and Earth Observation (ITC), Enschede,The Netherlands.* Retrieved from http://www.itc.nl/library/papers_2013/msc/nrm/asmare.pdf

Basuki, T. M., van Laake, P. E., Skidmore, A. K., & Hussin, Y. A. (2009). Allometric equations for estimating the above-ground biomass in tropical lowland Dipterocarp forests. *Forest Ecology and Management*, *257*(8), 1684–1694. https://doi.org/10.1016/j.foreco.2009.01.027

Böttcher, H., Eisbrenner, K., Fritz, S., Kindermann, G., Kraxner, F., McCallum, I., & Obersteiner, M. (2009). An assessment of monitoring requirements and costs of "Reduced Emissions from Deforestation and Degradation." *Carbon Balance and Management*, *4*, 7. https://doi.org/10.1186/1750-0680-4-7

Brown, S. (2002). Measuring carbon in forests: Current status and future challenges. *Environmental Pollution*, *116*(3), 363–372. https://doi.org/10.1016/S0269-7491(01)00212-3

Brown, S., Sathaye, J., Cannell, M., & Kauppi, P. (1996). Management of forests for mitigation of greenhouse gas emissions. In *climate change 1995: Impacts, adaptions and mitigation of climate change: scientific-technical analyses* (pp. 773–798).

Burrows, W. H., Henry, B. K., Back, P. V., Hoffmann, M. B., Tait, L. J., Anderson, E. R., … McKeon, G. M. (2002). Growth and carbon stock change in eucalypt woodlands in northeast Australia: Ecological and greenhouse sink implications. *Global Change Biology*, *8*(8), 769–784. https://doi.org/10.1046/j.1365-2486.2002.00515.x

Chave, J., Andalo, C., Brown, S., Cairns, M. A., Chambers, J. Q., Eamus, D., … Yamakura, T. (2005). Tree allometry and improved estimation of carbon stocks and balance in tropical forests. *Oecologia*, *145*(1), 87–99. https://doi.org/10.1007/s00442-005-0100-x

Chave, J., Condit, R., Aguilar, S., Hernandez, A., Lao, S., & Perez, R. (2004). Error propagation and scaling for tropical forest biomass estimates. *Philosophical Transactions of the Royal Society B: Biological Sciences*, *359*(1443), 409–420. https://doi.org/10.1098/rstb.2003.1425

Chave, J., Réjou-Méchain, M., Búrquez, A., Chidumayo, E., Colgan, M. S., Delitti, W. B. C., … Vieilledent, G. (2014). Improved allometric models to estimate the aboveground biomass of tropical trees. *Global Change Biology*, *20*(10), 3177–3190. https://doi.org/10.1111/gcb.12629

Cheng, S.-W., Dey, T. K., & Shewchuk, J. (2012). Three-dimensional delaunay triangulations. *Delaunay Mesh Generation*. https://doi.org/10.1201/b12987-3

Clark, D. a, Brown, S., Kicklighter, D. W., Chambers, J. Q., Thomlinson, J. R., Ni, J., … Holland, E. a. (2001). Net primary production in tropical forests: an evaluation and synthesis of existing field data. *Ecological Applications*, *11*(2), 371–384. https://doi.org/10.2307/3060895

Curtis, P. S. (2008). Estimating aboveground carbon in live and standing dead trees. In C. M. Hoover (Ed.), *Field Measurements for Forest Carbon Monitoring* (pp. 39–44). Durham, NH 03824: Northern Research Station. https://doi.org/10.1007/978-1-4020-8506-2

Dandois, J. P., Olano, M., & Ellis, E. C. (2015). Optimal altitude, overlap, and weather conditions for computer vision uav estimates of forest structure. *Remote Sensing*, *7*(10), 13895–13920. https://doi.org/10.3390/rs71013895

Davies, S. J., & Apr, N. (2007). Tree mortality and growth in 11 sympatric macaranga species in Borneo. *Growth (Lakeland)*, *82*(4), 920–932. https://doi.org/10.2307/2679892

Diana, R., Hadriyanto, D., Hiratsuka, M., Toma, T., & Morikawa, Y. (2002). Carbon stocks of fast growing tree species and baselines after forest fire in east Kalimantan, Indonesia. https://doi.org/10.13140/2.1.4899.4247

Drake, J. B., Dubayah, R. O., Clark, D. B., Knox, R. G., Blair, J. B., Hofton, M. A., … Prince, S. (2002). Estimation of tropical forest structural characteristics, using large-footprint lidar. *Remote Sensing of Environment*, *79*(2–3), 305–319. https://doi.org/10.1016/S0034-4257(01)00281-4

Du, H., Zhou, G., Ge, H., Fan, W., Xu, X., Fan, W., & Shi, Y. (2012). Satellite-based carbon stock estimation for bamboo forest with a non-linear partial least square regression technique. *International Journal of Remote Sensing*, *33*(6), 1917–1933. https://doi.org/10.1080/01431161.2011.603379

Dube, T., & Mutanga, O. (2015). Evaluating the utility of the medium-spatial resolution Landsat 8 multispectral sensor in quantifying aboveground biomass in uMgeni catchment, South Africa. *ISPRS Journal of Photogrammetry and Remote Sensing*, *101*, 36–46. https://doi.org/10.1016/j.isprsjprs.2014.11.001

Ebuy, J., Lokombe, J. P., Ponette, Q., Sonwa, D., & Picard, N. (2011). Allometric equation for predicting aboveground biomass of three tree species. *Journal of Tropical Forest Science*, *23*(2), 125–132.

Faculty of Forestry. University of Mulawarman. (2018)(Unpublished). Forest management plan long KPHP long-term forest management plan Unmul KRUS education forest.

Fritz, A., Kattenborn, T., & Koch, B. (2013). UAV-based photogrammetric point clouds- tree stem mapping in open stands in comparison to terrestrial laser scanner point clouds. *ISPRS - International Archives of the Photogrammetry, Remote Sensing and Spatial Information Sciences*, *XL-1/W2*(September), 141–146. https://doi.org/10.5194/isprsarchives-XL-1-W2-141-2013

Gibbs, H. K., Brown, S., Niles, J. O., & Foley, J. A. (2007). Monitoring and estimating tropical forest carbon stocks: Making REDD a reality. *Environmental Research Letters*, *2*(4). https://doi.org/10.1088/1748-9326/2/4/045023

Gonzalez, P., Asner, G. P., Battles, J. J., Lefsky, M. A., Waring, K. M., & Palace, M. (2010). Forest carbon densities and uncertainties from Lidar, QuickBird, and field measurements in California. *Remote Sensing of Environment*, *114*(7), 1561–1575. https://doi.org/10.1016/j.rse.2010.02.011

Guhardja, E., Fatawi, M., Sutisna, M., Mori, T., & Ohta, S. (2000). Rainforest ecosystems of East Kalimantan : el Niño, drought, fire and human impacts. *Ecological studies : analysis and synthesis* (Vol. v. 140). Retrieved from http://ci.nii.ac.jp/ncid/BA44703883

Hemery, G. E., Savill, P. S., & Pryor, S. N. (2005). Applications of the crown diameter-stem diameter relationship for different species of broadleaved trees. *Forest Ecology and Management*, *215*(1–3), 285–294. https://doi.org/10.1016/j.foreco.2005.05.016

Ho Tong Minh, D., Le Toan, T., Rocca, F., Tebaldini, S., D'Alessandro, M. M., & Villard, L. (2014). Relating P-band synthetic aperture radar tomography to tropical forest biomass. *IEEE Transactions on Geoscience and Remote Sensing*, *52*(2), 967–979. https://doi.org/10.1109/TGRS.2013.2246170

Holdaway, R. J., McNeill, S. J., Mason, N. W. H., & Carswell, F. E. (2014). Propagating uncertainty in plot-based estimates of forest carbon stock and carbon stock change. *Ecosystems*, *17*(4), 627–640. https://doi.org/10.1007/s10021-014-9749-5

Houghton, R. A., & Hackler, J. L. (2000). Changes in terrestrial carbon storage in the United States. 1: The roles of agriculture and forestry. *Global Ecology and Biogeography*, *9*(2), 125–144. https://doi.org/10.1046/j.1365-2699.2000.00166.x

Hunter, M. O., Keller, M., Victoria, D., & Morton, D. C. (2013). Tree height and tropical forest biomass estimation. *Biogeosciences*, *10*(12), 8385–8399. https://doi.org/10.5194/bg-10-8385-2013

IPCC. (2003). *Good practice guidance for land use, land use change and forestry. Institute for Global Environmental Strategies*. https://doi.org/citeulike-article-id:1260638

IPCC. (2006). Volume 4: Agriculture, forestry and other land use (AFOLU). *Draft 2006 IPCC guidelines for national greenhouse gas inventories*, *4*, 673. Retrieved from https://www.ipcc.ch/meetings/session25/doc4a4b/vol4.pdf

Terakunpisut, J., Gajaseni, N., Ruankawe, N. (2007). Carbon sequestration potential in aboveground biomass of Thong Pha Phum national forest, Thailand. *Applied Ecology and Environmental Research*, *5*(P 2728), 93–102.

Kachamba, D. J., Ørka, H. O., Gobakken, T., Eid, T., & Mwase, W. (2016). Biomass estimation using 3D data from unmanned aerial vehicle imagery in a tropical woodland. *Remote Sensing*, *8*(11). https://doi.org/10.3390/rs8110968

Ketterings, Q. M., Coe, R., Van Noordwijk, M., Ambagau, Y., & Palm, C. A. (2001). Reducing uncertain in the use of allometric biomass equation for predciting above-ground tree biomass in mixed secondary forests. *Forest Ecology and Management*, *146*, 199–209. https://doi.org/

Koh, L. P., & Wich, S. A. (2012). Dawn of drone ecology: Low-cost autonomous aerial vehicles for conservation. *Tropical Conservation Science*, *5*(2), 121–132. https://doi.org/10.1177/194008291200500202

Köhl, M., Magnussen, S., & Marchetti, M. (2006). Sampling Methods, Remote Sensing and GIS Multiresource Forest Inventory. *Tropical Forest Ecology*. https://doi.org/10.1007/978-3-540-32572-7

Kuuluvainen, T. (1991). Relationships between crown projected area and components of above-ground biomass in Norway spruce trees in even-aged stands: Empirical results and their interpretation. *Forest Ecology and Management*, *40*(3–4), 243–260. https://doi.org/10.1016/0378-1127(91)90043-U

Lo, E. (2005). Gaussian error propagation applied to ecological data: Post-ice-storm- downed woody biomass. *Ecological Monographs*, *75*(4), 451–466. https://doi.org/10.1890/05-0030

Lu, D., Mausel, P., Brondízio, E., & Moran, E. (2004). Relationships between forest stand parameters and Landsat TM spectral responses in the Brazilian Amazon Basin. *Forest Ecology and Management*, *198*(1–3), 149–167. https://doi.org/10.1016/j.foreco.2004.03.048

Magar, A. T. (2014). Estimation and mapping of forest biomass and carbon using point-clouds derived from airborne LiDAR and from 3D photogrammetric matching of aerial images, 79. Retrieved from http://www.itc.nl/library/papers_2014/msc/gem/thapamagar.pdf

Micheletti, N., Chandler, J. H., & Lane, S. N. (2015). Structure from motion (SfM) photogrammetry. *British Society for Geomorphology Geomorphological Techniques*, *2*(2), 1–12. https://doi.org/10.5194/isprsarchives-XL-5-W4-37-2015

Mlambo, R., Woodhouse, I. H., Gerard, F., & Anderson, K. (2017). Structure from motion (SfM) photogrammetry with drone data: A low cost method for monitoring greenhouse gas emissions from forests in developing countries. *Forests*, *8*(3). https://doi.org/10.3390/f8030068

Mtui, Y. P. (2017). Tropical rainforest above ground biomass and carbon stock estimation for upper and lower canopies using terrestrial laser scanner and canopy height model from unmanned aerial vehicle (UAV) in Ayer-Hitam, Malaysia (MSc Thesis). *University of Twente, Faculty of Geo-Information Science and Earth Observation (ITC), Enschede,The Netherlands*. Retrieved from http://www.itc.nl/library/papers_2017/msc/nrm/mtui.pdf

Nelson, R. F., Kimes, D. S., Salas, W. A., & Routhier, M. (2000). Secondary forest age and tropical forest biomass estimation using thematic mapper imagery. *BioScience*, *50*(5), 419. https://doi.org/10.1641/0006-3568(2000)050[0419:SFAATF]2.0.CO;2

Nevins, D. (1999). Carbon sequestration and storage in Irish forests. *Centre for Social and Economic Research on the Global Environment University of East Anglia*. Retrieved from http://www.coford.ie/media/coford/content/publications/projectreports/carbonseq-Irishforests.pdf

Nex, F. (2018). Unmanned aerial vehicles for earth observation and ESE applications. Retrieved from http://www.ncl.ac.uk/ceser/research/observation/uav-ese-applications/

Nguyet, D. A. (2012). Error propagation in carbon estimation using the combination of airborne LiDAR data and very high resolution Geo-eye satellite imagery in Ludhikhola watershed , Gorkha , Nepal (MSc Thesis). *University of Twente, Faculty of Geo-Information Science and Earth Observation (ITC), Enschede,The Netherlands*. Retrieved from http://www.itc.nl/Pub/Home/library/Academic_output/AcademicOutput.html?p=11&y=12&l=20

Odia, B. E. (2018). UAV tatasets for retrieval of forest parameters and estimation of aboveground biomass in Berkelah tropical forest, Malaysia. *University of Twente, Faculty of Geo-Information Science and Earth Observation (ITC), Enschede,The Netherlands.*

Okojie, J. A. (2017). Assessment of forest tree structural parameter extractability from optical imaging UAV datasets, in Ahaus Germany (MSc Thesis). *University of Twente, Faculty of Geo-Information Science and Earth Observation (ITC), Enschede,The Netherlands.* https:www.itc.nl/library/papers_2017/msc/nrm/okojie.pdf

Ota, T., Ogawa, M., Mizoue, N., Fukumoto, K., & Yoshida, S. (2017). Forest structure estimation from a UAV-based photogrammetric point cloud in managed temperate coniferous forests. *Forests*, *8*(9), 1–11. https://doi.org/10.3390/f8090343

Ota, T., Ogawa, M., Shimizu, K., Kajisa, T., Mizoue, N., Yoshida, S., … Ket, N. (2015). Aboveground biomass estimation using structure from motion approach with aerial photographs in a seasonal tropical forest. *Forests*, *6*(11), 3882–3898. https://doi.org/10.3390/f6113882

Perko, R., Raggam, H., Deutscher, J., Gutjahr, K., & Schardt, M. (2011). Forest assessment using high resolution SAR data in X-Band. *Remote Sensing*, *3*(4), 792–815. https://doi.org/10.3390/rs3040792

Powell, S. L., Cohen, W. B., Healey, S. P., Kennedy, R. E., Moisen, G. G., Pierce, K. B., & Ohmann, J. L. (2010). Quantification of live aboveground forest biomass dynamics with Landsat time-series and field inventory data: A comparison of empirical modeling approaches. *Remote Sensing of Environment*, *114*(5), 1053–1068. https://doi.org/10.1016/j.rse.2009.12.018

Roger A. Sedjo. (1989). Forests to offset the greenhouse effect: Resources for the future. *Journal of Forestry*, *Vol. 87*(No. 7), 12–16. Retrieved from http://www.rff.org/research/publications/forests-offset-greenhouse-effect

Ruiz, L. A., Hermosilla, T., Mauro, F., & Godino, M. (2014). Analysis of the influence of plot size and LiDAR density on forest structure attribute estimates. *Forests*, *5*(5), 936–951. https://doi.org/10.3390/f5050936

Saatchi, S. S., Harris, N. L., Brown, S., Lefskyd, M., Mitchard, E. T. A., Salas, W., Zuttaa, B. R., Buermannb, W., Lewis, S. L., Hagen, S., Petrova, S., Whiteh, L., Silman, M., & Morelj, M., & Morelj, A. (2011). Benchmark map of forest carbon stocks in tropical regions across three continents. *International Water Power and Dam Construction*, *65*(8), 30–32. https://doi.org/10.1073/pnas.1019576108

Sadadi, O. (2016). Accuracy of measuring tree height using airborne lidar and terrestrial laser scanner and its effect on estimating forest biomass and carbon stock in Ayer Hitam tropical rain forest reserve , Malaysia (MSc Thesis). *University of Twente, Faculty of Geo-information Science and Earth Observation (ITC), Enschede, Netherlands.* Retrieved from http://www.itc.nl/library/papers_2016/msc/nrm/ojoatre.pdf

Samalca, I. K. (2007). Estimation of Forest Biomass and its Error A case in Kalimantan , Indonesia (MSc Thesis). *University of Twente, Faculty of Geo-information Science and Earth Observation (ITC), Enschede, Netherlands.*

Senthilnath, J., Kandukuri, M., Dokania, A., & Ramesh, K. N. (2017). Application of UAV imaging platform for vegetation analysis based on spectral-spatial methods. *Computers and Electronics in Agriculture*, *140*, 8–24. https://doi.org/10.1016/j.compag.2017.05.027

Sherali, H. D., Narayanan, A., & Sivanandan, R. (2003). Estimation of origin-destination trip-tables based on a partial set of traffic link volumes. *Transportation Research Part B: Methodological*, *37*(9), 815–836. https://doi.org/10.1016/S0191-2615(02)00073-5

Shimano, K. (1997). Analysis of the relationship between DBH and crown projection area using a new model. *Journal of Forest Research*, *2*(4), 237–242. https://doi.org/10.1007/BF02348322

Sium, M. T. (2015). Estimating carbon stock using very high resolution imagery and terrestrial laser scanning in tropical rain forest of Royal Belum, Malaysia (MSc Thesis). *University of Twente, Faculty of Geo-information Science and Earth Observation (ITC), Enschede, Netherlands.*

Stöcker, C., Bennett, R., Nex, F., Gerke, M., & Zevenbergen, J. (2017). Review of the current state of UAV regulations. *Remote Sensing*, *9*(5). https://doi.org/10.3390/rs9050459

Strahler, A. H., Jupp, D. L. B., Woodcock, C. E., Schaaf, C. B., Yao, T., Zhao, F., … Boykin-Morris, W. (2008). Retrieval of forest structural parameters using a ground-based lidar instrument. *Canadian Journal of Remote Sensing*, *34*, S426–S440. https://doi.org/10.5589/m08-046

Toma, T., Warsudi, Osone, Y., Sutedjo, Sato, T., S. (2017). Sixteen years changes in tree density and aboveground biomass of a logged and burned dipterocarp forest in East Kalimantan, Indonesia. *Biodiversitas, Journal of Biological Diversity*, *18*(3), 1159–1167. https://doi.org/10.13057/biodiv/d180337

Villard, L., Le Toan, T., Tang Minh, D. H., Mermoz, S., & Bouvet, A. (2016). Forest biomass from radar remote sensing. *Land Surface Remote Sensing in Agriculture and Forest*, 363–425. https://doi.org/10.1016/B978-1-78548-103-1.50009-1

Westoby, M. J., Brasington, J., Glasser, N. F., Hambrey, M. J., & Reynolds, J. M. (2012). 'Structure- from-Motion' photogrammetry: A low- cost, effective tool for geoscience applications. *Geomorphology*, *179*, 300–314. https://doi.org/10.1016/j.geomorph.2012.08.021

Wikipedia. (2015). Unmul botanical garden Samarinda - Indonesian Wikipedia, the free encyclopedia. Retrieved August 25, 2018, from https://id.wikipedia.org/wiki/Kebun_Raya_Unmul_Samarinda

Zarco-Tejada, P. J., Diaz-Varela, R., Angileri, V., & Loudjani, P. (2014). Tree height quantification using very high resolution imagery acquired from an unmanned aerial vehicle (UAV) and automatic 3D photo-reconstruction methods. *European Journal of Agronomy*, *55*, 89–99. https://doi.org/10.1016/j.eja.2014.01.004

APPENDICES

Appendix 1: Biometric data collection sheet

Collection Sheet (KRUS Education Forest, East Kalimantan, Indonesia 2018)									
Recorder:			Plot No:		Plot Radius:		Date:		
Plot Centre	Latitude:				Slope (%):				
	Longitude:								
Photograph Number:				Photographer Name:					
Tree No.	Latitude	Longitude	Species	DBH (cm)	Tree Height (m)	Tree Shapes	Crown Diameter (m)	Canopy Density (%)	Remarks

Appendix 2: Ground control point (GCP) marker
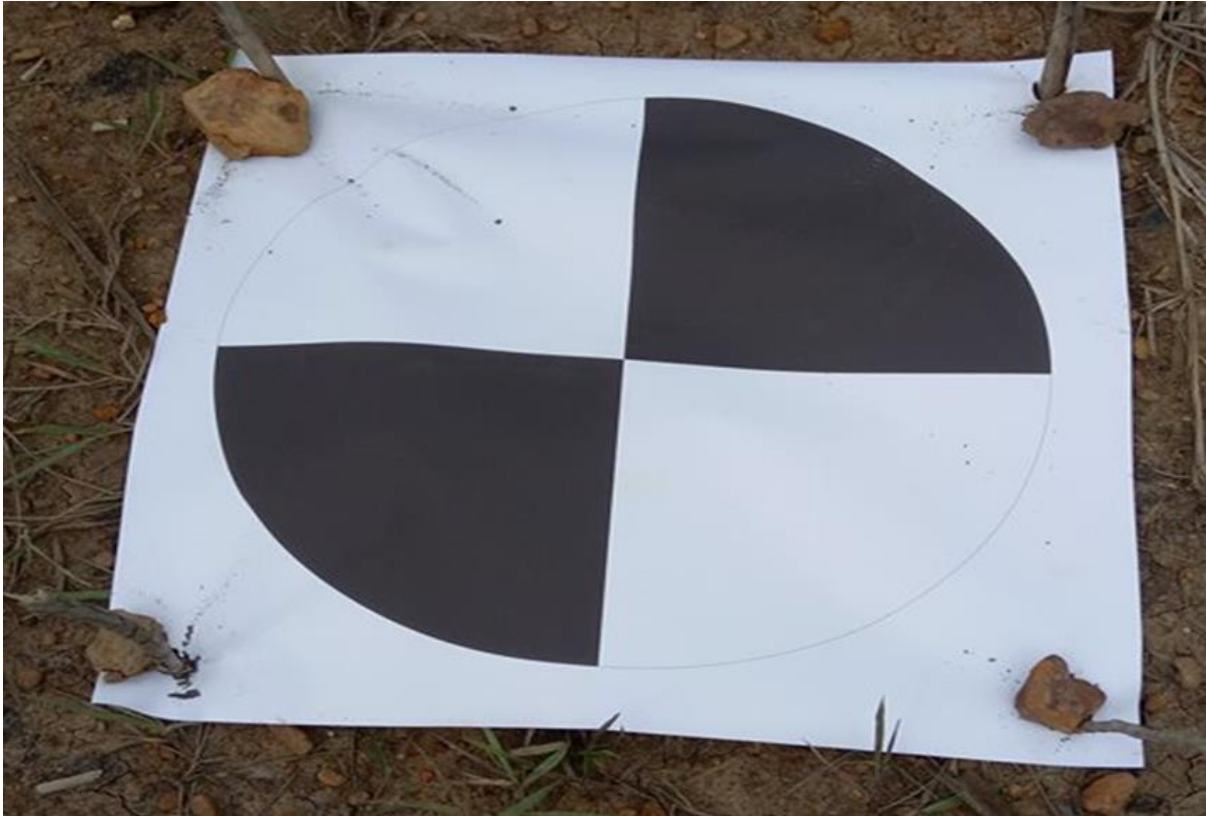
Appendix 3: Slope correction table

Plot Size: 500 m²					
Slope%	Radius(m)	Slope%	Radius(m)	Slope%	Radius(m)
0	12.62				
1	12.62	36	13.01	71	13.97
2	12.62	37	13.03	72	14.00
3	12.62	38	13.05	73	14.04
4	12.62	39	13.07	74	14.07
5	12.62	40	13.09	75	14.10
6	12.63	41	13.12	76	14.14
7	12.63	42	13.14	77	14.17
8	12.64	43	13.16	78	14.21
9	12.64	44	13.19	79	14.24
10	12.65	45	13.21	80	14.28
11	12.65	46	13.24	81	14.31
12	12.66	47	13.26	82	14.35
13	12.67	48	13.29	83	14.38
14	12.68	49	13.31	84	14.42
15	12.69	50	13.34	85	14.45
16	12.70	51	13.37	86	14.49
17	12.71	52	13.39	87	14.52
18	12.72	53	13.42	88	14.56
19	12.73	54	13.45	89	14.60
20	12.74	55	13.48	90	14.63
21	12.75	56	13.51	91	14.67
22	12.77	57	13.53	92	14.71
23	12.78	58	13.56	93	14.74
24	12.79	59	13.59	94	14.78
25	12.81	60	13.62	95	14.82
26	12.82	61	13.65	96	14.85
27	12.84	62	13.68	97	14.89
28	12.86	63	13.72	98	14.93
29	12.87	64	13.75	99	14.97
30	12.89	65	13.78	100	15.00
31	12.91	66	13.81	101	15.04
32	12.93	67	13.84	102	15.08
33	12.95	68	13.87	103	15.12
34	12.97	69	13.91	104	15.15
35	12.99	70	13.94	105	15.19

Appendix 4: Entry of biometric and UAV data in Microsoft Excel

Sl No	Tree No	X	Y	UAV Height	CPA (Sq. M)	Biometric DBH	UAV DBH	Biometric Height	UAV AGB	Field AGB
1	3	-0.45041	117.21778	18.85	28.87	33.5	32.47	17.5	609.37	602.34
3	7	-0.45034	117.2177	22.85	22.00	11.5	27.59	23.5	534.87	99.63
4	9	-0.45036	117.21771	19.30	30.87	47.4	33.84	19.8	675.77	1337.87
5	10	-0.45043	117.21771	31.50	61.72	83	51.65	30.2	2489.14	6029.43
6	12	-0.45049	117.21779	25.60	9.29	32	17.75	24.7	252.79	771.03
7	13	-0.45043	117.21783	26.85	47.57	41.7	44.24	25.8	1573.85	1348.95
8	15	-0.4505	117.21774	19.85	14.13	29.4	21.62	17.8	289.71	474.65
9	16	-0.45052	117.21775	15.62	42.86	13	41.48	14.9	818.24	81.13
10	17	-0.45047	117.21779	26.75	116.46	87.5	68.27	25.8	3658.18	5731.78
11	20	-0.4504	117.21782	17.20	10.85	28	19.02	17.7	196.08	429.16
12	21	-0.45044	117.21783	18.85	26.27	36	30.66	18.3	544.72	724.11
13	22	-0.45053	117.21775	24.10	27.60	19.3	31.59	23.2	734.06	270.32
14	23	-0.45046	117.2178	20.63	6.78	28	15.69	19.3	160.87	466.99
15	25	-0.45033	117.21771	13.50	17.83	15.5	24.47	12.6	253.34	97.10
16	26	-0.45035	117.2177	11.85	53.44	15.5	47.47	11.5	812.91	88.82
17	27	-0.45031	117.21774	18.20	18.98	34	25.34	17.3	363.01	613.10
Total AGB in Kg									13966.9	19166.41
Total AGB in Mg									13.96	19.16
Total AGB (Mg ha^{-1})									279.33	383.32

Appendix 5: Comparison between field-based AGB/AGC and UAV-based AGB/AGC 2017

Plot No	Field-based AGB and AGC 2017		UAV-based AGB and AGC 2017	
	AGB (Mg ha⁻¹)	AGC (Mg ha⁻¹)	AGB (Mg ha⁻¹)	AGC (Mg ha⁻¹)
1	409.27	204.64	271.69	135.84
2	332.51	166.26	339.53	169.76
3	246.65	123.33	278.34	139.17
4	449.42	224.71	306.20	153.10
5	125.23	62.62	171.89	85.95
6	325.35	162.68	319.17	159.59
7	502.61	251.30	319.97	159.99
8	280.47	140.23	288.69	144.35
9	280.85	140.42	252.02	126.01
10	260.24	130.12	223.52	111.76
11	150.91	75.45	137.26	68.63
12	157.27	78.63	189.32	94.66
13	201.10	100.55	243.07	121.54
14	313.57	156.78	267.76	133.88
15	165.20	82.60	170.13	85.06
16	358.98	179.49	241.18	120.59
17	155.12	77.56	166.64	83.32
18	375.56	187.78	307.76	153.88
19	200.41	100.21	222.74	111.37
20	111.65	55.82	129.49	64.74
21	251.60	125.80	246.84	123.42
22	429.42	214.71	349.27	174.64
23	165.84	82.92	202.64	101.32
24	281.59	140.79	209.74	104.87
25	222.62	111.31	216.74	108.37
26	301.02	150.51	268.51	134.26
27	150.63	75.32	186.31	93.15
28	267.11	133.56	254.12	127.06
29	260.75	130.37	232.34	116.17
30	281.21	140.61	273.87	136.94
31	193.74	96.87	212.81	106.40
32	402.41	201.21	340.04	170.02
33	181.96	90.98	186.39	93.19
34	176.21	88.11	187.34	93.67
35	164.20	82.10	145.63	72.82
36	71.23	35.62	141.15	70.58
37	585.46	292.73	331.39	165.69
38	264.53	132.27	228.23	114.12
39	123.03	61.51	157.95	78.97
40	170.87	85.43	183.65	91.82
41	259.19	129.59	248.80	124.40

Appendix 6: Comparison between field-based AGB/AGC and UAV-based AGB/AGC 2018

Plot No	Field-based AGB and AGC 2018		UAV-based AGB and AGC 2018	
	AGB (Mg ha^{-1})	AGC (Mg ha^{-1})		AGB (Mg ha^{-1})
1	433.00	216.50	279.34	139.67
2	350.64	175.32	343.34	171.67
3	264.51	132.25	289.77	144.89
4	474.68	237.34	313.32	156.66
5	142.74	71.37	194.81	97.41
6	341.32	170.66	333.93	166.96
7	524.52	262.26	328.17	164.08
8	296.93	148.47	307.72	153.86
9	302.73	151.36	264.04	132.02
10	280.69	140.35	239.56	119.78
11	170.74	85.37	159.76	79.88
12	173.88	86.94	199.58	99.79
13	221.92	110.96	263.27	131.63
14	337.13	168.57	274.38	137.19
15	191.28	95.64	188.51	94.26
16	380.47	190.24	258.35	129.17
17	174.43	87.22	179.18	89.59
18	403.38	201.69	318.34	159.17
19	220.66	110.33	238.16	119.08
20	125.94	62.97	150.99	75.50
21	270.97	135.48	265.59	132.80
22	454.81	227.41	354.17	177.09
23	181.23	90.61	224.95	112.47
24	302.70	151.35	235.57	117.79
25	239.04	119.52	233.91	116.95
26	320.18	160.09	272.11	136.06
27	165.96	82.98	190.66	95.33
28	290.36	145.18	272.95	136.47
29	283.78	141.89	248.65	124.32
30	301.60	150.80	292.22	146.11
31	211.01	105.51	218.15	109.07
32	420.83	210.41	358.82	179.41
33	199.92	99.96	189.10	94.55
34	193.54	96.77	203.95	101.98
35	193.96	96.98	149.84	74.92
36	84.44	42.22	147.69	73.84
37	612.01	306.00	340.66	170.33
38	285.57	142.78	239.37	119.68
39	141.41	70.71	170.77	85.38
40	188.31	94.15	193.79	96.89
41	282.95	141.48	280.77	140.38